Declaration

I, Othman Ahmad Othman, confirm that the work presented in this thesis is my own, and not substantially the same as any I have submitted for a degree or diploma or other qualification at any other university. Where information has been derived from other sources, I confirm that this has been indicated in the thesis.

Abstract

Among its various biological functions, NAD metabolism regulates axon degeneration, which is an early and often causative event in a variety of neurodegenerative diseases including Huntington's disease (HD) and Alzheimer's disease (AD).

Our research group previously found that reducing the levels of the NAD precursor nicotinamide mononucleotide (NMN) pharmacologically with the NMN-synthesizing enzyme nicotinamide phosphoribosyl transferase (NAMPT) inhibitor FK866 or genetically by expressing the bacterial enzyme NMN deamidase in mammalian neurons remarkably reduces axon degeneration after acute injury. Here, we asked whether FK866 could also improve axonal pathology and behavioral symptoms in *in vitro* and *in vivo* models of HD and AD, and compared its effect to that of memantine, an N-methyl-D-aspartate receptor (NMDAR) antagonist with a well-defined neuroprotective action.

An inducible PC12 cell line expressing wild type (Q21 PC12 cells) and HD-associated mutant Huntingtin (mHTT) protein (Q72 PC12 cells) was used as an *in vitro* model of HD, while amyloid-beta (Aβ) treatment in mouse cortical neurons was used to mimic AD-associated Aβ toxicity *in vitro*. We found that FK866 in combination with nicotinic acid (NA) that maintains NAD levels while reducing NMN levels significantly rescued axonal pathology and ameliorated nuclear morphology in HD and AD cellular models. NMN added together with FK866/NA significantly reverted FK866-mediated axonal protection. In contrast, memantine improved nuclear abnormalities while showing no effect in the axonal compartment. The similarity between our result in cellular HD and Aβ toxicity models and that observed in a model of Wallerian degeneration (Di Stefano et al. 2014) suggests that FK866-induced neuroprotection is linked to the reduction in NMN production and it is not due to off-target effects of FK866 and underlines shared mechanisms between axon pathology in disease and that after an acute injure.

I tested FK866 efficacy *in vivo* using HdhQ140 mice, a knock-in mouse model of HD, and APP_{swe}/PS1dE9 mice, a transgenic mouse model of AD, crossed with the yellow fluorescent protein (YFP)-H transgenic mouse line. In these mice, YFP protein is expressed in restricted subsets of neurons, allowing imaging of individual neuronal structures. The point here is to see at which neuronal compartment pathology begins. Consistent with previous reports (Adalbert et al. 2009; Marangoni et al. 2014), I found that axonal swellings and dystrophies appear early in HdhQ140 /YFP-H mice and in APP_{swe}/PS1dE9/YFP-H mice and were the

major structural abnormalities detected in these mice at the time-point considered. FK866 in combination with NA significantly decreased the number of axonal swellings detected in HdhQ140/YFP-H mice and that of axonal dystrophies detected in APP_{swe}/PS1dE9/YFP-H mice without causing any alteration in nuclear or dendritic morphology of these mice. In addition, FK866 significantly reduced APP_{swe}/PS1dE9/YFP-H mice hyperactivity, a known behavioral abnormality in these mice. On the other hand, memantine significantly restored the reduction in locomotor activity of HdhQ140/YFP-H mice and improved the sensorimotor gating abnormalities of APP_{swe}/PS1dE9/YFP-H mice.

Our results underlines potential mechanistic similarities between axonal abnormalities induced by mHTT and Aβ *in vitro* and in *in vivo* and those after acute injury, and they highlight the possible therapeutic value of limiting NMN levels with FK866.

Acknowledgment

First and above all, I praise God for providing me with the opportunity and the capability to proceed successfully, and being with me all the time during the hard moments that I faced throughout my PhD study.

I would like to express my sincere gratitude to my supervisors Dr Laura Conforti and Dr Marie-Christine Pardon for their continuous support, guidance, patience, motivation, and enthusiasm all the time during research and writing of this thesis.

I would like to thank Dr Federico Dajas-Bailador and my fellow lab mates Jamie Webster, Michele Di Stefano, Martina Marangoni, Francesca Rossi, Andrea Loreto, and Philippine Geiszler for precious assistance during my study.

Special thanks go to the people working at The Advanced Microscopy Unit Emma King and Ian ward, and the people working at The Institute of Cell Signalling Tim Self and Seema Rajani for support with microscopy and imaging.

I take this opportunity to thank my sponsor The Higher Committee for Education Development in Iraq (HCED-IRAQ) for providing the financial support for my study at The University of Nottingham, one of the most globally reputable universities.

I would like to thank my father, my mother, and my father in law, my mother in law, and other family members who they deserve my sincere gratitude and profound appreciation for their continuous encouragement during my study.

My deepest gratitude is for my wife Rafal for being the guiding light when life threw me in the darkest of corners. Thanks for being my leash when I was running too fast and my push when I was moving too slow. Thanks for being my anchor when I was sinking too deep and my rope when I was flying too high. You and our lovely kids Hayf and Yazin helped me to regain hope after despair, resume life after obstructions, restart journeys after detours, and revive strength after defeat.

List of Abbreviations

AD	Alzheimer's disease
APP	amyloid precursor protein
APP	amyloid precursor protein gene
Aβ	amyloid-β
BAC	bacterial artificial chromosome
BACE	β-site amyloid precursor protein cleaving enzyme
BDNF	brain derived neurotrophic factor
CAG	cytosine adenine guanine
CBP	CREB binding protein
CREB	cyclic-AMP response element binding protein
Dox	doxycycline
GFAP	glial fibrillary acidic protein
GFP	green fluorescent protein
HD	Huntington's disease
HDCRG	Huntington Disease Collaborative Research Group
HTT	huntingtin gene
HTT	huntingtin protein
IL	interleukin
mHTT	mutant huntingtin protein
MSNs	medium spiny neurons
NA	nicotinic acid
NAMPT	nicotinamide phosphoribosyl transferase

NMDARs	N-methyl-D-aspartate receptors
NMN	nicotinamide mononucleotide
NMNAT	nicotinamide mononucleotide adenylyl transferase
PBS	phosphate buffered saline
PC12	pheochromocytoma cells
PFA	phosphate buffered paraformaldehyde
PGC-1α	PPAR-γ coactivator 1α
PolyQ	polyglutamine
PPI	prepulse inhibition
PrP	prion protein
PS	presenilin gene
PS	presenilin protein
PSD95	postsynaptic density 95
RT-PCR	reverse transcription polymerase chain reaction
SAM	sterile α-motif
SARM1	sterile alpha and TIR motif–containing 1
TIR	Toll interleukin-1 receptor
TLR	Toll-like receptor
TNF	tumor necrosis factor
Wld^S	Wallerian degeneration slow gene
WLD^S	Wallerian degeneration slow protein
YAC	yeast artificial chromosome
YFP	yellow fluorescent protein

List of Figures

Page

Figure 1: George Huntington's 1872 paper "On Chorea" in The Medical and Surgical Reporter ---------- 16

Figure 2: Schematic diagram of HTT protein structure ---------- 20

Figure 3: Key cellular pathogenic mechanisms in HD ---------- 22

Figure 4: HD brain (right side) and normal brain (left side) ---------- 26

Figure 5: Alois Alzheimer and his patient Auguste D ---------- 33

Figure 6: AD brain (right side) and normal brain (left side) ---------- 35

Figure 7: The amyloid cascade pathway ---------- 36

Figure 8: Structure-activity relationship of WLD^S ---------- 46

Figure 9: NAD biosynthetic pathway from nicotinamide (NAM) and nicotinic acid (NA) - 47

Figure 10: Tet-On PC12 cells characterization ---------- 62

Figure 11: FK866 co-administered with NA reduced mHTT-induced toxicity in Tet-On PC12 cells ---------- 64

Figure 12: FK866 co-administered with NA reduced mHTT-induced toxicity in Q72 Tet-On PC12 cells, and neuroprotective effects of 10 nM and 100 nM FK866 were undistinguishable

Figure 13: NMN reverted the axonal protection of FK866/NA ---------- 67

Figure 14: Memantine attenuated mHTT-induced nuclear but not axonal toxicity in Tet-On PC12 cells ---------- 70

Figure 15: Expression of NMDARs subunits in Tet-On PC12 cells ---------- 71

Figure 16: Effect of Aβ on axonal viability of primary cortical neurons ---------- 72

Figure 17: FK866 co-administered with NA rescued Aβ -induced toxicity in cortical neuronal culture ---------- 75

Figure 18: Rotarod performance was impaired in HdhQ140/YFP-H model of HD and in APP_{swe}/PS1dE9/YFP-H model of AD in comparison to their YFP+ controls ---------- 85

Figure 19: Spatial working memory and locomotor activity was not impaired both in HdhQ140/YFP-H model of HD and in APP_{swe}/PS1dE9/YFP-H model of AD ---------- 87

Figure 20: Post-treatment rotarod performance did not change both in HdhQ140/YFP-H model of HD and in APP_{swe}/PS1dE9/YFP-H model of AD ---------- 89

Figure 21: Post-treatment spatial working memory was preserved both in HdhQ140/YFP-H model of HD and in APP_{swe}/PS1dE9/YFP-H model of AD ---------- 90

Figure 22: Post-treatment anxiety-like behaviour did not change both in HdhQ140/YFP-H model of HD and in APP_{swe}/PS1dE9/YFP-H model of AD ---------- 92

Figure 23: FK866/NA and memantine improved the locomotor activity of APP_{swe}/PS1dE9/YFP-H mice and HdhQ140/YFP-H mice respectively ---------- 95

Figure 24: Memantine and FK866/NA improved the sensorimotor gating abnormalities of APP_{swe}/PS1dE9/YFP-H mice. Drug treatment did not alter PPI parameters in HdhQ140/YFP-H mice ---------- 100

Figure 25: Fluorescent microscopy image (2.5X) of sagittal brain sections (50 μm) of 6-months old WT/YFP-H mouse ---------- 109

Figure 26: Corticostriatal neurons show no change in axonal swellings both in HdhQ140/YFP-H model of HD and in APP_{swe}/PS1dE9/YFP-H model of AD at 6-months old

Figure 27: Axonal swellings in stria terminalis of HdhQ140/YFP-H mice are ameliorated with FK866/NA and memantine ---------- 113

Figure 28: Cortical dystrophies in APP_{swe}/PS1dE9/YFP-H mice are decreased with FK866/NA and memantine ---------- 114

Figure 29: Cortical dystrophies in APP_{swe}/PS1dE9/YFP-H mice co-localized with the deposition of Aβ plaques ---------- 115

Figure 30: Nuclear morphology did not change both in HdhQ140/YFP-H model of HD and in APP_{swe}/PS1dE9/YFP-H model of AD at 6-months old ---------- 117

Figure 31: Gross dendritic morphology was preserved both in HdhQ140/YFP-H model of HD and in APP_{swe}/PS1dE9/YFP-H model of AD at 6-months old ---------- 119

Figure 32: Structure-activity relationship of SARM1 ---------- 127

List of Tables

Page

Table 1: Commonly used genetic mouse models of HD ---------- 28

Table 2: Commonly used genetic mouse models of AD ---------- 39

Table 3: Memantine and HD ---------- 51

Table 4: Memantine and AD ---------- 53

Table 5: Forward and reverse primer sequences for NMDARs NR1, NR2A and NR2B subunits ---------- 60

Table of Contents

Page

Chapter 1: Introduction ---------- 14

1.1 Huntington's Disease (HD) ---------- 16

1.1.1 History ---------- 16

1.1.2 Epidemiology ---------- 17

1.1.3 Clinical findings ---------- 17

1.1.4 Pathogenesis ---------- 19

1.1.5 Neuropathology ---------- 25

1.1.6 Models of Huntington's Disease (HD) ---------- 26

1.2 Alzheimer's Disease (AD) ---------- 32

1.2.1 History ---------- 32

1.2.2 Epidemiology ---------- 33

1.2.3 Clinical Findings ---------- 34

1.2.4 Pathogenesis and Neuropathology ---------- 34

1.2.5 Models of Alzheimer's Disease (AD) ---------- 37

1.3 Axon Degeneration and The Role of FK866 ---------- 44

1.4 Memantine ---------- 47

1.4.1 History ---------- 47

1.4.2 Pharmacology of NMDARs ---------- 48

1.4.3 Pharmacology of Memantine ---------- 50

1.4.4 Memantine and Huntington's Disease (HD) ---------- 51

1.4.5 Memantine and Alzheimer's Disease (AD) ---------- 53

1.5 Aims and Objectives ---------- 54

Chapter 2: Inhibiting NMN synthesis with FK866 rescued axonal degeneration in *in vitro* models of Huntington's disease (HD) and Alzheimer's disease (AD) ---------- 56

2.1 Introduction ---------- 57

2.2 Aims of The Study ---------- 58

2.3 Materials and Methods ---------- 58

- Tet-On PC12 cells culture ---------- 58
- Tet-On PC12 cells characterization and drug treatment ---------- 59
- RT-PCR ---------- 59
- Primary neuronal culture characterization and drug treatment ---------- 60
- Immunocytochemistry ---------- 60
- Statistical analysis ---------- 61

2.4 Results ---------- 61

- FK866 reduced mHTT-induced toxicity in Tet-On PC12 cells ---------- 61
- FK866/NA combination rescued Aβ -induced toxicity in cortical neuronal culture- 71

2.5 Discussion ---------- 75

Chapter 3: FK866 restored some of the behavioural abnormalities in *in vivo* models of Huntington's disease (HD) and Alzheimer's disease (AD) ---------- 78

3.1 Introduction ---------- 79

3.2 Aims of The Study ---------- 80

3.3 Materials and Methods ---------- 80

- Mouse origins and breading ---------- 80
- Genotyping ---------- 81
- Treatment groups ---------- 82
- Behavioural assays ---------- 82
- Statistical analysis ---------- 84

3.4 Results ---------- 84

- Motor functions were impaired both in HdhQ140/YFP-H mice and in APP_{swe}/PS1dE9/YFP-H mice, while learning, memory and locomotor activity remained intact ---------- 84
- FK866/NA and memantine restored the locomotor abnormalities of APP_{swe}/PS1dE9/YFP-H mice and HdhQ140/YFP-H mice respectively ---------- 87
- Memantine and FK866/NA improved the sensorimotor gating abnormalities of APP_{swe}/PS1dE9/YFP-H mice ---------- 95

3.5 Discussion ---------- 100

Chapter 4: FK866 ameliorated axonal swelling and dystrophy abnormalities in *in vivo* models of Huntington's disease (HD) and Alzheimer's disease (AD) respectively ----- 104

4.1 Introduction ---------- 105

4.2 Aims of The Study ---------- 107

4.3 Materials and Methods ---------- 107

- Tissue preparation and sectioning ---------- 107
- Immunohistochemistry ---------- 107
- Imaging and quantitative analysis ---------- 108
- Statistical analysis ---------- 109

4.4 Results ---------- 109

- Axonal swellings in stria terminalis were an early feature of HdhQ140/YFP-H mice, while cortical dystrophies were a characteristic phenomenon of APP_{swe}/PS1dE9/YFP-H mice ---------- 109
- FK866/NA and memantine improved swelling and dystrophy abnormalities detected in HdhQ140/YFP-H mice and APP_{swe}/PS1dE9 mice respectively ---------- 119

4.5 Discussion ---------- 120

Chapter 5: General Discussion ---------- 124

Chapter 6: Conclusive Results and Future Directions ---------- 129

References ---------- 132

Chapter 1:

Introduction

Axon loss is an early event in most neurodegenerative diseases including Huntington's disease (HD) and Alzheimer's disease (AD), where it correlates with symptom onset and progression and precedes cell body loss. This opens new possibilities for therapeutic strategies that selectively target the axonal compartment, since treatments based on the protection of the cellular compartment have shown to be largely ineffective. Recent evidences shown that modulation of nicotinamide adenine dinucleotide (NAD) synthesis pathway with the drug FK866 strongly protect axons *in vitro, ex-vivo* and *in vivo* after acute injury (Di Stefano et al. 2014). The present thesis aims to test the hypothesis that FK866 axon protective properties after acute injury could extend to models of neurodegeneration. In particular, we studied whether FK866 reduces axonal damage and attenuates behavioural symptoms in *in vitro* and *in vivo* models of HD and AD, and we compared its effect to that of the reported neuroprotective and axon protective properties of the N-methyl-D-aspartate receptors (NMDARs) antagonist memantine.

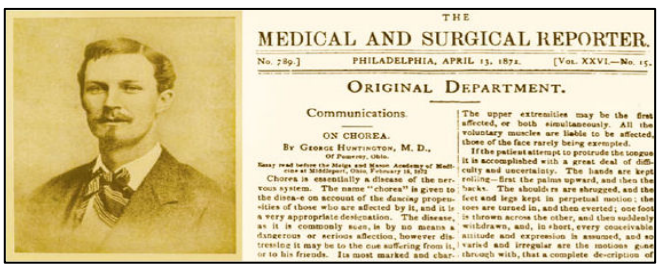
1.1 Huntington's Disease (HD)

HD is an autosomal dominantly inherited neurodegenerative disorder caused by expansion of a cytosine adenine guanine (CAG) repeat coding for polyglutamine (polyQ) tract in the Huntingtin *(HTT)* gene on the short arm of chromosome 4p 16.3, and manifested clinically by triad of psychiatric, motor, and cognitive symptoms.

1.1.1 History

The majority of HD cases in the United States can be traced back to three England travellers, who came to North America in 1630 (Vessie, 1932). The families of these three settlers had been persecuted in England for witchcraft. One of the three travellers settled in East Hampton, Long Island, New York. His descendant, the Mulford family, was locally known to suffer from strange and frightening disease (Vessie, 1932).

George Huntington (April 9, 1850 – March 3, 1916) was fascinated by the condition affecting the Mulford family. He used to visit the patients with his father and grandfather, George Lee Huntington (1811–1881) and Abel Huntington (1778–1858), both of whom were family physicians in East Hampton (Cangemi and Miller, 1998). George Huntington graduated from The University of Colombia in 1871, and in 1872, when he was 22 years old, he wrote his first and only paper, "On Chorea" (Figure 1), that describes the genetic illness that bears his name, Huntington's disease (Huntington, 1872). The condition was a general interest for Huntington family, firstly recognized by his grandfather Abel Huntington, then classified by his father George Lee Huntington, and finally formally described by George Huntington (Cangemi and Miller, 1998).



THE
MEDICAL AND SURGICAL REPORTER.
No. 789.] PHILADELPHIA, APRIL 13, 1872. [Vol. XXVI.—No. 15.

ORIGINAL DEPARTMENT.

Communications.

ON CHOREA.

By George Huntington, M. D.,
of Pomeroy, Ohio.

Read before the Meigs and Mason Academy of Medicine at Middleport, Ohio, February 18, 1872

Chorea is essentially a disease of the nervous system. The name "chorea" is given to the disease on account of the dancing propensities of those who are affected by it, and it is a very appropriate designation. The disease, as it is commonly seen, is by no means a dangerous or serious affection, however distressing it may be to the one suffering from it, or to his friends. Its most marked and characteristic features are the following: The upper extremities may be the first affected, or both simultaneously. All the voluntary muscles are liable to be affected, those of the face rarely being exempted. If the patient attempt to protrude the tongue it is accomplished with a great deal of difficulty and uncertainty. The hands are kept rolling—first the palms upward, and then the backs. The shoulders are shrugged, and the feet and legs kept in perpetual motion; the toes are turned in, and then everted; one foot is thrown across the other, and then suddenly withdrawn, and, in short, every conceivable attitude and expression is assumed, and so varied and irregular are the motions gone through with, that a complete description of

Figure 1: George Huntington's 1872 paper "On Chorea" in The Medical and Surgical Reporter

Research in the disease continued steadily during the 20th century, reaching a major breakthrough in 1983 when the US-Venezuela Huntington's Disease Collaborative Research Project discovered the approximate location of a causal gene (Gusella et al. 1983). This was the result of an extensive research began in 1979, focusing on the populations of two isolated Venezuelan villages, Barranquitas and Lagunetas, where there was an unusually high prevalence of HD. In 1993, there was another landmark discovery, which was the identification of the precise causal gene at 4p16.3, making this the first autosomal disease locus found using genetic linkage analysis (HDCRG, 1993).

1.1.2 Epidemiology

Prevalence of HD shows a stable prevalence pattern in most white populations of about 5-7 affected individuals per 100,000 (Walker, 2007). Prevalence can be much higher in areas where the population can be traced back to a few founders, as in the isolated population of the Lake Maracaibo region of Venezuela, where HD affects up to seven thousand per million people (Young et al. 1986). In contrast, HD appears less frequently in Japan, China, and Finland, and among African blacks. The prevalence in Japan has been estimated between 0.1 and 0.38 per 100,000 (Warby et al. 2011). Currently, the higher prevalence of HD in white populations compared with Asian or African individuals has been attributed to the high frequency of huntingtin alleles with 28-35 CAG repeats in white people (Harper and Jones, 2002).

1.1.3 Clinical Findings

Patients with HD typically develop symptoms around 35-50 years of age, although the onset may occur at any time, between the age of 1 and 80 years, and before that they are usually healthy and have no apparent clinical findings (Myers, 2004). This asymptomatic period merges unnoticeably with a prediagnostic period, when HD patients develop subtle abnormalities of personality, cognition, and motor control. Both the asymptomatic and prediagnostic periods are often called presymptomatic period, but in fact this period is accompanied with non-specific clinical manifestations including progressive weight loss, alterations in sexual behaviour, and disturbances in the wake-sleep cycle, and the patients can be unaware of them (Snowden et al. 1998; Walker, 2007, Politis et al. 2008). The mean

duration of HD is 17-20 years, and as the disease progresses and becomes more complicated, patients become more dependent in their daily life, and they finally die, most commonly due to pneumonia (Roos, 2010).

Clinical manifestations of HD patients can be divided into three major categories, psychiatric, motor, and cognitive symptoms.

Psychiatric disturbances, of which depression is the most frequent one, are seen in the early stages of the disease, and before the onset of other manifestations, and they usually have a highly negative impact on the family, and on the normal daily life functioning (Wheelock et al. 2003). Anxiety is also a common finding (34-61%), in addition to apathy, inactivity, obsessions, compulsions, irritability, suicidal ideation, feeling of guilt and low self-esteem (Roos, 2010).

The key diagnostic feature in HD patients is chorea. Chorea is an involuntary, nonrepetitive, non-periodic jerking movement, initially involving muscles in the distal extremities, like toes and fingers, and later involving small facial muscles (Warby et al. 2011). Although useful for diagnosis, chorea is a poor marker of disease severity (Mahant et al. 2003). As the disease progresses, other movement disorders occur, like dystonia, rigidity, and bradykinesia, while chorea becomes less prominent (Young et al. 1986).

Cognitive dysfunction in HD patients is particularly in relation to executive functions, such as organising, planning, checking, or adapting alternatives (Snowden et al. 2002). Normal persons are able to distinguish things that are relevant and those that can be ignored, but HD patients lose this capability (Roos, 2010). They are unable to organize their daily life, and can no longer make mental adjustments. Unlike psychiatric disturbances, which develop with some frequency and do not progress as the disease becomes more severe, cognitive symptoms worsen over time and speech deteriorates faster than comprehension (Walker, 2007).

Diagnosis is based on the presence of clinical symptoms in an individual whose parent is a proven HD patient. The clinical criteria for diagnosis are motor changes with or without psychiatric or cognitive manifestations. However, in the majority of cases, combination of psychiatric, motor, and cognitive symptoms usually present (Roos, 2010). The difficulty in recognizing the clinical picture is when the parent has died at younger age due to another cause. The current standard to solve this is DNA determination, showing expanded CAG

repeat in the first exon of the *HTT* gene on the short arm of chromosome 4p 16.3 (Myers, 2004).

1.1.4 Pathogenesis

In 1993, a group of 58 scientists from all over the world, The Huntington Disease Collaborative Research Group (HDCRG), characterized the gene responsible for HD and named it interesting transcript 15, IT15. HDCRG team found that the first exon of the IT15 gene observed on HD chromosomes from 75 disease families examined, comprising a variety of ethnic backgrounds, contained a repetitive DNA element consisting of three nucleotides: C (cytosine), A (adenine), and G (guanine), collectively known as CAG, that was longer than the normal range in non-HD controls (HDCRG, 1993).

An inverse relationship has been described between the length of the CAG repeat, and the age of onset of HD (Andrew et al. 1994). The longer the CAG repeats, the earlier the onset of the disease. The length of this repeat explains 40-50% of the overall variance in the age of onset, and the remaining is influenced by genetic and environmental factors, such as paternal inheritance (Brinkman et al. 1997; Wexler et al. 2004).

The IT15 gene, later renamed the Huntingtin gene (*HTT*), encodes a 350 kDa very large protein called Huntingtin (HTT) (Figure 2) (HDCRG, 1993). An obvious feature of HTT structure is the PolyQ tract at its NH_2 terminus, followed by a proline-rich sequence (Zuccato et al. 2010). This protein is also enriched in approximately 40 amino acid long consensus sequences, called huntingtin, elongation factor 3, protein phosphatase 2a, and tor 1 (HEAT) repeats (Li et al. 2001). This protein is mainly cytoplasmic, although a small proportion is intranuclear (Kegel et al. 2002).

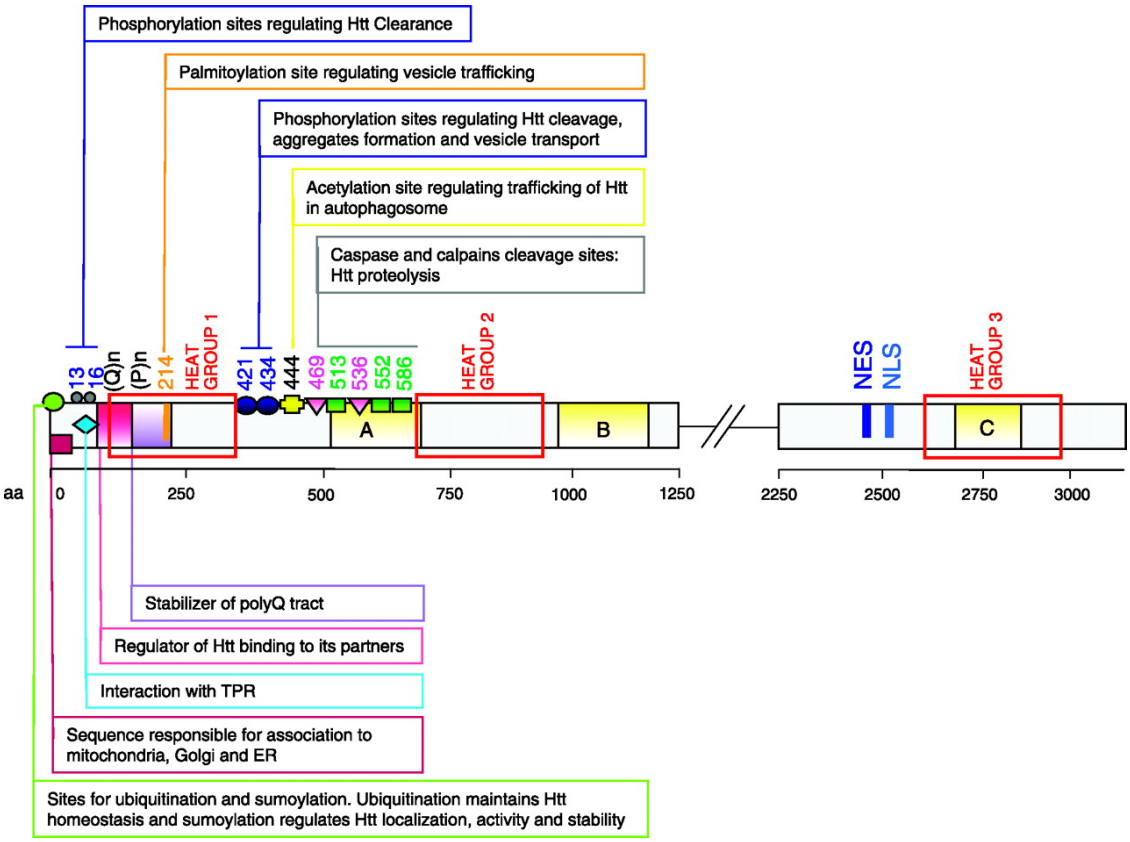


Figure 2: Schematic diagram of HTT protein structure (Zuccato et al. 2010). (Q)*n* indicates polyQ tract, which is followed by the polyproline sequence (P)*n*; the red emptied rectangles indicate the three main groups of HEAT repeats (HEAT group 1, 2, 3). The small green rectangles indicate the caspase cleavage sites and their amino acid position, while the small pink triangles indicate the calpain cleavage sites and their amino acid positions. Boxes in yellow: B, regions cleaved preferentially in the cerebral cortex; C, regions cleaved preferentially in the striatum; A, regions cleaved in both. Posttranslational modifications: ubiquitination (UBI) and/or sumoylation (SUMO) sites (green); palmitoylation site (orange); phosphorylation at serines 13, 16, 421, and 434 (blue); acetylation at lysine 444 (yellow).

Cellular functions of HTT are still not completely understood, but it was found that knocking out its gene in mice is embryonic lethal, and this means it is essential for normal embryonic development (Zeitlin et al. 1995). In addition, conditional knockout of HTT in forebrain and testes had resulted in progressive degenerative neuronal phenotype and sterility, suggesting that this protein is required for neuronal function and survival in the brain (Dragatsis et al. 2000). Different *in vitro* and *in vivo* studies have shown that HTT also has antiapoptotic role (Rigamonti et al. 2000; Dragatsis et al., 2000; Rigamonti et al. 2001), and although the mechanisms of HTT antiapoptotic properties have been partially explained, it could be due to the direct inhibitory effects of HTT on the proteolytic actions of caspases such as caspase 3

and 9 (Rigamonti et al. 2000; Rigamonti et al. 2001). In addition, biological and molecular findings have linked HTT to the production of brain derived neurotrophic factor (BDNF), a neurotrophin that is particularly important for the survival of striatal neurons and for the activity of the corticostriatal synapses (Zuccato and Cattaneo, 2007). HTT stimulates cortical BDNF production by acting at the level of BDNF gene transcription (Zuccato et al. 2001). HTT is found predominantly in the cytoplasm of neurons and is enriched in compartments containing vesicle-associated proteins (Velier et al. 1998), where it enhances both anterograde and retrograde transport of vesicles containing neurotransmitters and also factors such as BDNF through binding to the microtubules (Block-Galarza et al. 1997; Gunawardena et al. 2003).

All the above *in vitro* and *in vivo* data indicate that wild-type HTT has beneficial functions in the mature brain, and it is therefore possible that its loss in HD reduces the ability of neurons to survive and even contributes to neuropathology. In support of this, several lines of evidence both in humans and in mouse models have shown that homozygosity for the HD mutation leads to a more severe phenotype than heterozygosity with the same CAG expansion in the *HTT* gene (Reddy et al. 1998, Wheeler et al. 2000; Squitieri et al. 2003).

Expansion of CAG in the *HTT* gene, which is the codon for the amino acid glutamine, leads to an abnormally expanded polyQ tract in HTT (HDCRG, 1993). The wild-type *HTT* gene contains CAG repeats ranging from 6 – 35, while the mutant *HTT* gene is associated with 36 repeats or more, and definite clinical manifestations occur if the repeats exceed 40 (Zuccato et al. 2010). CAG repeats in the range 36-39 leads to incomplete penetrance of the disease or to a very late onset (Zuccato et al. 2010).

There is now strong support for the idea that the rate limiting step in the pathogenesis of HD is cleavage of mutant HTT (mHTT) by different proteases, like caspases and calpains, resulting in the formation of N-terminal toxic fragments containing the polyglutamine expansion (Imarisio et al. 2008). Different molecular pathways have been described to explain the mechanisms by which mHTT toxic fragments promote neuronal dysfunction in HD (Figure 3).

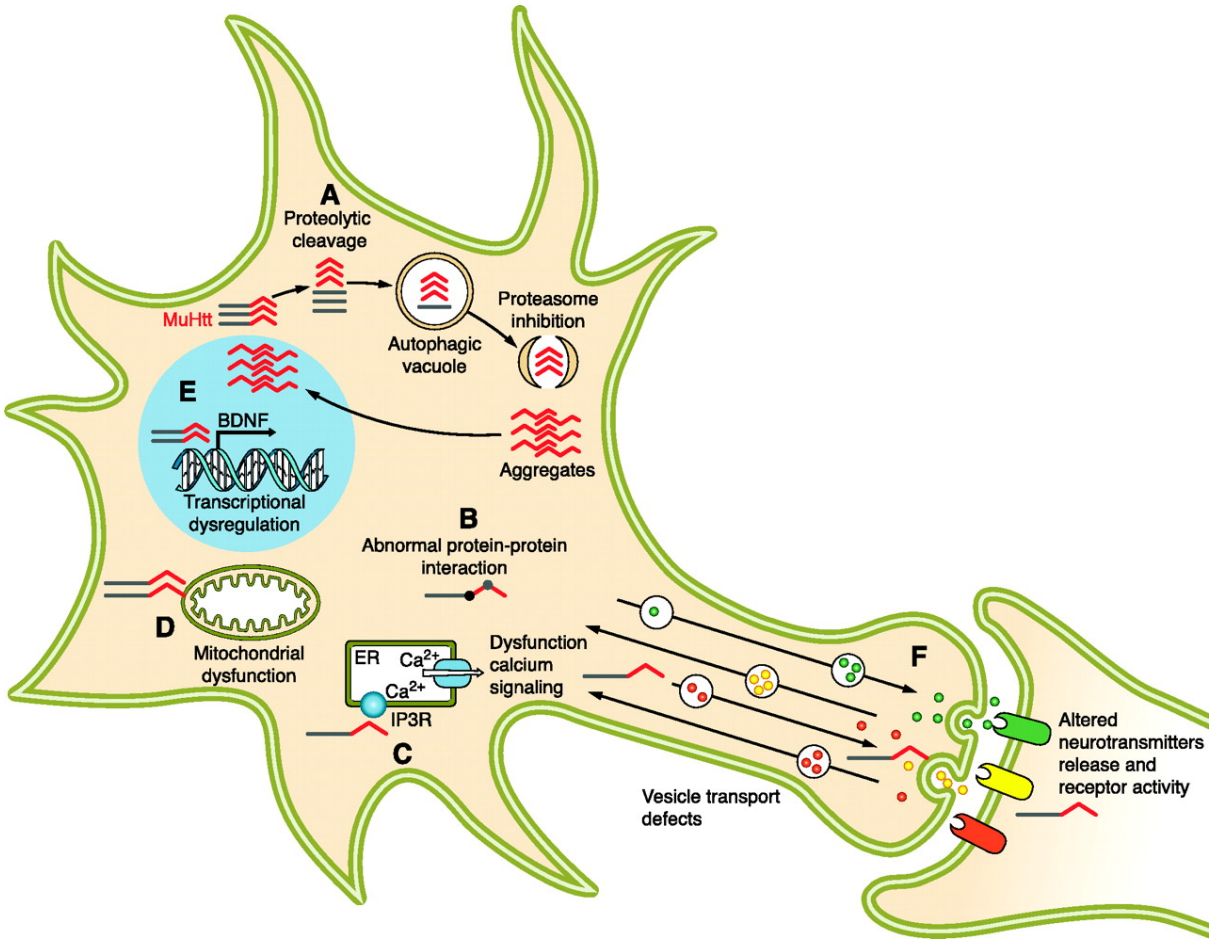


Figure 3: Key cellular pathogenic mechanisms in HD (Zuccato et al. 2010)

1. **Neuronal inclusions:** mHTT toxic fragments can easily aggregate and accumulate in the nucleus forming what is called nuclear neuronal inclusions (or aggregates). Inclusion formation in cultured cells was associated with cell death (Hackam, et al. 1998; Ho et al. 2001). In a conditional mouse model expressing exon 1 fragment of the mutant *HTT* gene with 94 CAG repeats, inclusion formation increases as HD becomes more progressive, and these inclusions disappear when the expression of the mutant *HTT* gene is turned off (Yamamoto et al. 2000). The toxicity of nuclear neuronal inclusions could arise from the recruitment of transcriptional factors and transcriptional regulators that are important for the expression of neuronal survival genes (Cha, 2007; Nucifora et al. 2003). However, several lines of evidence support the idea that neuronal inclusions are rather a defensive mechanism of the cells to sequester toxic soluble fragments of mHTT (Saudou et al. 1998; Kuemmerle et al. 1999), and neurons developing inclusions survived significantly longer than those without inclusions (Arrasate et al. 2004). A more recent view supports

the hypothesis that mHTT toxic fragments in the form of small oligomers intermediates, globular intermediates, or protofibrils are neurotoxic, while those in the form of large inclusions are neuroprotective (Arrasate et al. 2004; Bennet et al. 2007). Extranuclear neuronal inclusions are more likely toxic, since they disrupt the axonal transport between the cell body and the synaptic terminal (Li et al. 2001; Gunawardena et al. 2003).

2. **Excitotoxicity:** Excessive activation of NMDARs, due to increased release or decreased uptake of the excitatory amino acid glutamate, can result in stress or even death of striatal neurons (Raymoned, 2003). It has been found that mHTT and its toxic fragments increase the expression and activity of extrasynaptic NMDARs in the striatum by different mechanisms. Expression of this mutant protein induces tyrosine phosphorylation of NR2B subunits of NMDARs, which consequently promote over activation of these receptors (Song et al. 2003). In addition, mHTT was found to interfere with the ability of HTT to interact with postsynaptic density 95 (PSD95), a scaffolding protein of the post synapse, resulting in the sensitization of NMDARs (Sun et al. 2001). NMDARs over activation could preferentially activate a number of pro-death pathways, like the forkhead box pathway and the proteases calpains, and inhibit a number of pro-survival pathways, like cyclic-AMP response element binding protein (CREB) and extracellular signal-regulated kinase 1/2 (ERK1/2) pathways (Hardingham and Bading, 2010). All these processes will eventually result in dysfunction of neuronal interaction at the corticostriatal synapses.

3. **Loss of BDNF:** Quantitative assessment of BDNF in human cortices affected by HD revealed lower BDNF mRNA and protein levels, indicating reduced production of this factor in the brain of HD sufferers (Zuccato et al. 2008). Many laboratories have confirmed reduced BDNF levels in brain samples from a large panel of HD animal models including both transgenic and knock-in mice models (Zuccato and Cattaneo, 2007; Zuccato and Cattaneo, 2009). It has been found that mHTT reduces BDNF levels by altering the transcription of CREB, CREB binding protein (CBP), specificity protein 1 (Sp1), TBP associated factor 130 (TAF130), and other transcription factors that regulate the activity of BDNF promoters (Zuccato et al. 2001; Cha, 2007). In addition, mHTT can interact with both the glutamine-rich activation domain and the acetyltransferase domain of CBP that ultimately reduce BDNF mRNA levels further (Steffan et al. 2000). The importance of BDNF in supporting the survival of striatal medium spiny neurons

(MSNs), leads to the assumption that disturbance in BDNF signalling is the cause for the differential vulnerability of striatal neurons in HD patients (Zuccato and Cattaneo, 2007).

4. **Mitochondrial dysfunction:** The observation that 3-nitropropionic acid, which is a mitochondrial toxin, and an inhibitor of the tricarboxylic acid cycle, can induce lesions in the striatum that are similar to the cell loss in HD (Beal et al. 1993), leads to the assumption that dysfunctional mitochondria could be implicated in the pathogenesis of HD. It has been found that mHTT interferes with transcription of genes involved in mitochondrial function, thereby altering their motility and metabolic activity within the cells (Orr et al. 2008). This mutant protein could increase the level of the transcription factor p53, resulting in mitochondrial membrane depolarization, as well as upregulation of two proapoptotic downstream elements, bcl2-associated x protein, and p53-upregulated modulator of apoptosis (Bae et al. 2005). In addition, mHTT could repress transcription of PPAR-γ coactivator 1α (PGC-1α), a gene encoding for a transcriptional coactivator that regulates expression of genes involved in mitochondrial biogenesis and respiration, resulting in mitochondrial defects (Cui et al. 2006). Consistent with this, PGC-1α knockout mice have shown to exhibit mitochondrial dysfunctions accompanied by hyperkinetic movement disorder and striatal degeneration (Cui et al. 2006).

5. **Transcriptional dysregulation:** The first evidence highlighting the presence of transcriptional dysregulation in HD came from in situ hybridization studies documenting specific alternations in mRNA expression in post-mortem human HD brains and also in cellular and mouse models of HD (Augood et al. 1996; Augood et al. 1997; Arzberger et al. 1997). Cleavage of mHTT has also been shown to activate the stress-signalling kinase (SEK1)-JUN N-terminal kinase (JNK) pathway and induce apoptosis in a hippocampal neuronal cell line (Liu, 1998). Consistent with these early findings, microarray studies revealed alternations in mRNA of genes associated with transcriptional processes, neurotransmitter receptors, synaptic transmission, cytoskeletal and structural proteins, intracellular signalling, and calcium homeostasis, all implicated in HD (Luthi-Carter et al. 2000; Luthi-Carter et al. 2002; Chan et al. 2002; Sipione et al. 2002). Decreases in mRNA levels were more than increases, and the set of genes that were decreased at symptomatic stages was larger than the one affected at presymptomatic stages, suggesting that transcriptional dysregulation is an early and progressive event in HD (Zuccato et al. 2010).

To sum up, mHTT and its toxic fragments promote neuronal dysfunction in HD by multiple mechanisms, and it is therefore difficult to attribute the broad clinical picture of this neurodegenerative disease to a single mechanism, and unlikely that a single therapeutic regimen will be able to manage HD patients, especially if started after symptom onset.

1.1.5 Neuropathology

The basal ganglia are an interconnected set of subcortical brain structures involved in various aspects of motor control and cognition (Han et al. 2010). Within the basal ganglia is the striatum, which serves the function of filtering multiple input pathways originating from different cortical regions (Mitchell et al. 1999). Information processed in the striatum ultimately returns to the cerebral cortex to complete what is called the corticobasal ganglia-thalamocortical loop (Parent and Hazrati, 1995).

The striatum represented by the caudate and putamen is composed mainly (up to 95%) of projection neurons, which are morphologically characterized by long axons, medium-sized cell bodies, and spiny dendrites, hence they are commonly termed MSNs (Gerfen, 1988). Based on their projection targets, MSNs in the striatum can be divided into two main groups: MSNs in the direct or striatonigral pathway (dMSNs), which project axons to the internal segment of the globus pallidus (GPi), and MSNs in the indirect or striatopallidal pathway (iMSNs), which project axons to the external segment of the globus pallidus (GPe) (Han et al. 2010). The most pronounced neuropathology in HD is found in the striatum, with prominent atrophy and cell loss in the caudate and putamen (Gutekunst et al. 1999).

There is selective vulnerability within MSNs subclasses. MSNs in the indirect pathway are affected at earlier stages and to a greater extent than those in the direct pathway (Reiner et al. 1988). This could explain the development of chorea as an early functional abnormality in patients with HD, since a broad array of experimental evidence supports the proposition that iMSNs help to suppress cortical selection of unwanted movement (Eidelberg and Surmeier, 2011).

Although less pronounced than in the striatum, other brain areas could also be affected, especially in patients with advanced HD. Neuropathological changes have been found in the substantia nigra, the cortical layers 3, 5, and 6, the CA1 region of the hippocampus, the angular gyrus in the parietal lobe, the Purkinje cells of the cerebellum, the lateral tuberal

nuclei of the hypothalamus, and the centromedialparafascicular complex of the thalamus (Figure 4) (Walker, 2007).

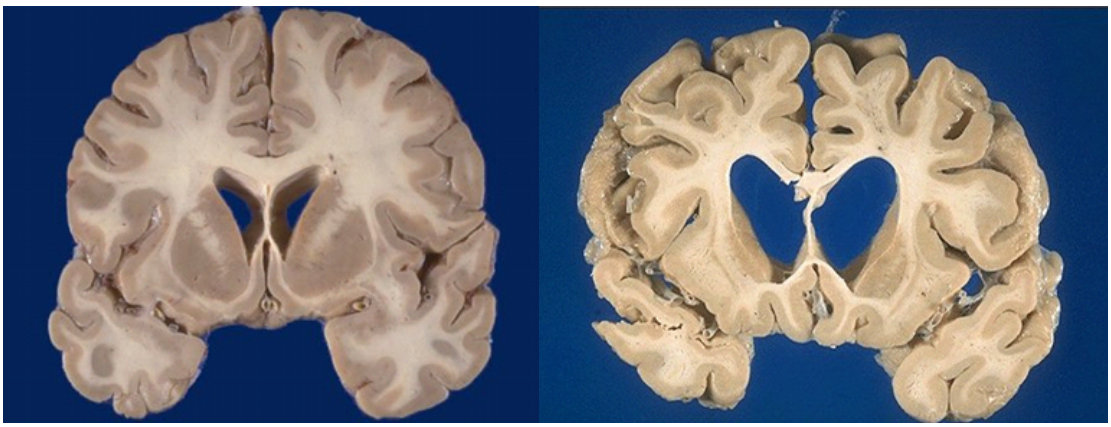


Figure 4: HD brain (right side) and normal brain (left side)

1.1.6 Models of Huntington's Disease (HD)

In the late 1970s, and before discovering the *HTT* gene, several lines of investigation converged to generate animal models of HD (Coyle, 1979). The earliest models used toxins to induce death of striatal neurons, either by excitotoxic mechanisms, or by disruption of mitochondrial machinery (Ramaswamy et al. 2007). The selective NMDARs agonists quinolinic acid and kainic acid have been the two most commonly used agents to produce rodent and non-human primate models of HD (Schwartz et al. 1983; Beal et al. 1986; Beal et al. 1991). The mitochondrial toxin 3-nitropropionic acid, which is an inhibitor of the tricarboxylic acid cycle, has also been used because it produced lesions in the striatum that were similar to the cell loss in HD (Beal e al., 1993). Although these toxin models have been reliable models for specific aspects of HD, they were limited because it was not possible to use them in studying the progression of the disease, or to replicate the widespread neuropathology observed in the human condition (Cepeda et al. 2010). The discovery of the *HTT* gene in 1993 led to the creation of genetic models that opened the doors for mechanistic studies, and permit examination of the progression of the disease in detail.

A. Cellular Models of HD

To gain insight into some of the molecular mechanisms of HD, several cellular models have been developed that stably express the mutant *HTT* gene in an inducible or constitutive form. Exon 1 fragment of the mutant *HTT* gene with various CAG repeats has been mainly used in these models, since it is much more toxic and more liable to aggregation than the full length form (Ross and Margolis, 2002).

The pheochromocytoma12 (PC12) cell line is widely utilized as a cellular model for HD, and its properties are well known (Greene and Tischler, 1976). This cell line has been created from rat adrenal pheochromocytoma. One week's exposure of PC12 cell line to nerve growth factor (NGF) results in differentiation of these cells and expression of processes that are similar to those produced by sympathetic neurons in primary culture. The Tet-On gene expression system has been utilized to create a stable inducible PC12 Tet-On cell line expressing a green fluorescent protein (GFP)-tagged exon 1 fragment of the mutant *HTT* gene (see chapter 2: materials and methods for the details). Expression of the mutant *HTT* gene has been achieved by transfecting the PC12 cell line with a vector containing this gene under the control of a tetracycline-responsive promoter. The expression of this gene is induced in these cells by the addition of doxycycline (dox) to the culture medium (Gossen et al. 1995). As a result, PC12 cells start to display abnormal morphology, intranuclear aggregate formation, and increasing susceptibility to apoptotic stimulation. These cells also start to lose the neurite extension response to NGF, and to show altered gene expression (Li et al. 1999; Wyttenbach et al. 2000).

B. Genetic Mouse Models of HD

With the discovery of the *HTT* gene in 1993, it became possible to create genetic models that attempt to recapitulate the neuropathology and symptomatology of HD. Ideally, mouse models should reproduce the key features of the disease in humans, and display an early, easy to measure, and highly reproducible phenotype that can be used for preclinical therapeutic trials (Menalled et al. 2003). The first of these models were created in the laboratory of Gillian Bates in 1996, and named the R6 lines (R6/2, R6/1, R6/5, and R6/0) (Mangiarini et al. 1996). Since then, numerous genetic rodent models have been generated that differ regarding the type of mutation expressed, portion of the protein included in the transgene, promoter

employed, and level of expression of mHTT (Li et al. 2005). These models express either a truncated or full-length form of the mutant *HTT* gene, inserted either randomly in the rodent genome (transgenic models), or carry expanded CAG repeats contained within the native murine *HTT* gene (knock-in models) (Table 1) (Ramaswamy et al. 2007). Knockout models are not good models of HD because nullizygous animals die during embryonic development, but they have demonstrated that HTT plays a crucial role during embryogenesis (Menalled, 2005).

Genetic mouse models of Huntington's disease (HD)							
Transgenic mouse models of Huntington's disease (HD)							
Mouse model	**Construct**	**Promoter**	**CAG repeats**	**Age at death**	**Earliest abnormal behaviour**	**Nuclear inclusions**	**References**
R6/1	Exon 1 fragment of the human *HTT* gene	Human *HTT* promoter	115	40 weeks	15-21 weeks of age	5 months of age	Mangiarini et al. 1996 Menalled and Chesselet, 2002
R6/2	Exon 1 fragment of the human *HTT* gene	Human *HTT* promoter	150	10-13 weeks	5-6 weeks of age	4 weeks of age	Mangiarini et al. 1996 Menalled and Chesselet, 2002
YAC72	Full-length form of the human *HTT* gene	Human *HTT* promoter	72	Not reported (> 12 months)	7 months of age	Extremely rare	Hodgson et al. 1999 Menalled and Chesselet, 2002
YAC128	Full-length form of the human *HTT* gene	Human *HTT* promoter	128		3 months of age	15 months of age	Hodgson et al. 1999 Bayram-Weston et al. 2012
BACHD	Full-length form of the human *HTT* gene	Human *HTT* promoter	97		2 months of age	Extremely rare	Gray et al. 2008
Knock-in mouse models of Huntington's disease (HD)							
Mouse model	**Construct**	**Promoter**	**CAG repeats**	**Age at death**	**Earliest abnormal behaviour**	**Nuclear inclusions**	**References**
Hdh94	Exon 1 fragment of the human *HTT* gene	Mouse *HTT* promoter	94	Not reported (> 12 months)	2 months of age	6 months of age	Menalled et al. 2002 Menalled et al. 2003
Hdh140	Exon 1 fragment of the human *HTT* gene	Mouse *HTT* promoter	140		1 months of age	1 months of age	Menalled et al. 2003

Table 1: Commonly used genetic mouse models of HD

Transgenic Mouse Models of HD

Transgenic Mouse Models Expressing Truncated Form of The Human *HTT* Gene

The R6/1 and R6/2 transgenic mice were the first transgenic mouse models developed. They both express exon 1 fragment of the human *HTT* gene with around 115 and 150 CAG repeats respectively (Mangiarini et al. 1996). The truncated mutant *HTT* gene is randomly inserted into the mouse genome, and the resulting mouse expresses the mutant gene copies, in addition to its endogenous wild-type copies. The human *HTT* promoter drives the transgene expression in these mice, and the resulting mutant gene is expressed in all cells of the mouse and at 31% and 75% of the wild-type gene level in the R6/1 and R6/2 models respectively (Mangiarini et al. 1996).

The R6 mouse models, and in particular the R6/2 line offer many advantages that make them a popular choice and the most widely used in therapeutic trials. They manifest a very aggressive, rapidly progressing form of HD, with signs of motor deficits as early as 5-6 weeks of age, nuclear inclusions of mHTT at 4 weeks, reduced brain (44%) and striatal (41%) volume at 12 weeks, and death at approximately 10-13 weeks of age (Davies et al. 1997; Menalled and Chesselet, 2002). The R6/1 line presents with phenotypic alterations that are similar to the R6/2, but in a more protracted form, and death could be delayed to 40 weeks of age (Mangiarini et al. 1996).

The R6 transgenic mouse models are not without limitations. First, since the mutant *HTT* gene is randomly inserted in the mouse genome of these lines, there could be interference with the normal functions of other genes not related to HD. Second, as these mice contain multiple copies of the *HTT* gene, some researchers believe that they may not be representative of the genetics of the disease as it appears in humans, who usually have only one normal allele and one mutant allele of this gene (Ramaswamy et al. 2007). Third, the transgene expression in these mice is driven by human promoter and not by their endogenous promoter, and this may lead to a phenotype that does not correctly mimic the disease. For instance, loss of striatal neurons, which is widely reported in HD patients, is minimal in the R6 lines, and appears evident only at a very late stage of the disease, after the appearance of behavioural symptoms (Davies et al. 1997).

Transgenic Mouse Models Expressing Full-length Form of The Human *HTT* Gene

Hayden and colleagues created another transgenic mouse model in 1999, using a yeast artificial chromosome (YAC) vector system to express a full-length form of the human *HTT* gene under the control of the human *HTT* promoter (Hodgson et al. 1999). The resulting mutant gene is expressed in all cells of the mouse and at 30-50% of the wild-type gene level (Menalled and Chesselet, 2002). YAC mice contain either 72 or 128 CAG repeats. YAC72 mice display abnormal behaviour around 7 months of age, with preferential loss of lateral striatal neurons at 12 months, while those with 128 CAG repeats display earlier and more severe manifestations (Slow et al. 2003). YAC128 mice exhibit hyperkinesia and increased open-field activity at 3 months of age, but then begin to show signs of hypokinesia at 6 months, and by 12 months, open-field activity diminishes significantly compared with controls (Slow et al. 2003). In addition, at 48 weeks of age, these mice show reduced striatal

(10–15%) and cortical (7–9%) volume, and reduced striatal (9.1%) and cortical (8.3%) neuron number. An attractive feature of the YAC lines compared to the R6 lines is that the neuronal loss they present is limited to striatum; also since YAC mice live much longer than their R6 counterparts, this mouse model is a favourite candidate for long-term therapeutic studies (Ramaswamy et al. 2007). Presence of nuclear inclusions of mHTT is extremely rare in these mice (Menalled and Chesselet, 2002).

A more recently transgenic mouse model was created in the laboratory of William Yang in 2008, using a bacterial artificial chromosome (BAC) vector system to express a full-length form of the human *HTT* gene, with 97 CAG repeats, under the control of the human *HTT* promoter (Gray et al. 2008). BACHD mice exhibit progressive motor deficits starting from 2 months of age, and these symptoms become robust and more severe by 6 months of age. These mice also show neuronal synaptic dysfunction, and late-onset selective neuropathology, which includes significant cortical and striatal atrophy and striatal dark neuron degeneration. Unlike R6/2 mouse model and consistent with YAC mouse model, BACHD mice do not show early and diffuse nuclear inclusions of mHTT (Gray et al. 2008). By 12 months of age, BACHD brains have only a few small inclusions predominantly in the cortical neuropils, in addition to very tiny inclusions in the striatum. This interesting finding suggests that the pathogenetic process in these mice can occur without early and diffuse nuclear accumulation of aggregated mHTT.

Both YAC and BAC mice display normal life span, and premature death has not been reported in any of these transgenic models (Zuccato et al. 2010).

Knock-in Mouse Models of HD

Knock-in mouse models carry expanded CAG repeats contained within the native murine *HTT* gene, and they are considered the most accurate representative for HD from a genetic standpoint, because they carry the mutation in its appropriate genomic and protein context. These models may contain either expanded CAG repeats within an unmodified mouse gene, or a chimeric mouse/human exon 1 carrying the expanded CAG repeats region and the human polyproline region (Menalled et al. 2012). Initial results with knock-in mouse models were disappointing as the first line generated termed HdhQ70-80, with 70-80 CAG repeats, had normal life-span and did not show the classical HD motor deficits (Shelbourne et al. 1999).

However, sensitive and careful testing of knock-in mice with longer CAG repeats revealed that subtle behavioural abnormalities were present as early as 1-2 months of age (Menalled et al. 2000).

HdhQ94 is a chimeric knock-in mouse model of HD with 94 CAG repeats (Levine et al. 1999). These mice displayed a biphasic motor phenotype, starting with increased motor activity at 2 months, followed by hypoactivity at 4 months. Nuclear staining and microaggregates of mHTT in HdhQ94 mouse model were restricted to the striatum, and appeared consistently at 6 months. However, no nuclear inclusions were found in the cerebral cortex (Menalled and Chesselet, 2002).

In an attempt both to confirm the relationship between CAG repeats length and age of onset characteristic of polyglutamine expansions disease, and to provide a model with a faster onset of abnormal behaviour for drug testing; Scott Zeitlin's group created HdhQ140 knock-in mouse model (Menalled et al. 2003). These mice express chimeric mouse/human exon 1 containing 140 CAG repeats inserted in the murine *HTT* gene. Impairment in locomotor activity as seen using open field test is observed in HdhQ140 mouse model as early as 1 months of age (Menalled et al. 2003), which is around the time when abnormalities were detected in R6/2 mice (Luesse et al. 2001), and much earlier when abnormalities were observed in YAC128 mice (Slow et al. 2003). In addition, at 12 months of age HdhQ140 mice display a more apparent motor dysfunction as measured by a decrease in stride length similar to what is characterized in HD patients (Menalled et al. 2003). Moreover, nuclear inclusions and staining of mHTT are observed in these mice at 4 month of age, particularly in the striatum. Later as the animal aged, the size and number of nuclear inclusions and the intensity of nuclear staining are increased in the striatum, and also start to be detected in the olfactory system, cerebral cortex, hippocampus, and cerebellum (Menalled et al. 2003). Like YAC128 mice though, HdhQ140 mice display normal life span. Because of their early behavioural anomalies and regionally specific pathology, HdhQ140 knock-in mouse model provide a powerful tool with which to evaluate the effectiveness of novel therapies and to study the mechanisms involved in the neuropathology of HD.

C. Invertebrate Models of HD

Invertebrate models of HD like Drosophila melanogaster and Caenorhabditis elegans offer the potential of using powerful genetic techniques to search for genetic factors that enhance or suppress an experimentally induced phenotype (Margolis and Ross, 2003). The Drosophila model expresses the expanded CAG repeats in the eye of the fly, resulting in subsequent degeneration of its photoreceptors (Jackson et al. 1996). The Caenorhabditis model expresses the expanded CAG repeats in the nervous system of the worm, resulting in overall decreased motility (Brignull et al. 2006). Invertebrates have short life span, which makes it easy to generate large numbers of animals, but research to develop novel therapeutic strategies for HD ultimately requires animal models with more complexity (Ramaswamy et al. 2007).

1.2 Alzheimer's Disease (AD)

AD is an age-related neurodegenerative disease, and it is the most common cause of dementia worldwide, characterized by extracellular depositions of amyloid-β (Aβ) plaques, intracellular aggregates of neurofibrillary tangles, and neuronal loss, and manifested clinically by memory loss and progressive decline of cognitive functions.

1.2.1 History

The story of AD begins at the beginning of the 20th century when a 51-year-old woman, Auguste D, was admitted to the Frankfurt State Asylum where she was examined by a young psychiatrist, Alois Alzheimer, who was interested in her case until her death in Frankfurt on April 8, 1906 (Figure 5). He reported the patient findings at a conference in Tubingen on November 3, 1906 under the title "On a peculiar disease process of the cerebral cortex" (Alzheimer, 1907). Alzheimer discussed Auguste D's case and mentioned she had a striking cluster of symptoms that included severely impaired memory, aphasia, erratic behaviour, paranoia, and auditory hallucinations. Moreover, on post-mortem examination, he found argyrophilic plaques, tangles and atherosclerotic changes in the brain.



Figure 5: Alois Alzheimer and his patient Auguste D

Unfortunately, Alzheimer notes were lost for almost a century but were discovered in the basement of the University of Munich by Konard Maurer who published Auguste D photograph and handwritten notes of Alzheimer on Auguste D's case in the journal The Lancet (Maurer et al. 1997). The slides prepared from Auguste D brain on which Alzheimer had based his diagnosis were also discovered later and a team of scientists succeeded in extracting DNA from these samples and found that Auguste D did not carry the e4 allele of the apolipoprotein E gene which made her at risk for developing early onset disease (Graeber et al. 1998).

1.2.2 Epidemiology

Aging has become a worldwide universal phenomenon, and recent reports from the UN Aging Program and the US Centers for Disease Control and Prevention have estimated that the number of older people aged 65+ years in the world is expected to increase from 420 million in 2000 to nearly 1 billion by 2030 (Kalaria et al. 2008). Since occurrence of AD is strongly associated with increasing age, hence it would be expected that AD cases are constantly increasing which would pose substantial burden on caregivers. It has been estimated that 25 – 30 million people worldwide currently suffer from AD and these cases will approximately triplicate by 2040 (Ferri et al. 2005). AD is the most common cause of dementia accounting for up to 75% of all dementia cases, and caring for late onset dementia patients in UK are estimated to cost over £17 billion per year (Dementia UK, the full report 2007). Early-onset familial AD is often caused by autosomal dominant mutations, and accounts for only about 2% of all AD patients, while the majority of AD cases are sporadic,

and present considerable heterogeneity in terms of risk factor profiles (Blennow et al. 2006).

1.2.3 Clinical Findings

Clinical findings in AD patients follow three distinct phases, the forgetfulness phase, the confusional phase and the dementia phase (Schneck, Reisberg and Ferris, 1982). These manifestations reflect the accumulation of the extracellular amyloid plaques and the intracellular neurofibrillary tangles in the hippocampus, amygdala, basal forebrain, and the cerebral cortex, with consequent synaptic loss and axon degeneration in these brain areas.

In the first phase, the forgetfulness phase, there is usually poor short-term memory, tendency to forget where objects have been placed, and difficulty in recalling names of familiar people and places (Mohanaruban, Sastry and Finucane, 1989; Greene, Hodges and Baddeley, 1995; Goldblum, et al. 1998). Sufferers maybe unable to concentrate on tasks, and there is significant lack of curiosity, in addition to some emotional changes such as anxiety and irritability (Goudie, 1993; Thompson, 1997).

In the second phase, the confusional phase, memory, both short-term and long-term deteriorate, with decline in generalized intellectual performance, changes to speech for example inability to find a word, and difficulty in performing complex tasks with complete loss of social independence skills (Reisberg, 1983; Goldblum, et al. 1998). Lack of interest in social life follows quickly and can be extremely distressing to family and friends (Thompson, 1997).

In the third phase, the dementia phase, memory deteriorates further, and sufferers become highly dependent on the others for self-care skills such as dressing, toileting and feeding (Thompson, 1997). In the late stages, AD patients become bedridden and typically acquire comorbidities such as pneumonia and decubitus ulcers.

1.2.4 Pathogenesis and Neuropathology

AD is an irreversible progressive neurodegenerative disease that predominantly affects cerebral cortex and hippocampus, which loose mass and shrink (atrophy) as the disease advances. Progressive atrophy of the frontal, parietal, and temporal cortical lobes is the main

gross anatomical correlate of AD, with relative sparing of occipital, and primary motor and sensory regions (Minati et al. 2009). Atrophy of the hippocampus is significant and can extend to the amygdala. Enlargement of the ventricles, particularly the temporal horns are also one of the unique neuropathological changes observed in the AD brain (Figure 6) (Mott and Hulette, 2005).

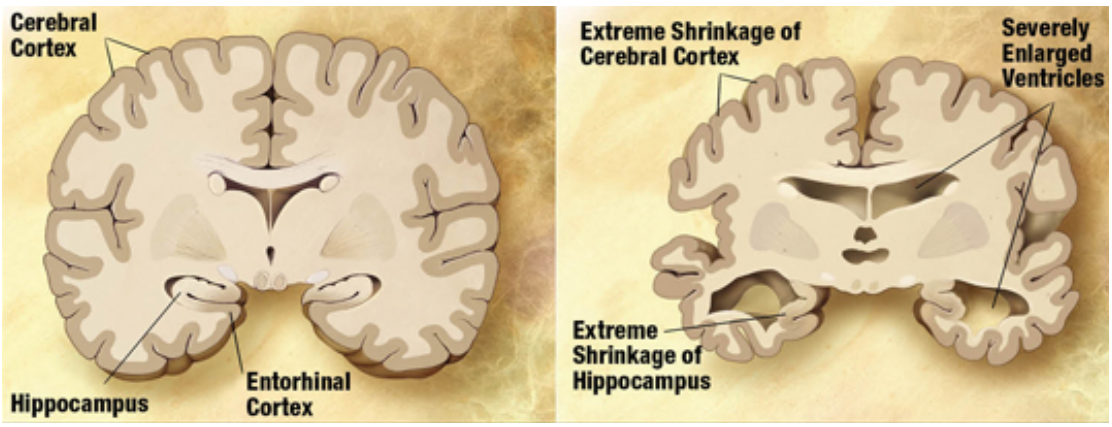


Figure 6: AD brain (right side) and normal brain (left side)

Amyloid-Beta, Amyloid Plaques, and The Amyloid Cascade

As previously described by Alois Alzheimer himself more than a century ago, the presence of extracellular amyloid plaques of which Aβ – a peptide formed by enzymatic cleavage of the transmembrane protein amyloid precursor protein (APP) – is one of the key histopathological hallmarks of the AD brain (Alzheimer, 1907).

Diffuse plaques, commonly referred to as preamyloid deposits, represent an early stage in the formation of senile plaques, they are much less dense and consist of nonfibrillary forms of Aβ (Tagliavino et al. 1988). Senile plaques represent a mature form of neuritic plaques. They have a diameter ranging between 10 and 160 μm, and appear as radiating bundles of amyloid with or without a dense central core (Mott and Hulette, 2005).

It is believed that Aβ is a critical factor in the pathogenesis of AD, both in familial and sporadic forms, and its accumulation is an early event leading to neurodegeneration. APP is a transmembrane protein that can undergo a series of proteolytic cleavage by secretase enzymes α-secretase and β-secretase (also called β-site amyloid precursor protein cleaving enzyme (BACE)), releasing soluble extracellular fragments α-sAPP and β-sAPP respectively

(Minati et al. 2009) (Figure 7). Cleavage by β-secretase takes place at the N-terminus of the Aβ sequence, and this leaves the Aβ region attached to the C-terminus fragment (β-CTF), while cleavage by α-secretase takes place within the Aβ region and thus prevents the release of the full-length Aβ peptide (α-CTF) (Minati et al. 2009). γ-secretase, another enzyme complex in the amyloid cascade, composed of presenilin 1 and 2 (PS1 and PS2), subsequently cleaves α-CTF and β-CTF releasing, respectively, either a harmless p3 fragment or multiple isoforms of Aβ peptide (Nathalie and Jean-Noel, 2008). The most predominant form of this peptide is 40 residues in length ($A\beta_{1\text{-}40}$), whereas a small proportion (approximately 10%) is the 42 residue variant ($A\beta_{1\text{-}42}$) (Citron, 2010). $A\beta_{1\text{-}42}$ is significantly more prone to aggregate into oligomers, a process called oligomerization, forming larger insoluble fibrils that subsequently develop into mature senile plaques, and hence it is considered more neurotoxic than $A\beta_{1\text{-}40}$, and deposition of these plaques around cerebral neurons are confirmed to be the major cause of neurodegeneration associated with AD (Citron, 2010).

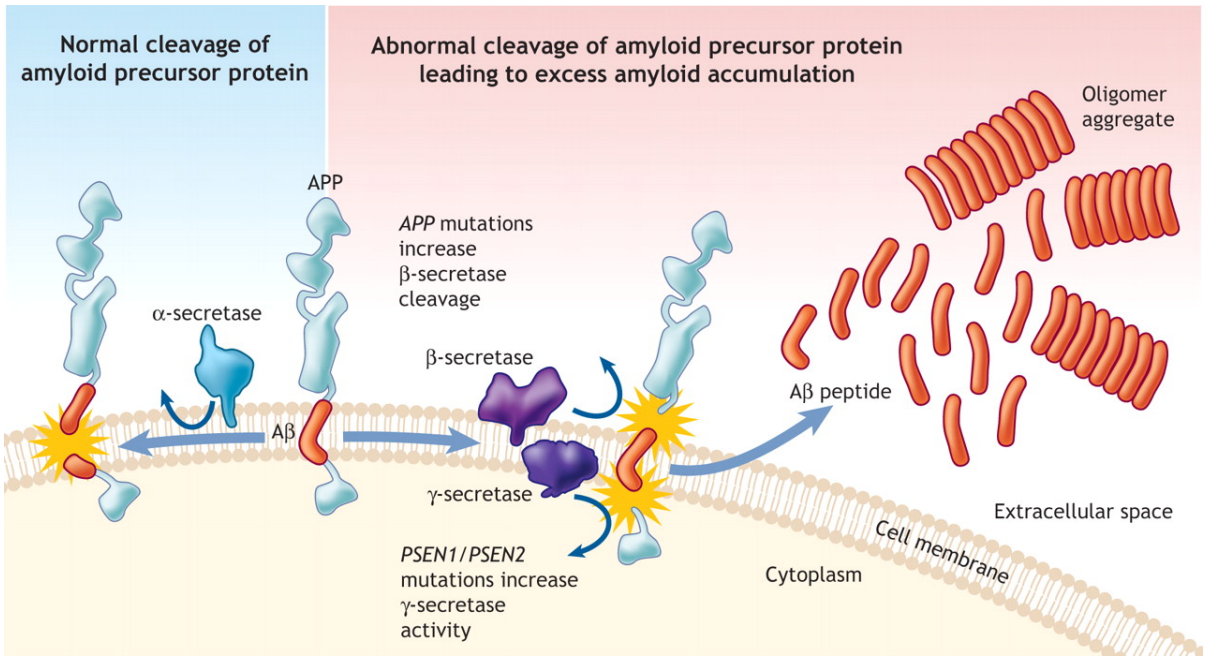


Figure 7: The amyloid cascade pathway (Patterson et al. 2008). Cleavage of the transmembrane protein APP takes place through competing α-secretase and β-secretase. Cleavage by α-secretase takes place within the Aβ region and thus prevents the release of the full-length Aβ peptide. Cleavage by β-secretase takes place at the N-terminus of the Aβ region, and subsequent cleavage by γ-secretase result in the release of Aβ peptide

Mutation in three genes - *APP, PS1 and PS2* – is known to shift the balance in the amyloid cascade in favour of the amyloidogenic pathway, and the commonality of these mutations is they all end up in the production of more amyloidogenic Aβ ($A\beta_{1-42}$), and manifest in early-onset AD pathogenesis (St George-Hyslop and Petit, 2005). One commonly studied mutation in *APP* gene is known as the Swedish mutation (APP_{swe}), in which a double amino-acid change leads to increased cleavage by β-secretase, and subsequently more β-CTF and Aβ produced (Haass et al. 1995). Mutation in *PS1* gene and its homolog *PS2* cause shift in $A\beta_{1-40}$:$A\beta_{1-42}$ ratio, and so more amyloidogenic $A\beta_{1-42}$ will be produced, leading to early-onset AD (Guo et al. 1999; Jankowsky et al. 2004).

Neurofibrillary Tangles

Another histopathological hallmark of the AD brain is development of neurofibrillary tangles, a flame-shaped, helical deposits of the hyperphosphorylated axonal proteins tau, which are integral components of microtubules, and they play an important role in maintaining the structure and stability of neurons as well as participating in essential neurons functions, such as axonal transport (Alzheimer, 1907; Goedert, 1993; Braak et al. 1994; Goedert et al. 2006). Under normal conditions, phosphorylation of tau proteins is at 5 epitopes. In AD, Aβ plaques deposition results in altered ionic homeostasis that consequently shift the balance between phosphorylating protein kinases and dephosphorylating protein phosphatases toward more tau proteins phosphorylation (at up to 21 epitopes) (Noble et al. 2003; Goedert et al. 2006). As a result, there will be tau protein hyperphosphorylation, release of tau from microtubules and their consequent accumulation in the perykaria and dendrites, polymerization and tangle formation, and finally synaptic dysfunctions and axon degeneration (Brion, 1998; Sorrentino and Bonavita, 2007).

1.2.5 Models of Alzheimer's Disease (AD)

Animal models of AD have been created to recapitulate the major neuropathological hallmarks of this neurodegenerative disease in order to understand the pathological mechanisms that occur as the disease progress and also to investigate the effectiveness of potential novel medicines (Wenk and Olton, 1987; Wenk and Olton, 1989). The ideal model of AD would develop the full range of AD features, both pathological, biochemical and

behavioural, including cognitive deficits, amyloid plaques, neurofibrillary tangles, in addition to synaptic, axonal and neuronal loss and neurodegeneration. However, it is important to emphasise that there is no existing AD model that exhibits all these features, and all the lines that have been created display some but not all AD phenotypes to varying degrees and in different combinations.

Numerous knockout mouse models have been created to investigate a particular aspect of AD which is suppression of genes that encode proteins involved in the pathogenesis of this neurodegenerative disease, in particular *APP* gene that encode β-secretase (BACE), and *PS1 and PS2* genes that encode γ-secretase (Shen et al. 1997; Herreman et al. 1999; Luo et al. 2001).

Although BACE had no clear physiological functions, BACE knockout mice were perfectly viable with no obvious defects and they no longer produced any Aβ (Luo et al. 2001; Roberds et al. 2001). However, later studies revealed that these mice showed significantly reduced level of myelination and myelin thickness (Hu et al. 2006; Willem et al. 2006), suggesting a vital role of this enzyme in the development of the nervous system.

PS (both *PS1 and PS2*) knockout mice developed severe neurodegeneration of cerebral cortex and impairment of memory and synaptic function (Shen et al. 1997; Saura et al. 2004), which highlighted that the encoded protein of these genes, γ-secretase, has several other functions besides cleaving β-CTF and releasing Aβ peptide, including cleavage of other γ-secretase substrates, neurogenesis, cell adhesion, synapse formation, calcium homeostasis, and apoptosis (Thinakaran and Parent, 2004).

The first attempt to generate transgenic mouse models of AD, which are the oldest and the most widely used models of this neurodegenerative disease, counted only on overexpression of the entire sequence of human APP in the brain (Quon et al. 1991; Yamaguchi et al. 1991; Buxbaum et al. 1993; Lamb et al. 1993; Moran et al. 1995). Despite the successful expression of APP transgene in these mouse brains, neuropathology was very limited and in the majority of cases there was no amyloid deposit. This could be attributed to the absence of a disease-causing mutation in the transgene, to the genetic background of mice, or to other unknown factors inherent to the mouse brain compared to human (Saraceno et al. 2013).

The next transgenic mouse models generated did not take in consideration overexpression of human APP only, but also that this protein must be mutated for the production of high levels of Aβ, and as a result these mice developed age-dependent AD-like pathology including amyloid deposit (Table 2) (Games et al. 1995; Hsiao et al. 1996; Andra et al. 1996; Chishti et al. 2001). However, these transgenic mice are not without limitations. They do not develop extensive neuronal loss like human AD patients, and this could be attributed to the amount of time needed to develop this characteristic neuropathological feature. While AD progresses over decades of human life, transgenic mice are maintained only for 2 years (Saraceno et al. 2013).

Genetic mouse models of Alzheimer's disease (AD)				
Transgenic mouse models of Alzheimer's disease (AD) expressing mutant form of the human *APP* gene				
Mouse model	**Construct**	**Promoter**	**Pathological and Behavioural Abnormalities**	**References**
PDAPP	Human *APP* gene with "Indiana" mutation	Platelet-derived growth factor-β	• At 3 months: Hippocampal atrophy • At 6-9 months: Deposition of Aβ plaques in hippocampus, and cerebral cortex • At 18 months: Microgliosis, synaptic alternations and behavioural deficits	Games et al. 1995; Dodart et al. 1999; Irizarrry et al. 1997a
Tg2576	Human *APP* gene with "Swedish" double mutation	Hamster prion protein	• At 2-9 months: Elevated Aβ level, in particular the amyloidogenic $Aβ_{1-42/43}$ • At 11-13 months: Deposition of Aβ plaques in cortex, hippocampus, and cerebellum • At 9-10 months: Signs of memory deficits as evident by Y-maze and Morris water maze	Hsiao et al. 1996
CRND8Tg	Human *APP* gene with both "Indiana" and "Swedish" mutations	Syrian hamster prion protein	• At 3 months: Deposition of Aβ plaques • At 6 months: 3,200-4,600 pmol of $Aβ_{1-42}$/gm brain, with an excess of $Aβ_{1-42}$ over $Aβ_{1-40}$ • At 3 months: Signs of memory deficits as evident by Morris water maze	Chishti et al. 2001
Double transgenic mouse models of Alzheimer's disease (AD) expressing mutant form of the human *APP* gene and mutant form of the human *Presenilin* (*PS*) gene				
Mouse model	**Construct**	**Promoter**	**Pathological and Behavioural Abnormalities**	**References**
PSAPP	Human *APP* gene with "Swedish" double mutation, and *PS* gene with M146L mutation	Platelet-derived growth factor-β	• At 8-10 weeks: Deposition of Aβ plaques in cerebral cortex and hippocampus, with selective 41% increase in $Aβ_{1-42}$/43, in addition to reduced spontaneous alternation performance as evident by Y maze before substantial Aβ deposition was apparent	Holcomb et al. 1998
TASTPM	Human *APP* gene with "Swedish" double mutation, and *PS* gene with M146V mutation	Thy-1	• At 3 months: Deposition of Aβ plaques, which increase with age, and were greater in females than in males at all ages investigated • At 6, 8 and 10 months: Signs of cognitive deficits as evident by object recognition test	Howlett et al. 2004
APP_{swe}/ PS1dE9	Chimeric human/mouse *APP* gene with "Swedish" double mutation, and *PS1* gene with deletion at exon 9	Mouse prion protein	• At 4-6 months: Deposition of Aβ plaques, with a progressive increase in plaques number up to 12 months, and a similar increase in Aβ levels • At 6 months: Astrocytosis with severe gliosis especially in the vicinity of Aβ plaques • At 15 months: Extensive staining throughout the cortex for glial fibrillary acidic protein, the main astrocytic intermediate filament • At 18 months: Higher Aβ with significant decrease in cholinergic markers (cortex and hippocampus) and somatostatin levels (cortex), in addition to impairment of the cognitive tasks measured in Morris water maze	Borchelt et al. 1997; Jankowsky et al. 2001; Garcia-Alloza et al. 2006; Jankowsky et al. 2004; Savonenko et al. 2005; Kamphuis et al. 2012

Table 2: Commonly used genetic mouse models of AD

More than 20 autosomal dominant *APP* mutations linked to AD had been characterized, and the commonality of these mutations is they all enhance the production and/or aggregation of Aβ. Of these, only few have been used to generate transgenic mouse models of AD, and they are named according to the geographic location from which the affected family originated. K670D/M671L double mutation at the β-secretase cleavage site, originally found in a Swedish family, results in increased β-secretase cleavage activity, and subsequently more Aβ produced, both $Aβ_{1-40}$ and $Aβ_{1-42}$ (Citron et al. 1992; Mullan et al. 1992; Suzuki et al. 1994).

V7171 “London” mutation (Goate et al. 1991), V717F “Indiana” mutation (Murrell et al. 1991), and other mutations at the γ-secretase cleavage site shift the balance in $A\beta_{1-40}$:$A\beta_{1-42}$ ratio, and so more amyloidogenic $A\beta_{42}$ produced, leading to early-onset AD. Mutations within the Aβ sequence, such as E693G “Artic” mutation (Nilsberth et al. 2001), increase fibrillogenesis or resistance to proteolysis. In addition to the aforementioned *APP* point mutations, increases for example duplications in the *APP* gene copy number can result in early-onset AD (Cabrejo et al. 2006), and this explain why patients with Down Syndrome who have extra copy of chromosome 21, the site of the *APP* gene, and therefore have three copies of this gene, develop AD very early, usually in their 40s (Heston, 1984). Thus, mice overexpressing the wild-type human *APP* gene, even without mutation, may serve as useful models for AD (Hall and Robrson, 2012).

PS mutations, in particular *PS1* mutation, another common autosomal dominant mutation linked to AD, have been used also to generate transgenic mouse models of AD (Borchelt et al. 1996; Duff et al. 1996; Citron et al. 1997; Chui et a. 1999; Dewachter et al. 2000). Despite the increased production of Aβ in these mice, they fail to develop significant AD-like pathology, and this could be due to the sequence differences between mouse and human APP/Aβ (Selkoe, 1989). Mouse APP differs from human APP by 17 amino acids, 3 of which are within the Aβ region (Hall and Robrson, 2012). The β-secretase enzyme BACE generates Aβ by cleavage at either Asp^{1} (β-site) or Glu^{11} (β`-site), ultimately leading to the production of full-length $A\beta_{1-40/42}$ or truncated $A\beta_{11-40/42}$ (Huse et al. 2002). While mouse BACE cleaves human APP to produce $A\beta_{1-40/42}$, this enzyme is more likely to cleave mouse APP to form the truncated $A\beta_{11-40/42}$, which is less amyloidogenic and also cause not that efficient aggregation (Cai et al. 2001; Huse et al. 2002). The hypothesis that mice transgenic for *PS* mutations only are unable to develop AD-like pathology was confirmed by crossing them with mice transgenic for either human or mouse APP (Hall and Robrson, 2012). While *PS* mutant mice crossed with a mouse line overexpressing mouse APP have no AD pathology (Jankowsky et al. 2007), the same mutant mice crossed with a mouse line overexpressing human APP develop extensive amyloid deposit and cognitive deficits (Savonenko et al. 2005). Thus expression of human APP appears to be essential for the development of AD phenotype in mice.

Transgenic Mouse Models of AD Expressing Mutant Form of The Human *APP* Gene

The PDAPP model was the first transgenic mouse model of AD developed that successfully recapitulated several neuropathological features characteristic of AD (Games et al. 1995). These mice overexpress the human *APP* gene with V717F "Indiana" mutation under the control of platelet-derived growth factor beta (PDGF-β) promoter. At 3 months of age, these mice display significant hippocampal atrophy, and at 6-9 months of age, Aβ plaques start to deposit in the hippocampus, corpus callosum, and cerebral cortex, and the density of these plaques increases with age (Dodart et al. 1999). Although other AD-like pathology features had been characterized in 18-months old PDAPP mice, like microgliosis, synaptic alternations and behavioural deficits, neuronal loss was absent, and so this mouse model fail to meet all criteria of the neuropathology of human AD (Irizarrry et al. 1997a). The Tg2576 model was another transgenic mouse model of AD that showed age-dependent Aβ deposits formation and also age-related cognitive impairment (Hsiao et al. 1996). These mice overexpress the human *APP* gene with K670D/M671L"Swedish" double mutation under the control of hamster prion protein (PrP) promoter. At 2-8 months of age, these mice start to show elevated levels of Aβ, in particular the amyloidogenic $A\beta_{1\text{-}42/43}$, and this increased to 14-fold by 11-13 months of age, where Aβ started to deposit in frontal, temporal, and entorhinal cortex, hippocampus, presubiculum, subiculum, and cerebellum (Hsiao et al. 1996). At 9-10 months of age, Tg2576 mice demonstrate signs of memory deficits as evident by Y-maze and Morris water maze behavioural tests. As for PDAPP mice, Tg2576 mice also do not develop neuronal loss (Irizarrry et al. 1997a). Overexpressing the human *APP* gene with both the "Indiana" and "Swedish" mutation resulted in a more aggressive transgenic mouse model of AD, named the CRND8Tg model (Chishti et al. 2001). Transgene expression in these mice was driven under the control of Syrian hamster PrP promoter and as a result of this double mutation, these mice start to deposit thioflavine S-positive Aβ plaques as early as 3 months, with dense-cored plaques and neuritic pathology evident from 5 months of age. In addition, early deposition of Aβ in these mice was associated with an early impairment in acquisition and learning reversal in the reference memory version of the Morris water maze, present by 3 months of age (Chishti et al. 2001).

Double Transgenic Mouse Models of AD Expressing Mutant Form of The Human *APP* Gene and Mutant Form of The Human *Presenilin* (*PS*) Gene

To accelerate deposition of Aβ plaques in transgenic mouse models of AD, multiple *APP* and *PS* mutations were inserted in mice. While Tg2576 transgenic mice develop extracellular Aβ deposits by 9-12 months of age, crossing this line with M146L transgenic line, a *PS* mutant mice, under the control of PDGF promoter, resulted in a double transgenic progeny, the PSAPP model, that develop large numbers of fibrillar Aβ deposits in cerebral cortex and hippocampus around 8-10 weeks of age that is far earlier than their singly transgenic Tg2576 littermates (Holcomb et al. 1998). Furthermore, PSAPP mice show a selective 41% increase in $A\beta_{1\text{-}42/43}$ in their brains. Interestingly, both doubly and singly transgenic mice showed reduced spontaneous alternation performance in a Y maze before substantial Aβ deposition was apparent, and this suggests that some aspects of the behavioural phenotype in these mice may be related to an event that precedes plaques formation (Holcomb et al. 1998). The TASTPM is another double transgenic mouse model of AD that is created by crossing Tg2576 line with M146V transgenic line, a *PS* mutant mice, under the control of Thy-1 promoter (Howlett et al. 2008). At 3 months of age, TASTPM mice start to deposit Aβ, and these depositions increase with age, and were greater in females than in males at all ages investigated. While there was no evident cognitive impairment in these mice at 3-4 months of age, both male and female TASTPM mice exhibited similar significant cognitive impairment at 6, 8 and 10 months of age in the object recognition test, compared to wild-type littermates.

APP_{swe}/PS1dE9 Mouse Model

Transgenic lines made by crossing animals expressing mutant human *APP* to mutant *PS* allow for incremental increases in the amyloidogenic $A\beta_{1\text{-}42}$ and provide a potentially attractive model system in which to study AD progression and therapeutic modulation. Single mutation insertion is not the only strategy used to manipulate *PS1* gene, and *PS1* with deletion at exon 9 was co-expressed with chimeric human/mouse *APP* gene with the ”Swedish” double mutation to generate APP_{swe}/PS1dE9 line (Borchelt et al. 1997; Lee et al. 1997). The cDNA for PS1 with deletion at exon 9 was cloned into the MoPrP.Xho vector at the Xho I site between PrP exon 2 and 3, and this vector contains the mouse PrP promoter which directs the transgene expression predominantly to CNS neurons (Jankowsky et al. 2001). The cDNA for mouse *APP* humanized within the Aβ region and containing the

”Swedish” double mutation was similarly cloned into the MoPrP.Xho vector, and again under the control of mouse PrP promoter (Jankowsky et al. 2001). APP_{swe}/PS1dE9 transgenic mouse model was created by co-injection into pronuclei of the two transgene constructs with a single genomic insertion site, resulting in the two transgenes being transmitted as a single locus (Garcia-Alloza et al. 2006). At 4-6 months of age, APP_{swe}/PS1dE9 mice showed visible Aβ plaques deposition that is far earlier than their singly transgenic APP_{swe} littermates, with a progressive increase in plaques number up to 12 months, and a similar increase in Aβ levels (Jankowsky et al. 2004; Savonenko et al. 2005; Garcia-Alloza et al. 2006). However, at 6 months of age, transgenic mice expressing APP_{swe} and PS1dE9, alone and in combination were indistinguishable from their nontransgenic littermates in all cognitive parameters measured in a standard Morris water maze task, followed by assessment of episodic-like memory in repeated reversal and radial water maze tasks (Savonenko et al. 2005). Astrocytosis develops in parallel with Aβ plaques deposition in these mice, with severe gliosis starting around 6 months of age, especially in the vicinity of plaques (Kamphuis et al. 2012). The number of cells positive for glial fibrillary acidic protein (GFAP), the main astrocytic intermediate filament, progressively increases with age in this double transgenic model, with extensive staining throughout the cortex by 15 months (Kamphuis et al. 2012). APP_{swe}/PS1dE9 mice have a high incidence of spontaneous epileptic seizures, including generalized seizures, as detected by video-EEG (Minkeviciene et al. 2009). In two recording episodes at the onset of Aβ plaques deposition, at least one unprovoked seizure was detected in 65% of these mice, of which 46% had multiple seizures and 38% had a generalized seizure, and none of the wild-type mice had seizures (Minkeviciene et al. 2009). At 18 months of age, APP_{swe}/PS1dE9 mice showed higher amyloid burdens than their singly transgenic littermates with statistically significant but mild decrease in cholinergic markers (cortex and hippocampus) and somatostatin levels (cortex) (Savonenko et al. 2005). In addition, the performance of all the cognitive tasks in the 18 months old double transgenic mice was worse than that of mice from all other genotypes (Savonenko et al. 2005). The consistent and early onset of Aβ plaques deposition in APP_{swe}/PS1dE9 transgenic mice and the availability of these animals through a commercial source, confirms its utility for studying the biochemical and pathological mechanisms underlying AD pathogenesis, and also for assessing the efficacy of new AD therapeutic interventions.

1.3 Axon Degeneration and The Role of FK866

Axon degeneration is an early event in many neurodegenerative diseases including HD, AD, Parkinson's disease (Galvin et al. 1999), multiple sclerosis (Ferguson et al. 1997) and amyotrophic lateral sclerosis (Fischer and Glass, 2007), where it precedes cell body loss and correlates with symptom onset and progression (Conforti et al. 2014). There is currently no cure for these progressive, highly debilitating and unavoidably fatal age-associated conditions, which are increasingly prevalent in our society. As treatments based on the protection of neuronal cell bodies have shown to be largely ineffective, targeting axon degeneration could be a valid therapeutic alternative. Therefore, understanding the mechanisms by which axons are lost in each of these pathologies is the basis for effective treatments.

Neuritic dystrophies have been reported in post-mortem brain samples of patients affected by HD (Graveland et al. 1985; Ferrante et al. 1991), and they generally precede neurodegeneration (Li and Conforti, 2013). Fibre loss has been observed in post-mortem brain samples of pre-clinical HD patients (Reading et al. 2005) and in presymptomatic HD patients by longitudinal diffusion tensor imaging (Reading et al. 2005; Weaver et al. 2009). Neuritic abnormalities and fibre loss have also been observed in mouse models of HD, where neuronal loss is not present or it occurs at very late stages (Klapstein et al. 2001). Early axon degeneration in these models is associated with the presence of neuropil mHTT aggregates while its correlation with the deposition of the large neuronal intranuclear inclusions (NII) is less clear (Li et al. 2001). HTT has a role in axonal transport (DiFiglia et al. 1995; Block-Galarza et al. 1997; Gunawardena et al. 2003), and a perturbation of vesicular axonal transport is one way in which mHTT has been proposed to perturb axonal integrity (Gauthier et al. 2004; Colin et al. 2008; Zala et al. 2013). Moreover, mHTT causes tubulin deacetylation (Dompierre et al. 2007), and inhibits fast axonal transport (FAT) in models of HD by increasing the expression of axonal cJun N-terminal kinase 3 (JNK3) that in turn phosphorylates a residue in the kinesin-1 motor domain and reduces kinesin-1 binding to microtubules (Morfini et al. 2009). Large axonal swellings developing age-dependently first in stria terminalis and then in corticostriatal axons, in the absence of any abnormalities in other neuronal compartments, have been reported recently in the HdhQ140 knock-in mouse model of HD, supporting the concept that axonal dysfunction occurs at early stages (Marangoni et al. 2014).

Similarly, axon and synapse degeneration preceding cell body loss have been reported in post-mortem patients and models of AD. Synaptic dysfunctions are early events in AD and precede any other neuronal abnormalities (Selkoe, 2002). Defects in axonal transport are widely documented in AD (Pigino et al. 2003; Zhang et al. 2004; Stokin et al. 2005; Salehi et al. 2006; Lazarov et al. 2007), and can be directly caused by Aβ plaques deposition in proximity of axons (Adalbert et al. 2009), or by other toxic effects of Aβ, for example on mitochondrial function (Rui et al. 2006; Decker et al. 2010). Significant reduction in axonal transport rates as Aβ increases, even before plaques formation, was shown in Tg2576 transgenic mice, by manganese-enhanced magnetic resonance imaging (MEMRI) (Smith et al. 2007). Early axonal swellings and dystrophies have been observed in mouse models of AD (Adalbert et al. 2009; Crowe et al. 2013) in proximity of Aβ plaques, while axons appear still intact elsewhere and are connected to cell bodies which appear normal. This is important as it underlines a window of opportunity where restoring axonal function locally could in principle completely rescue neuronal function. Exposure of axonal terminals to $A\beta_{1-42}$ leads to an excessive release of the excitatory neurotransmitter glutamate and impairment of axonal transport (Hiruma et al. 2003; Molnar et al. 2004; Rosales-Corral et al. 2012), accompanied by axonal degeneration and damage to the neurons.

While these observations highlight axons and synapses as potential effective therapeutic targets in these disorders, how to delay the degeneration of these neuronal compartments has long remained elusive. Studying axon degeneration after injury – known as Wallerian degeneration (Waller A, 1850) – greatly enhanced our understanding on mechanisms leading to axon degeneration. The discovery of the Wallerian degeneration slow (Wld^S) spontaneous mutant mouse where Wallerian degeneration is delayed by 10-fold (Lunn et al. 1989; Conforti et al. 2000; Mack et al. 2001), have led to the identification of an active pro-axon death pathway initiated after an acute injury. The presence of an 85-kb tandem triplication in the mutant mouse (Coleman et al., 1998) leads to the formation of the chimeric gene encoding for the axon protective chimeric protein known as Wallerian degeneration slow (WLD^S) (Figure 8). WLD^S is a modified form of nuclear NAD-biosynthetic enzyme nicotinamide mononucleotide adenylyl transferase 1 (NMNAT1) with an N-terminal sequence that relocates this enzyme to cytoplasm and axons (Conforti et al. 2000; Mack et al. 2001).

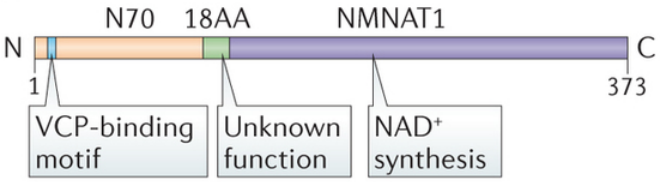


Figure 8: Structure-activity relationship of WLD^S (Conforti et al. 2014). WLD^S is a chimeric protein that results from a tandem triplication and encodes full-length NMNAT1 fused to 70 amino-terminal amino acids (N70) from the ubiquitin conjugation factor E4 B ligase (UBE4B). N70 does not contain UBE4B catalytic activity but retains a small motif within the N-terminal 16 amino acids that binds to the ubiquitous cytoplasmic protein valosin-containing protein (VCP), and its important for translocation of WLD^S to the cytoplasm and axoplasm.

In wild types, where WLD^S is not present, the endogenous labile axonal isoform NMNAT2 provides the essential enzymatic activity required for axon survival and growth (Gilley and Coleman, 2010; Gilley et al. 2013; Milde et al. 2013). Its rapid degradation after injury has been suggested to initiate axon degeneration. NMNAT2 maintains axons by scavenging its substrate nicotinamide mononucleotide (NMN), a nucleotide precursor of NAD, which triggers a rapid pathway of axon degeneration when its levels accumulate after acute injury, as a consequence of NMNAT2 depletion (Di Stefano et al. 2014). When WLD^S is present, due to its higher stability, it can substitute for NMNAT2, providing the enzymatic activity required for preserving axon integrity. Consistent with this model, blocking NMN synthesis with the drug FK866 (also known as APO866, WK175, or (E)-N-[4-(1-benzoylpiperidin-4-yl) butyl] acrylamide-3-(pyridine-3-yl), a highly potent and specific non-competitive low-molecular weight inhibitor of the NMN-synthesising enzyme nicotinamide phosphoribosyl transferase (NAMPT) (Hasmann and Schemainda, 2003) (Figure 9), strongly protects axons *in vitro, ex-vivo* and *in vivo* after acute injury (Di Stefano et al. 2014). WLD^S also shows a protective effect in some disease models, indicating shared mechanisms and translational potential (Conforti et al. 2014). In addition, FK866 also shows a remarkable neuroprotective effect in the vincristine model of chemotherapy-induced axon degeneration (Di Stefano et al. 2014), where axons are not physically separated from their cell bodies. However, the potential efficacy of FK866 in models of disease remains unexplored. The early axon pathology observed in models of HD and AD, where disruption of axonal transport might still isolate axons from their cell bodies, shares some features with axon degeneration after an acute injury (Conforti et al. 2014). Thus, the NAMPT inhibitor FK866 could also attenuate

axon pathology induced by mHTT and Aβ in *in vitro* and even in *in vivo* models of these neurodegenerative diseases.

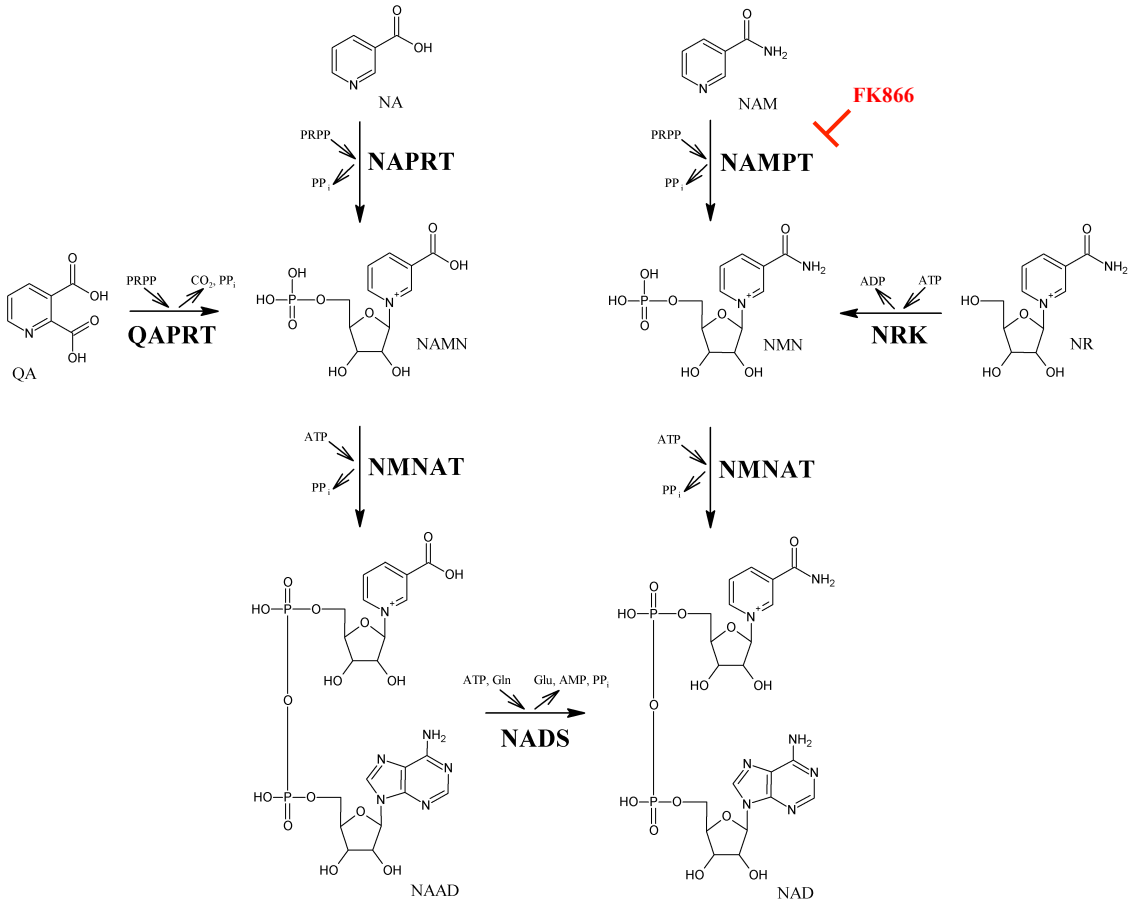


Figure 9: NAD biosynthetic pathway from nicotinamide (NAM) and nicotinic acid (NA) (Di Stefano et al. 2014). The enzymes involved are NAMPT, nicotinic acid phosphoribosyl transferase (NAPRT), NMNAT and nicotinamide adenine dinucleotide synthetase (NADS). The site of action of FK866, a highly specific inhibitor of NAMPT, is shown.

1.4 Memantine

1.4.1 History

Memantine (1-amino-3,5-dimethyl-adamantane) was first synthesized in 1963 by researchers at Eli Lilly in an attempt to prepare a blood glucose lowering agent (Gerzon et al. 1963), but it was completely devoid of such property. In the 1970s, memantine (code D140) was found

to have activity on the central nervous system, and this interesting finding opened the way for three researcher groups to start evaluating the biochemical, pharmacological, and pharmacokinetic properties of this compound, which later had been given the international non-proprietary name memantine (Parsons et al. 1999). In 1989, extensive preclinical research found that the most probable mechanism of action of memantine is via inhibiting the activity of NMDARs (Bormann, 1989; Kornhuber et al. 1989) with an IC_{50} of approximately 1 μM, which corresponds well with its therapeutic concentration range (Bresink et al. 1996). Since then, and based on these results, clinical research had focused mainly on the efficacy of memantine on cerebral ischemia and AD (Parsons et al. 1999). Nowadays, memantine is regarded as a novel therapeutic agent, and it is the first drug to be approved by the United States Food and Drug Administration for the treatment of moderate to severe AD, after its approval for the same indication in the European Union (Witt et al. 2004).

1.4.2 Pharmacology of NMDARs

Molecular Composition of NMDARs

NMDARs are heteromeric ligand-gated ion channels made up of different subunit families, NR1 (whose presence is mandatory), NR2A-D, (Dingledine et al. 1999), and in some neurons NR3A or 3B (Sasaki et al. 2002). NMDARs are unique among all neurotransmitter receptors in that their activation requires the simultaneous binding of two different agonists, glutamate at NR2 subunit, and glycine at NR1 subunit (Johnson and Kotermanski, 2006). Glutamate is the major excitatory neurotransmitter in the brain that is involved in almost every CNS function especially in cortical and hippocampal regions. The subtype of NR2 subunit that combines with NR1 subunit can influence the biophysical and pharmacologic characteristics of endogenous NMDARs, providing significant potential for functional diversity. During early postnatal development, many synaptic NMDARs are composed of NR1 and NR2B subunits, producing receptors with very long lasting synaptic currents. After the first few weeks of brain development, NR2B subunits start to be replaced gradually by NR2A ones, yielding receptors with shorter synaptic currents. Moreover, there is strong evidence that the majority of synapses in the adult brain preferentially express NR1-NR2A vs. NR1-NR2B NMDARs.

Alteration of NMDARs Functions in HD

Based on the probable involvement of NMDARs in the pathogenesis of HD (described previously), a great deal of interest had focused on whether functions of these receptors are altered in HD models. This hypothesis had been directly confirmed by assessing NMDARs-mediated currents with electrophysiological recordings (Fernandes and Raymond, 2009). Results of these assessments revealed significant enhancement of NMDARs-mediated currents in MSNs acutely dissociated from striata of presymptomatic and symptomatic R6/2 (Starling et al. 2005), YAC72 (Cepeda et al. 2010), HdhQ94 (Levine et al. 1999), and HdhQ100 (Laforet et al. 2001) mouse models of HD compared to slices from their wild-type counterparts. All these observations indicate that alterations in NMDARs activity is present prior to, and possibly plays a causative role in the behavioural changes associated with HD (Fernandes and Raymond, 2009). Further investigations have been performed to determine whether the mutant *HTT* gene selectively alter the functions of various NMDARs subunits. One of these studies used HEK293 cells overexpressing NR1/NR2A or NR1/NR2B NMDARs in conjunction with full-length form of the mutant *HTT* gene with 15 or 138 CAG repeat (Chen et al. 1999). Results of this study suggested that the mutant *HTT* gene might increase numbers of functional NR1/NR2B NMDARs compared to NR1/NR2A ones. Another study used the same cellular model confirmed these findings, and found that the mutant *HTT* gene selectively enhanced apoptotic cell death in HEK293 cells cotransfected with NR1/NR2B NMDARs compared to that in HEK293 cells cotransfected with NR1/NR2A NMDARs (Zeron et al. 2001). All these results indicate that the mutant *HTT* gene modulates the response of NR2B-containing NMDARs, and this is possibly implicated in the pathogenesis of HD (The NR2B-selective hypothesis) (Fernandes and Raymond, 2009). Actually this possibility is not surprising since the striatum (which is the most important part affected in HD), had been shown to express higher levels of NR2B subunits relative to other NR2 subunits, compared to other regions of the brain (Landwehrmeyer et al. 1995; Rigby et al. 1996).

Alteration of NMDARs Functions in AD

Disturbances in glutamate neurotransmission have been linked with the pathological mechanisms underlying AD (Hardy and Cowburn, 1987; Greenamyre and Young, 1989; Palmer and Gershon, 1990; Cacabelos et al. 1999; Francis, 2003; Wenk et al. 2006). Many

studies had linked neuronal dysfunction in AD and its consequent neurodegeneration to the increased sensitivity and/or activity of the glutamatergic NMDARs by various toxic factors such as Aβ plaques deposition, soluble Aβ oligomers, hyperphosphorylated tau protein in neurofibrillary tangles, and mitochondrial dysfunction (Gray and Patel, 1995; Wenk, 2006; Wenk et al. 2006; De Felice et al. 2007a; Parihar and Brewer, 2007). Aβ, both $A\beta_{1-40}$ and its amyloidogenic variant $A\beta_{1-42}$ has been shown to directly activate NMDARs, induce increases in intracellular Ca^{2+} level and a state of excitotoxctity, and consequently neurotoxicity in cultured neuroblastoma cells (Lee et al. 1995), and in HEK293 cells transiently expressing NR1/NR2A or NR1/NR2B NMDARs subunits (Domingues et al. 2007), an effect which is partially prevented with the NMDARs antagonist MK-801. Aβ effect on NMDARs may be secondary to the binding of this peptide to the postsynaptic proteins PSD95 and synaptophysin, with consequent down-regulation of these anchoring proteins, and indirect suppression of NR2A NMDARs subunits function but activation of NR2B NMDARs subunits function (Roselli et al. 2005; De Felice et al. 2007a; Lacor et al. 2007; Liu et al. 2010). All these ultimately induces a number of pro-death pathways, like the proteases caspase 3 and caspase 8 (Liu et al. 2010). This Aβ effect is blocked with the NMDARs antagonist MK-801 and also with the selective NR2B NMDARs subunit antagonist ifenprodil (Roselli et al. 2005). In addition to the aforementioned effects of Aβ seen *in vitro*, *in vivo* studies had also found that Aβ and in particular the amyloidogenic $A\beta_{1-42}$ potentiates NMDARs responses to 260%, an effect that is blocked by NMDARs antagonists (Molnar et al. 2004; Szegedi et al. 2005).

1.4.3 Pharmacology of Memantine

A variety of pharmacodynamic factors have been suggested as contributing to the improved tolerability of memantine among the many NMDARs antagonists that have been tested in human. Memantine is unique in that it binds only to open NMDARs; hence it is classified as an open channel blocker (Chen et al. 1992; Chen and Lipton, 1997). This pattern of antagonism increases the therapeutic efficacy of the drug, since more channels are open and available to be blocked during pathological conditions. Hence, memantine would be expected to treat patients with moderate-severe dementia involving excessive glutamate and NMDARs activity much more effectively than those with mild dementia involving only increased physiologic activity (Chen and Lipton, 2006). After blocking NMDARs, the channel can

close, glutamate can unbind, and memantine is trapped inside the receptor. However, unlike other trapping channel blockers like MK-801, ketamine, and phencyclidine, memantine has proposed to be trapped in some but not all NMDARs (Blanpied et al. 1997). This partial trapping phenomenon has been suggested to improve the clinical tolerability of the drug, based on the hypothesis that relief of channel block allows physiologic synaptic transmission to continue to a sufficient degree so as to avoid disrupting critical brain circuits function which require the integrity of NMDARs (Mealing et al. 2001; Rogawski and Wenk, 2003). Memantine has been considered a low-moderate affinity NMDARs antagonist, and this property increases the effective blocking rate of the drug since higher concentrations are required to exert the same degree of block. Another feature of memantine is the strong voltage dependency of NMDARs blockade, which allows the drug to exit the channel quickly under depolarized conditions, and this further maintain the normal synaptic activity (Muller et al. 1995). All these features in addition to multiple sites of block on NMDARs and multiple sites of action on targets other than NMDARs have been proposed as contributing to the unique clinical safety and efficacy of memantine.

1.4.4 Memantine and Huntington's Disease (HD)

There is a growing interest in the scientific community in evaluating the effect of memantine in cellular and mouse models of HD (Table 3).

Model	Memantine Dose	Memantine Effects	References
3-nitropropionic acid model	20 mg/kg/day i.p. for 5 days	1. Decreased striatal lesion volume, number of TUNEL+ cells, and Fluoro-Jade C+ degenerating neurons, 2. Decreased Bax level and huntingtin proteolytic fragments, 3. Increased Bcl-xl level.	Lee et al. 2006
3-nitropropionic acid model	20 mg/kg/day i.p. for 5 days	1. Restored motor function, & up-regulation of BDNF and GDNF expression, 2. Enhanced brain succinate dehydrogenase activity, 3. Decreased glutamate content, striatal loss, and GFAP immunoreactivity.	Ranju et al. 2015
YAC128 transgenic mouse model	1 mg/kg/day i.p. for 10 months	1. Blocked extrasynaptic (but not synaptic) NMDARs, 2. Ameliorated neuropathological and behavioural manifestations.	Okamoto et al. 2009
YAC128 transgenic mouse model	30 mg/kg/day i.p. for 10 months	1. Blocked both synaptic and extrasynaptic NMDARs, and worsened the outcome, 2. Decreased neuronal inclusions.	Okamoto et al. 2009
YAC128 transgenic mouse model	1 mg/kg/day i.p. for 2 months	1. Reversed the deficits in striatal nuclear CREB activity, 2. Improved rotarod performance.	Milnerwood et al. 2010

Table 3: Memantine and HD

Lee et al. 2006 investigated the neuroprotective effect of memantine in 3-nitropropionic acid-induced striatal degeneration model of HD. Either memantine (20 mg/kg/day) or phosphate buffered saline (PBS) was intraperitoneally administered for five days. In the memantine-

treated group, the striatal lesion volume, the number of TUNEL+ cells, and Fluoro-Jade C+ degenerating neurons were all decreased (Lee et al. 2006). In addition, memantine increased Bcl-xl level, decreased Bax level and huntingtin proteolytic fragments, and exerted an inhibitory effect on the micro-calpain level (Lee et al. 2006). Based on the probable involvement of extrasynaptic NMDARs in the pathogenetic mechanisms of HD, a great deal of interest has focused on whether low micromolar concentrations of memantine could preferentially inhibit the function of these receptors, while relatively preserve synaptic NMDARs whose function is essential for activating cell survival pathway. Okamoto et al. 2009 found that 10 months treatment of low-dose memantine (1 mg/kg body weight) blocked extrasynaptic (but not synaptic) NMDARs and ameliorated neuropathological and behavioural manifestations in 12-month old YAC128 mice. In contrast, high-dose memantine (30 mg/kg body weight) blocked both synaptic and extrasynaptic NMDARs, decreased neuronal inclusions, and worsened the outcomes of these mice. Milnerwood et al. 2010 confirmed these findings using the same genetic mouse model of HD, and found that 2 months treatment of low-dose memantine (1 mg/kg body weight) reversed the deficits in nuclear CREB activity in the striatum of 4-month old YAC128 mice, with a concomitant improvement in the rotarod learning task of these mice. Along with the shift in the balance of synaptic vs. extrasynaptic NMDARs signalling and localization with the resultant increase in extrasynaptic NMDARs activity, in particular NR1/NR2B-containing extrasynaptic NMDARs activity (Okamoto et al. 2009; Milnerwood et al. 2010), intracellular Ca^{+2} signalling pathways including calpain and p38 MAPK activation that couple to survival or death are also dysregulated early in striatal tissue of post-mortem HD human brains and presymptomatic 1-2 month old YAC128 mice (Gafni and Ellerby, 2002; Cowan et al. 2008; Fan et al. 2012). Dau et al. 2014 investigated the calcium-dependent pathways downstream of NR1/NR2B-containing extrasynaptic NMDARs in YAC128 mouse model of HD. They found that 2 months treatment of 4 month old YAC128 and WT mice with memantine (1 and 10 mg/kg/day) reduced striatal NR1/NR2B-containing extrasynaptic NMDARs expression and current without altering synaptic NMDARs levels (Dau et al. 2014). In addition, low dose 1 mg/kg/day memantine rescued CREB shut-off, while both doses suppressed p38 MAPK activation to WT levels (Dau et al. 2014). In a recent study, Ranju et al. 2015 investigated the role of memantine in improving motor function, regulation of neurotrophic factors, in addition to mitochondrial and neuronal functions in 3-nitropropionic acid model of HD. They found that memantine (20 mg/kg/day i.p.) treatment for 5 days restored motor function, with an associated up-regulation in BDNF and GDNF expression, enhanced brain

succinate dehydrogenase activity and decreased glutamate content (Ranju et al. 2015). In addition, memantine treatment ameliorated striatal neuronal loss, reduced GFAP immunoreactivity, and exhibited protective effect against neuronal apoptosis (Ranju et al. 2015).

1.4.5 Memantine and Alzheimer's Disease (AD)

Memantine is the first drug to be approved by the United States Food and Drug Administration and also by the European Union for the treatment of moderate to severe AD, and its effectiveness had been confirmed in many *in vitro* and *in vivo* studies (Table 4).

Model	Memantine Dose	Memantine Effects	References
Cortical neurons treated with $A\beta_{1-40}$ and its amyloidogenic variant $A\beta_{1-42}$	Various	Attenuates the toxic action induced by Aβ treatment	Tremblay et al. 2000; Hu et al. 2007
$A\beta_{1-40}$ directly injected into the hippocampus of Sprague-Dawley rats	15 mg/kg/day s.c. for 9 days	Exerted protective effects on progressive neuronal damage and apoptosis	Miguel-Hidalgo et al. 2002
APP_{swe}/PS1dE9 transgenic mouse model	30 mg/kg/day p.o. for 2-3 weeks	Improved the acquisition of Morris water maze, without affecting swimming speed, locomotor activity or aggressive behaviour	Minkeviciene et al. 2004
Tg2576 transgenic mouse model	10 & 20 mg/kg/day p.o. for 6 months	Decreased Aβ plaques deposition, increased synaptic density and the appearance of degenerating axons	Dong et al. 2008
Tg2576 transgenic mouse model	5 mg/kg/day p.o. for 6 months	Decreased Aβ plaques deposition, increased synaptic density, but with no effect on the appearance of degenerating axons	Dong et al. 2008
Triple-transgenic mouse model	30 mg/kg/day p.o. for 3 months	Restored cognition and reduced the levels of insoluble Aβ, Aβ dodecamers, prefibrillar soluble oligomers, and fibrillar oligomers specially in older animals	Martinez-Coria et al. 2010
APP_{swe}/PS1dE9 transgenic mouse model	10 mg/kg/day i.p. for 3 weeks	Improved the reversal phase of left-right discrimination, though equivalent to saline for Morris water maze, passive avoidance learning, and elevated plus maze	Filali et al. 2011

Table 4: Memantine and AD

Early data found that memantine attenuated the toxic action of $A\beta_{1-40}$ and its amyloidogenic variant $A\beta_{1-42}$ in cultured cortical neurons (Tremblay et al. 2000; Hu et al. 2007). Memantine ameliorates the deleterious action of Aβ not only *in vitro* but also *in vivo*. Semi-chronic infusion of memantine (15 mg/kg/day s.c.) for 9 days exerted protective effects on progressive neuronal damage and apoptosis induced by the direct injection of $A\beta_{1-40}$ into the hippocampus of Sprague-Dawley rats (Miguel-Hidalgo et al. 2002). In addition, memantine had been found to modulate the cognitive impairment in transgenic mouse models of AD. Memantine (30 mg/kg/day p.o.) for 2-3 weeks significantly improved the acquisition of Morris water maze in APP_{swe}/PS1dE9 double transgenic mice without affecting swimming speed, locomotor activity or aggressive behaviour (Minkeviciene et al. 2004). These data indicate that memantine improves hippocampus-based spatial learning in a transgenic mouse model of AD without producing nonspecific effects on locomotion or exploratory activity (Minkeviciene et al. 2004). The similarity of memantine mechanism of action to other

NMDARs antagonists has led to concerns that it may have neuroprotective as well as neurotoxic effects (Dong et al. 2008). To assess that, Tg2576 transgenic mice were given memantine (5, 10 and 20 mg/kg/day) for 6 months, and quantitative light in addition to electron microscopy were used to investigate Aβ plaques deposition and neuronal morphology in the hippocampus and overlying cortex (Dong et al. 2008). Administration of the two higher doses of memantine (10 and 20 mg/kg/day) was associated with a significant decrease in Aβ plaques deposition, increase in synaptic density and the appearance of degenerating axons. Administration of the lowest dose of memantine (5 mg/kg/day) was associated with a significant decrease in Aβ plaques deposition and a significant increase in synaptic density, but not a significant increase in degenerating axons. These results suggest that chronic memantine administration may have both neuroprotective and neurotoxic effects in a mouse model of AD (Dong et al. 2008). In another study, memantine (30 mg/kg/day p.o.) was administered to three groups of triple-transgenic AD mice (APP, PS1, and tau mutations) with differing levels of AD-like pathology (6, 9, and 15 months of age) for 3 month (Martinez-Coria et al. 2010). After the treatment, memantine-treated mice had restored cognition and significantly reduced the levels of insoluble Aβ, Aβ dodecamers, prefibrillar soluble oligomers, and fibrillar oligomers, and these effects on pathology were stronger in older, more impaired animals, than in younger, early stage animals (Martinez-Coria et al. 2010). Subchronic memantine administration (10 mg/kg/day i.p.) for 3 weeks was better than placebo during the reversal phase of left-right discrimination, though equivalent to saline for Morris water maze and passive avoidance learning in APP_{swe}/PS1dE9 double transgenic mice (Filali et al. 2011). The drug had no effect on non-learned behaviours in elevated plus-maze exploration and nest building, and these results support a specific action of NMDARs antagonism on behavioural flexibility in transgenic mice with Aβ pathology (Filali et al. 2011).

1.5 Aims and Objectives

Based on the involvement of axon degeneration in the pathogenesis of HD and AD, the present thesis aims to answer whether FK866 axon protective properties *in vitro, ex-vivo* and *in vivo* after acute injury could extend beyond that and also modulate axonal damage and

behavioural symptoms in *in vitro* and *in vivo* models of these neurodegenerative diseases, and to compare this to the reported neuroprotective and axon protective effects of memantine.

To accomplish these aims:

1. I used *in vitro* models of HD and AD where early axonal damage had been already reported, and treated them with FK866/NA combination to test how inhibiting NMN synthesis with FK866 while maintaining NAD level with NA could modulate axonal damage in these models. Then I co-administered NMN with FK866/NA to test whether this NAD precursor could revert FK866-mediated neuroprotection.

2. I used HdhQ140 and APP_{swe}/PS1dE9 *in vivo* models of HD and AD crossed with YFP-H mice to test how inhibiting NMN synthesis with FK866 while maintaining NAD level with NA could modulate behavioural symptoms and axonal damage in these models. I chose these particular animal models since signs of axon pathology had been reported in these mice at 6 months old, the time I planned to do the drug treatment and behavioural studies. I subjected HdhQ140 and APP_{swe}/PS1dE9 mice to a battery of motor and cognitive assays to test the effect of FK866/NA *in vivo*. In addition, expression of YFP protein marker allow visualizing signs of axonal damage in these mice and also gives a powerful tool to test whether FK866/NA treatment could modulate this damage.

Chapter 2:

Inhibiting NMN synthesis with FK866 rescued axonal degeneration in *in vitro* models of Huntington's disease (HD) and Alzheimer's disease (AD)

2.1 Introduction

As treatments based on the protection of neuronal cell bodies have shown to be largely ineffective, targeting axon degeneration, which had been confirmed to be an early event in many neurodegenerative diseases including HD, and AD, where it precedes cell body loss and correlates with symptom onset and progression (Conforti et al. 2014), could be a valid therapeutic alternative. Therefore, understanding the mechanisms by which axons are lost in each of these pathologies is the basis for effective treatments, and to accomplish this we used *in vitro* models of HD and Aβ toxicity where early axonal damage has been reported (Wyttenbach et al. 2000; Rosales-Corral et al. 2012).

Tet-On PC12 cells have proven to be a useful *in vitro* model of HD that recapitulates some of the typical features of this disease such as axonal pathology and mHTT aggregate formation, and therefore, can be valuable to gain insight into some of the molecular mechanisms of axon degeneration in this disease and also to test the activity of some neuroprotective agents (Wyttenbach et al. 2000; Li et al. 2001).

Primary neuronal culture is a powerful tool that has been used extensively for studying mechanisms of neuronal degeneration and regeneration. Treating these primary neurons and in particular cortical neurons with Aβ peptide was used to mimic AD-associated Aβ toxicity *in vitro*, and also to characterize the activity of novel drugs for this neurodegenerative disease.

Evidences for the involvement of axons and synapses in the pathogenesis of HD and AD are opening the way into potential effective therapeutic targets for these disorders, however how to delay the degeneration of these neuronal compartments is not always known. The serendipitous discovery of the spontaneous mutant mouse *Wld*^{S} where axon degeneration after an injury – known as Wallerian degeneration (Waller A, 1850) – is delayed by 10-fold (Lunn et al. 1989; Conforti et al. 2000; Mack et al. 2001), have led to the characterization of an active pro-axon death pathway stimulated after acute injury with shared mechanistic similarity to the axon pathology in some neurodegenerative diseases (Conforti et al. 2014). While maintenance of axon survival and growth depends on the activity of the cytoplasmic NAD-biosynthetic enzyme NMNAT2, acute injury quickly terminate the activity of this labile enzyme and result in accumulation of the NAD precursor NMN, which in turn triggers a rapid pathway of axon degeneration (Gilley and Coleman, 2010; Gilley et al. 2013; Milde et al. 2013; Di Stefano et al. 2014). Blocking NMN synthesis with the NMN-synthesising

enzyme NAMPT inhibitor FK866 (Hasmann and Schemainda, 2003) (Figure 9), strongly protects axons *in vitro, ex-vivo* and *in vivo* after acute injury (Di Stefano et al. 2014). In addition to its role in neurodegenerative diseases, emerging data implicate NAMPT in the pathogenesis of a number of different human diseases, in particular in the field of inflammation (Garten et al. 2009). NAMPT inhibition with FK866 has been shown to reduce disease burden in inflammatory animal models of arthritis and endotoxic shock (Busso et al. 2008; Van-Gool et al. 2009), as well as in experimental autoimmune encephalitis (Bruzzone et al. 2009). Moreover, FK866 has been shown to reduce the secondary inflammatory injury and partly reduce permanent damage in an experimental compression model of spinal cord injury (Esposito et al. 2012).

Both mHTT and Aβ increase the expression of extrasynaptic NR2B subunit of NMDARs, whose excessive activation causes excitotoxctity (Li et al. 2003). Extrasynaptic NMDARs activation leads to axonal and dendritic damage and axonal transport defects (Takeuchi et al. 2005; Hardingham et al. 2010), and compounds that selectively block these receptors, such as memantine, are protective in models of HD (Okamoto et al. 2009; Milnerwood et al. 2010), and already approved for clinical treatment of AD (Mount and Downton, 2006).

2.2 Aims of The Study

This study aims to test the hypothesis that FK866 neuroprotective properties after an acute injury could extend to *in vitro* models of HD and Aβ toxicity, and to compare this to the reported neuroprotective effects of memantine.

2.3 Materials and Methods

Tet-On PC12 cells culture. A stable inducible Tet-On PC12 cell line expressing GFP-tagged exon 1 fragment of the mutant *HTT* gene, with 21 (wild-type, Q21 PC12 cells) or 72 (mutant, Q72 PC12 cells) CAG repeats, was used as an *in vitro* model of HD (Wyttenbach et al. 2000). Expression of the mutant *HTT* gene was induced in this model by adding dox to the culture medium (Gossen et al. 1995). Tet-On PC12 cells were cultured in high glucose Dulbecco's Modified Eagle's Medium (DMEM) (Sigma-Aldrich™), supplemented with 5% Tet-approved heat-inactivated fetal bovine serum (FBS) (PAA™), 10% heat-inactivated horse

serum (HS) (Gibco™), 1% penicillin-streptomycin-glutamine (Gibco™), 50 µg/ml geneticin 418 (G418) (PAA™), and 70 µg/ml hygromycin B (Invitrogen™) (standard medium) at 37°C and 5% CO_2 in a humidified incubator. Tet-On PC12 cells were differentiated by replacing the standard medium with the differentiation medium consisting of high glucose DMEM, supplemented with 2% B27 (Invitrogen™), 1:1000 gentamycin (Gibco™), 50 µg/ml G418 (PAA™), 70 µg/ml hygromycin B (Invitrogen™) and 100 ng/ml NGF 7S (Invitrogen™).

Tet-On PC12 cells characterization and drug treatment. Tet-On PC12 cells were plated on type IV collagen-coated Ibidi 35 mm µ-dishes (Ibidi™), in standard medium. After 24 hours, this medium was replaced with the differentiation medium (day 1). Cells were fed every 48 hours with fresh medium containing 1 µg/ml dox (Sigma-Aldrich™) to induce expression of the mutant *HTT* gene. At day 6, Tet-On PC12 cells were fixed with 4% phosphate buffered paraformaldehyde (PFA) (Sigma-Aldrich™), and then stained using 1:500 Hoechst staining (Invitrogen™) according to the manufacturer's instructions. Five fields / dish were imaged using a DM IRB Leica fluorescent microscope. Percentage of cells which have axons, percentage of cells with morphologically healthy nuclei, and number of mHTT aggregates were quantified manually in each image, using ImageJ software, version 1.45. Hoechst-stained nuclear morphology was considered abnormal if the nucleus was fragmented or condensed to a small size (Wyttenbach et al. 2000). In drug treatment studies, 1-100 nM FK866, 1 mM NA (Sigma-Aldrich™), 1 mM NMN (Sigma-Aldrich™), and 5-30 µM memantine (Sigma-Aldrich™), was added to the differentiation medium at day 1, and this was repeated in four independent experiments (n=4).

RT-PCR. Total RNA was isolated from brain tissue or Tet-On PC12 cells cultured for 7 days as described above using TRIzol® reagent (Life Technologies™) according to the manufacturer's instructions. cDNA was reverse transcribed using SuperScript™ II reverse transcriptase (Invitrogen™) with random primers (Sigma-Aldrich™) following the manufacturer's instructions. Positive controls from rat brain and negative controls in which reverse transcriptase enzyme was omitted were included. Reverse transcription polymerase chain reaction (RT-PCR) for NMDARs subunits was performed in a BIOER™ thermal cycler using REDTaq DNA Polymerase (Sigma-Aldrich™) as per the manufacturer's instructions with 10 µM of the forward and reverse primers. Table 5 shows primer sequences for

NMDARs NR1, NR2A and NR2B subunits. Amplified fragments were analysed using gel electrophoresis in a 1.6% agarose gel stained with ethidium bromide.

Gene Symbol	Forward Primer	Reverse Primer
NMDARs NR1 Subunit	5'-ATAAGACATGGGTTCGGTATCAGG-3'	5'-CTCAGCTCTCCCTATGACGGGAAC-3'
NMDARs NR2A Subunit	5'-ATCACGCATGTGTGCGACCTCATG-3'	5'- ATGAGCTCTGTGTTCCCAGACACCA-3'
NMDARs NR2B Subunit	5'-ATGAAGCCCAGCGCAGAGTGCTGTT-3'	5'- CACGAAGCTGTTCTCGATGGTACTG-3'

Table 5: Forward and reverse primer sequences for NMDARs NR1, NR2A and NR2B subunits

Primary neuronal culture characterization and drug treatment. Cortices and stria were collected from E16 C57BL/6 mouse embryos, placed in a 5-cm petri dish containing 10 ml cold Hank's Balanced Salt Solution (HBSS) (Sigma-Aldrich™), transferred to 15 ml falcon tube, triturated up and down gently with 10 ml pipette, and plated in Ibidi 35 mm µ-dishes in neurobasal medium (Gibco™) supplemented with 1% B27 and 1% glutamine (Gibco™). At day 6, different treatment groups were established by changing the medium of the neuronal culture with fresh medium containing the added drug, 10 µM oligomeric Aβ (Sigma-Aldrich™), 10 nM FK866, 1 mM NA, and 10 µM memantine. After 48 hours, all groups were processed for toxicity, apoptosis and axonal damage studies, and this was repeated in four independent experiments (n=4).

Immunocytochemistry. After drug treatment, neuronal culture medium was removed and cells were washed once with PBS, fixed with 4% phosphate buffered PFA, permeabilized with 1% Triton in PBS, and blocked with 5% normal gout serum (Sigma-Aldrich™) in PBS. For toxicity and apoptosis studies, neuronal cultures were incubated with 4 µM Ethidium Homodimer-1 (Invitrogen™) and 1:500 Hoechst staining respectively. For axonal damage studies, neuronal culture was incubated with 1:500 SMI 31 (Covance™) primary antibody overnight, washed 3 times with 1x PBS, incubated with 1:200 Alexa Fluor 488 (Invitrogen™) secondary antibody for 1 hour, and then washed 3 times with PBS. Finally, images from five fields / dish were acquired using a DM IRB Leica fluorescent microscope. Percentage of area of axons, and percentage of cells with morphologically healthy nuclei were quantified manually in each image, using ImageJ software, version 1.45. To measure the area of axons with ImageJ software, images have to be converted to grayscale, SMI 31-

stained axons areas need to be highlighted using thresholding, and the thresholded areas need to be measured. Hoechst-stained nuclei morphology was considered abnormal if the nucleus was fragmented or condensed to a small size.

Statistical analysis. Data were expressed as mean ± SD. Two- or Three-way ANOVA was used for statistical analysis followed by Bonferroni post-hoc test. Comparison among multiple groups was performed using two-way ANOVA. $P < 0.05$ was considered to be statistically significant.

2.4 Results

FK866 reduced mHTT-induced toxicity in Tet-On PC12 cells.

The early axon pathology observed in models of neurodegenerative diseases shares some features with axon degeneration after an acute injury (Conforti et al. 2014), which is greatly delayed by the NAMPT inhibitor FK866 (Di Stefano et al. 2014). To investigate whether FK866 has any protective effect in these pathologies, I used *in vitro* models of HD and Aβ toxicity, where early axonal damage has been reported (Wyttenbach et al. 2000; Rosales-Corral et al. 2012).

First, I tested FK866 in a PC12 inducible model of HD, i.e. the Tet-On PC12 cells with 21 (wild-type, Q21 PC12 cells) or 72 (mutant, Q72 PC12 cells) CAG repeats (Wyttenbach et al. 2000). Upon dox treatment, Q72 PC12 cells express mutant *HTT* gene, develop abnormal cellular morphology and intranuclear aggregate formation resembling those described in HD patients, in addition to losing their neurite extension in response to NGF (Wyttenbach et al. 2000) (Figure 10A - C). In contrast, only homogeneous *HTT* expression is detected in Q21 cells, which show no morphological abnormality (Figure 10A).

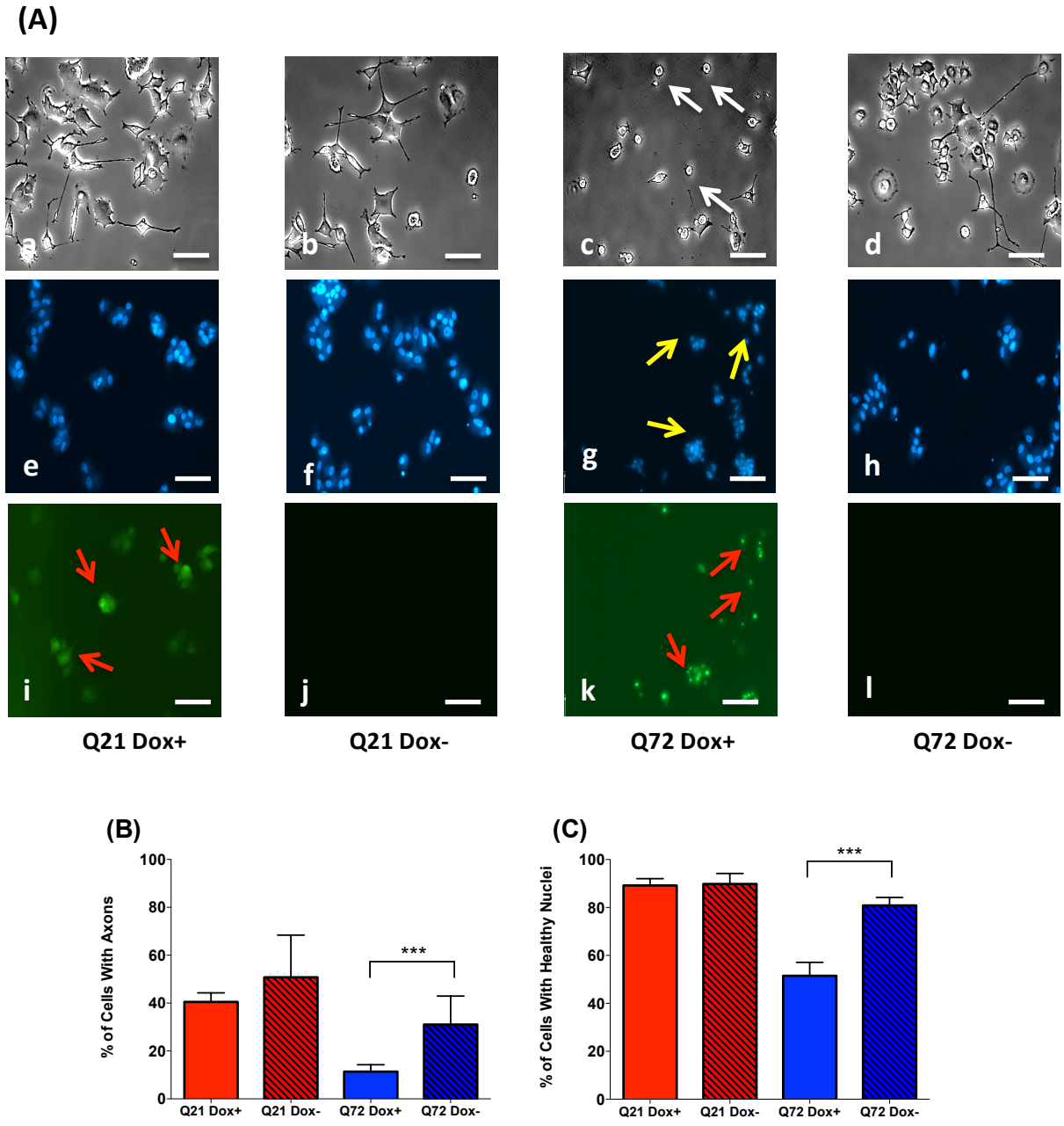
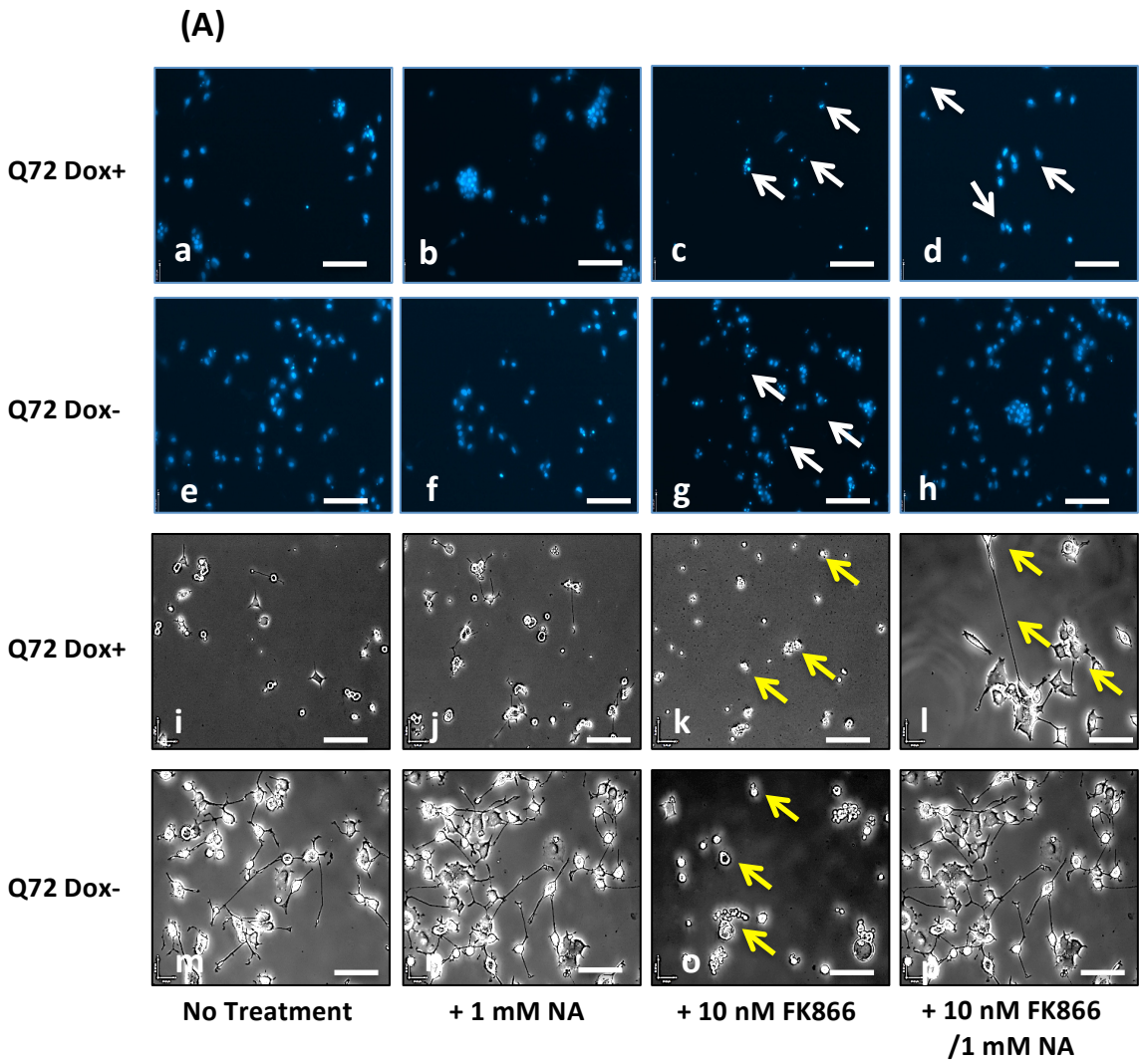


Figure 10: Tet-On PC12 cells characterization. (A) (a-d) bright-field images, (e-h) DAPI-field images, and (i-l) GFP-field images of Tet-On PC12 Cells. Dox-induced expression of mutant *HTT* exon 1 significantly ($p < 0.001$) impaired axonal morphology (white arrows in image c) and nuclear morphology (yellow arrows in image g) in Q72 Dox+ PC12 cells. Moreover, Q72 Dox+ PC12 cells accumulated mHTT aggregates upon dox treatment (red arrows in image k), while Q21 Dox+ PC12 cells displayed a diffuse homogenous localisation of mHTT GFP fluorescence (red arrows in image i). (B) Quantification (%) of Tet-On PC12 cells that have axons (cells with 3 or more processes). Q72 Dox+ PC12 cells developed the shortest and the least frequent axons in comparison to the three other Tet-On PC12 cells groups. (C) Quantification (%) of Tet-On PC12 cells with morphologically healthy nuclei (a nucleus was considered unhealthy if it was fragmented or condensed to a small size). (n=4, mean ± SD, two-way ANOVA followed by Bonferroni post-hoc test, ***, $p < 0.001$). Scale bar, 20 µm.

10-100 nM FK866 added to the culture medium significantly ($p < 0.001$) reduced cellular viability in both Q21 and Q72 PC12 cells (Figure 11A - C; Figure 12A, and B). However when supplied together with 1 mM NA, which maintains NAD biosynthesis in the presence of FK866 and limits any potential toxicity due to NAD depletion (Figure 9), 10-100 nM FK866 significantly ($p < 0.001$) rescued the axonal abnormalities and also ameliorated the nuclear morphology of Q72 dox+ PC12 cells (Figure 11A - C; Figure 12A, and B).



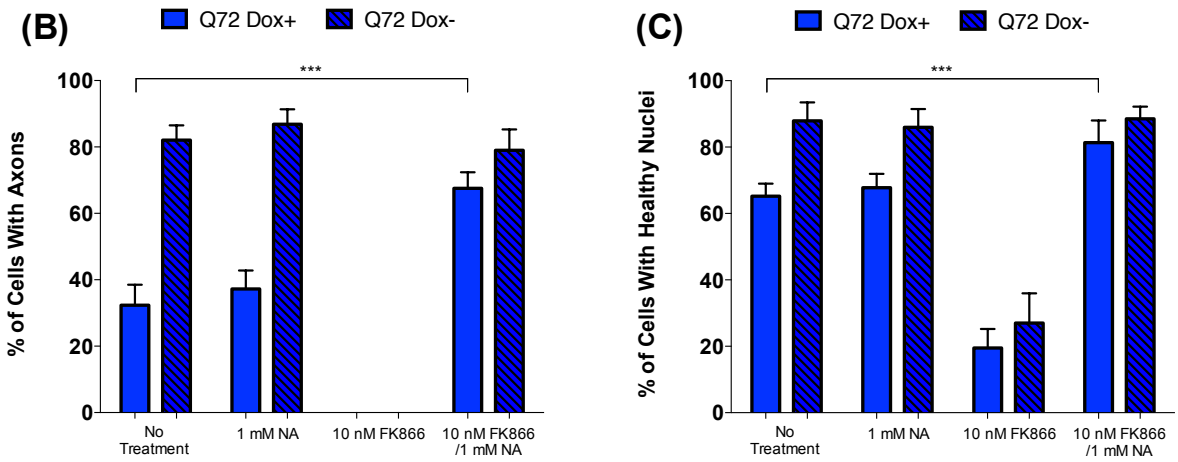


Figure 11: FK866 co-administered with NA reduced mHTT-induced toxicity in Tet-On PC12 cells. (A) (a-h) DAPI-field images and (i-p) bright-field images of Q72 PC12 cells cultured in the presence (a-d and i-l) or absence (e-h and m-p) of dox to induce mHTT expression and aggregate formation. The cells were then left untreated or treated as indicated. Consistent with a toxic effect of the block of NAD synthesis, 10 nM FK866 added to the culture medium significantly reduced cellular viability in both dox+ and dox- Q72 PC12 cells (white arrows in image c, and g; and yellow arrows in image k, and o); however, co-administration of 10 nM FK866 with 1 mM NA restored cell viability, significantly reduced axonal abnormalities (yellow arrows in image l), and ameliorated nuclear morphology (white arrows in image d) of Q72 Dox+ PC12 cells. (B) Quantification (%) of Q72 PC12 cells that have axons. (C) Quantification (%) of Q72 PC12 cells with morphologically healthy nuclei. (n=4, mean ± SD, two-way ANOVA followed by Bonferroni post-hoc test, ***, $p < 0.001$). Scale bar, 20 µm.

NA alone had no effect on axon or nuclear morphology (Figure 11A - C; Figure 12A, and B), and it does not affect axon degeneration after acute injury (Di Stefano et al. 2014). FK866 administered in combination with NA did not affect the number of mHTT aggregates in Q72 dox+ PC12 cells (data not shown). Neuroprotective effects of 10 nM and 100 nM FK866 were undistinguishable (Figure 12C, and D).

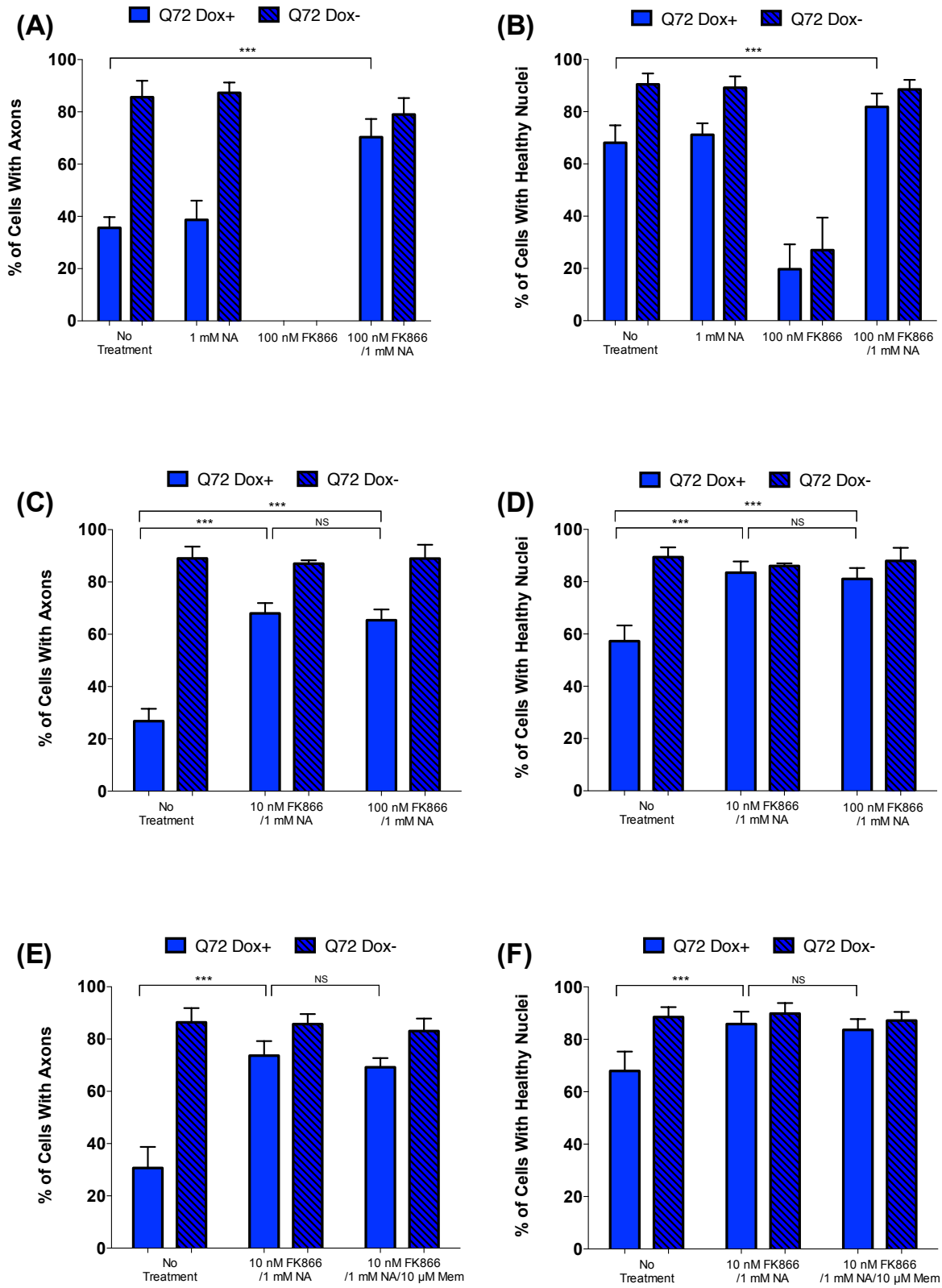
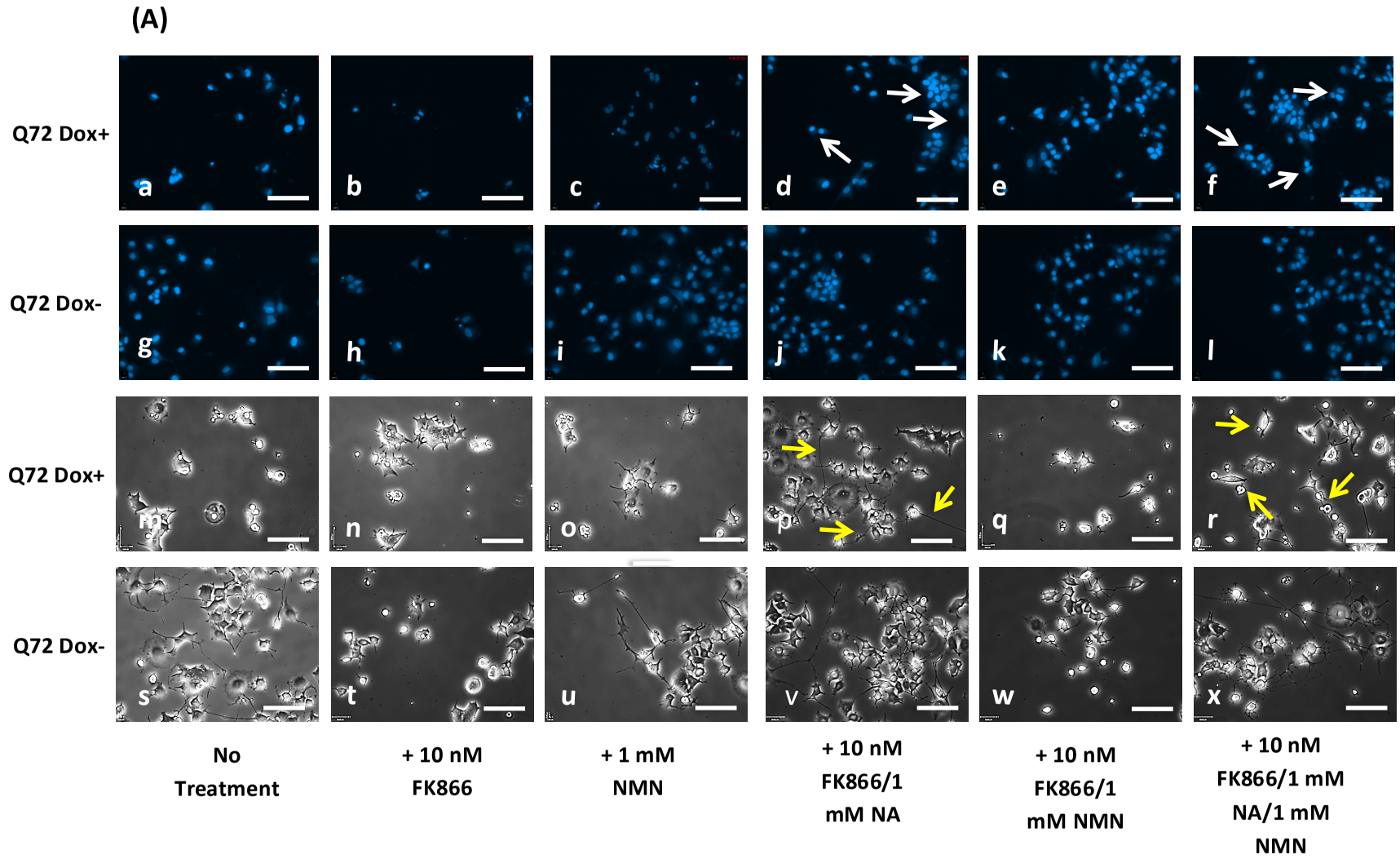

(A)
Q72 Dox+
Q72 Dox-
% of Cells With Axons
***
No Treatment
1 mM NA
100 nM FK866
100 nM FK866 /1 mM NA
(B)
Q72 Dox+
Q72 Dox-
% of Cells With Healthy Nuclei
***
No Treatment
1 mM NA
100 nM FK866
100 nM FK866 /1 mM NA
(C)
Q72 Dox+
Q72 Dox-
% of Cells With Axons
***
***
NS
No Treatment
10 nM FK866 /1 mM NA
100 nM FK866 /1 mM NA
(D)
Q72 Dox+
Q72 Dox-
% of Cells With Healthy Nuclei
***
***
NS
No Treatment
10 nM FK866 /1 mM NA
100 nM FK866 /1 mM NA
(E)
Q72 Dox+
Q72 Dox-
% of Cells With Axons
***
NS
No Treatment
10 nM FK866 /1 mM NA
10 nM FK866 /1 mM NA/10 µM Mem
(F)
Q72 Dox+
Q72 Dox-
% of Cells With Healthy Nuclei
***
NS
No Treatment
10 nM FK866 /1 mM NA
10 nM FK866 /1 mM NA/10 µM Mem

Figure 12: **FK866 co-administered with NA reduced mHTT-induced toxicity in Q72 Tet-On PC12 cells, and neuroprotective effects of 10 nM and 100 nM FK866 were undistinguishable.** (A, C, and E) Quantification (%) of Q72 PC12 cells that have axons, (B, D, and F) Quantification (%) of Q72 PC12 cells with morphologically healthy nuclei. 10-100 nM FK866 co-administered with 1 mM NA significantly ($p < 0.001$) reduced axonal abnormalities and ameliorated nuclear morphology in Q72 Dox+ PC12 cells. There was no significant difference between the neuroprotective effects of 10 and 100 nM FK866. Combining 10 μM memantine and 10 nM FK866/1 mM NA had no synergistic neuroprotective effects. (n=4, mean ± SD, two-way ANOVA followed by Bonferroni post-hoc test, ***, $p < 0.001$, NS, $p > 0.05$). Mem = Memantine.

1 mM NMN added together with 10 nM FK866/1 mM NA significantly ($p < 0.01$) reverted the axonal protection of FK866/NA combination (Figure 13A, and B). This result is similar to what observed in a model of Wallerian degeneration (Di Stefano et al. 2014), and suggests that FK866-induced neuroprotection is linked to the reduction in NMN production and it is not due to off-target effects of FK866. Interestingly, 1 mM NMN did not affect the neuroprotective effect of FK866/NA at the cellular body compartment ($p > 0.05$) (Figure 13A, and C), probably indicating that NMN can still be converted to NAD at this level, where multiple NMNAT enzymes likely operate.


(A)
Q72 Dox+
Q72 Dox-
Q72 Dox+
Q72 Dox-
a
b
c
d
e
f
g
h
i
j
k
l
m
n
o
p
q
r
s
t
u
v
w
x
No Treatment
+ 10 nM FK866
+ 1 mM NMN
+ 10 nM FK866/1 mM NA
+ 10 nM FK866/1 mM NMN
+ 10 nM FK866/1 mM NA/1 mM NMN

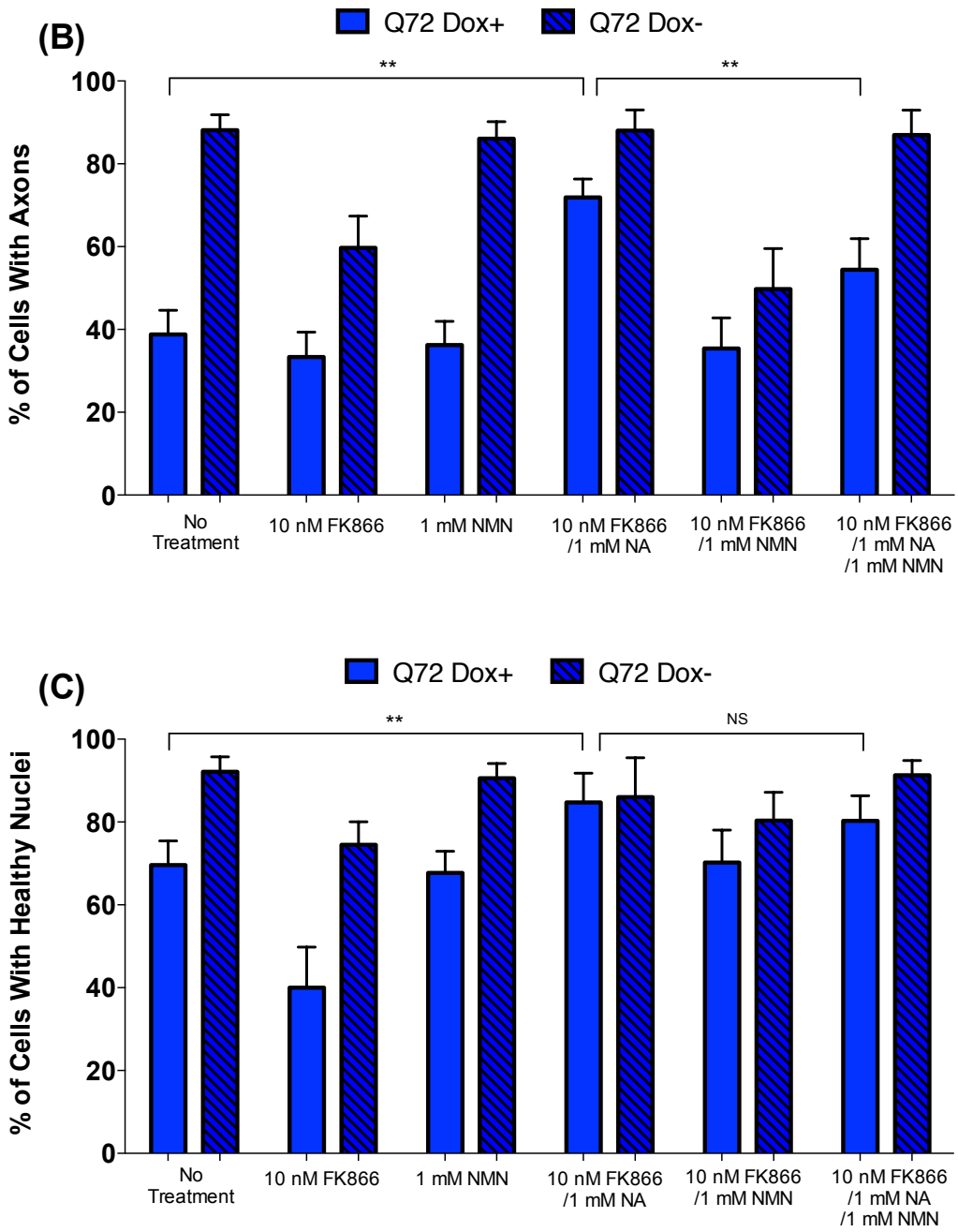
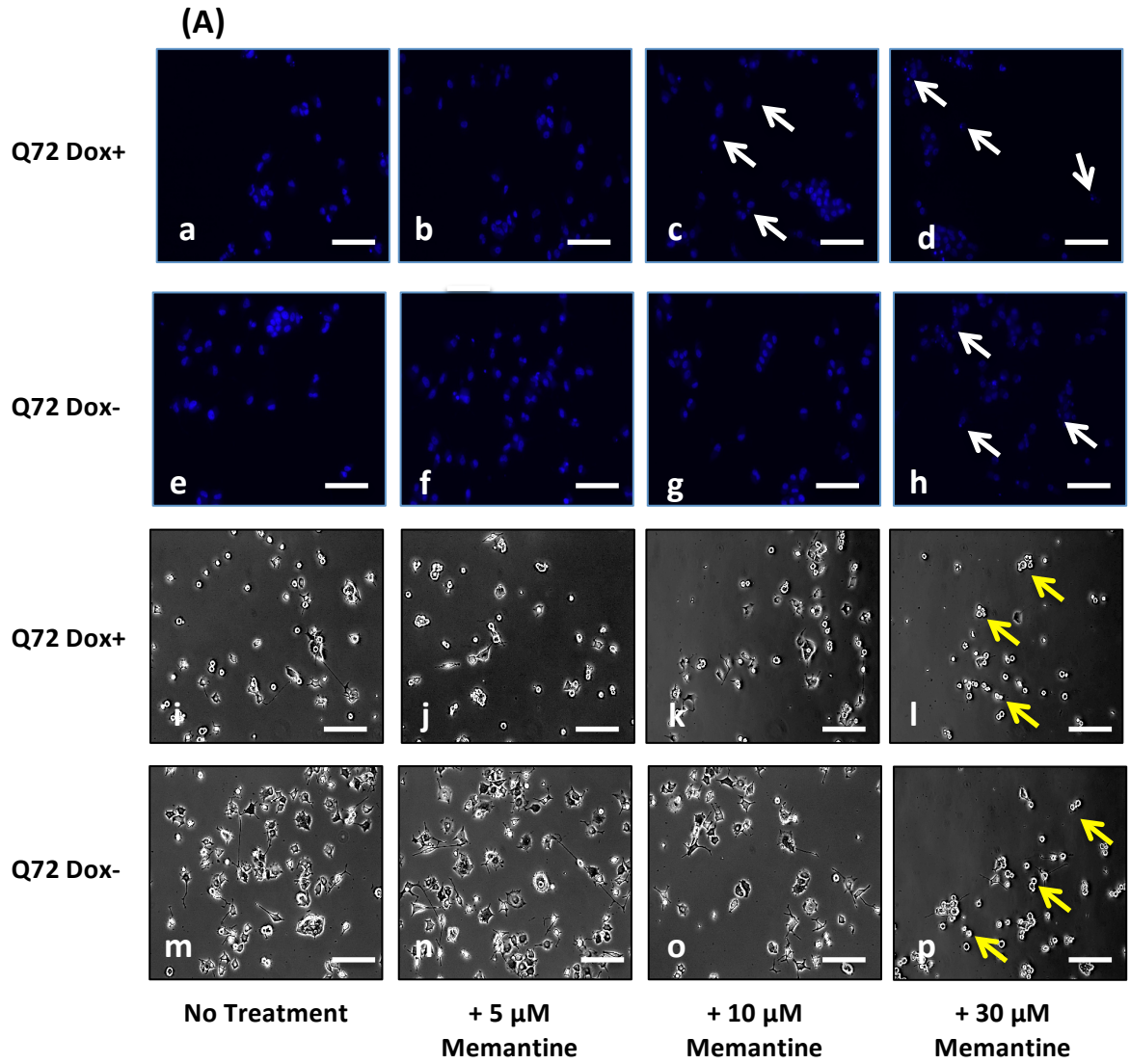


Figure 13: **NMN reverted the axonal protection of FK866/NA**. (A) (a-l) DAPI-field images and (m-x) bright-field images of Q72 PC12 cells, cultured in the presence (a-f and m-r) or absence (g-l and s-x) of dox to induce mHTT expression and aggregate formation. Cells were then left untreated (a, g, m, and s) or treated as indicated. 10 nM FK866/1 mM NA attenuated the axonal abnormalities and ameliorated the nuclear morphology of Q72 Dox+ PC12 cells (white arrows in image d; and yellow arrows in image p); 1 mM NMN significantly reverted the axonal protection of FK866/NA (yellow arrows in image r), suggesting that this neuroprotection is linked to the reduction in NMN production. 1 mM NMN however, did not affect FK866/NA neuroprotective effect at the cellular body compartment (white arrows in image f). (B) Quantification (%) of Q72 PC12 cells that have axons. (C) Quantification (%) of Q72 PC12 cells with morphologically healthy nuclei. (n=4, mean ± SD, two-way ANOVA followed by Bonferroni post-hoc test, **, $p < 0.01$, NS, $p > 0.05$). Scale bar, 20 μm.

I compared FK866 effect to that of memantine, an inhibitor of the extrasynaptic NMDARs with described neuro- and axon- protective effects (Takeuchi et al. 2005). 10 µM memantine resulted in a small, but significant ($p < 0.05$) improvement in nuclear morphology in Q72 dox+ PC12 cells but had no effect on axonal morphology in both Q21 and Q72 PC12 cells (Figure 14A - C). At 30 µM however, memantine significantly ($p < 0.001$) impaired axonal and nuclear morphologies in all Tet-On PC12 cell groups (Figure 14A - C).



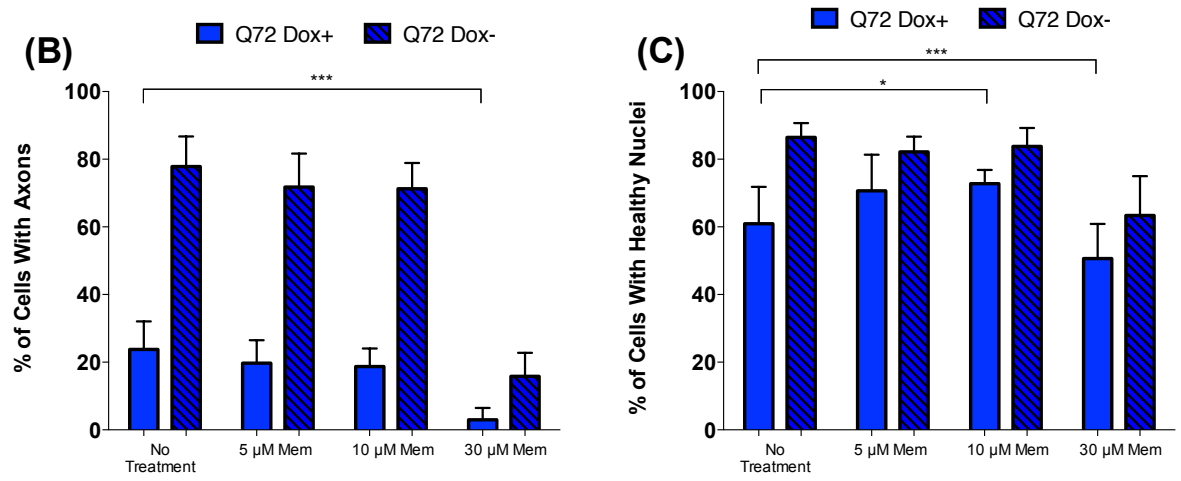


Figure 14: Memantine attenuated mHTT-induced nuclear but not axonal toxicity in Tet-On PC12 cells. (A) (a-h) DAPI-field and (i-p) bright-field images of Q72 PC12 cells cultured in the presence (a-d and i-l) or absence (e-h and m-p) of dox to induce mHTT expression and aggregate formation. 10 µM memantine significantly increased percentage of Q72 Dox+ PC12 cells with morphologically healthy nuclei (white arrows in image c). At 30 µM however, memantine significantly impaired axonal and nuclear morphologies in Q72 PC12 cells (white arrows in image d, and h; and yellow arrows in image i, and p). (B) Quantification (%) of Q72 PC12 cells that have axons. (C) Quantification (%) of Q72 PC12 cells with morphologically healthy nuclei. (n=4, mean ± SD, two-way ANOVA followed by Bonferroni post-hoc test, *, $p < 0.05$, ***, $p < 0.001$). Scale bar, 20 µm. Mem = Memantine.

The partial protection conferred by memantine could be due to lack of functional expression of NMDARs in Tet-On PC12 cells. To test this, I examined NMDARs subunits expression in these cells by RT-PCR. I found that while NMDARs NR1 subunit was expressed in Q21 and Q72 Tet-On PC12 cells; neither NMDARs NR2A nor NR2B subunits were expressed in any of these cells groups (Figure 15). In contrast to previous reports in other models (Okamoto et al. 2009), there was no effect of memantine on the number of mHTT aggregates in Q72 dox+ PC12 cells (data not shown). Combining 10 µM memantine and 10 nM FK866/1 mM NA had no synergistic neuroprotective effects ($p > 0.05$) (Figure 12E, and F).

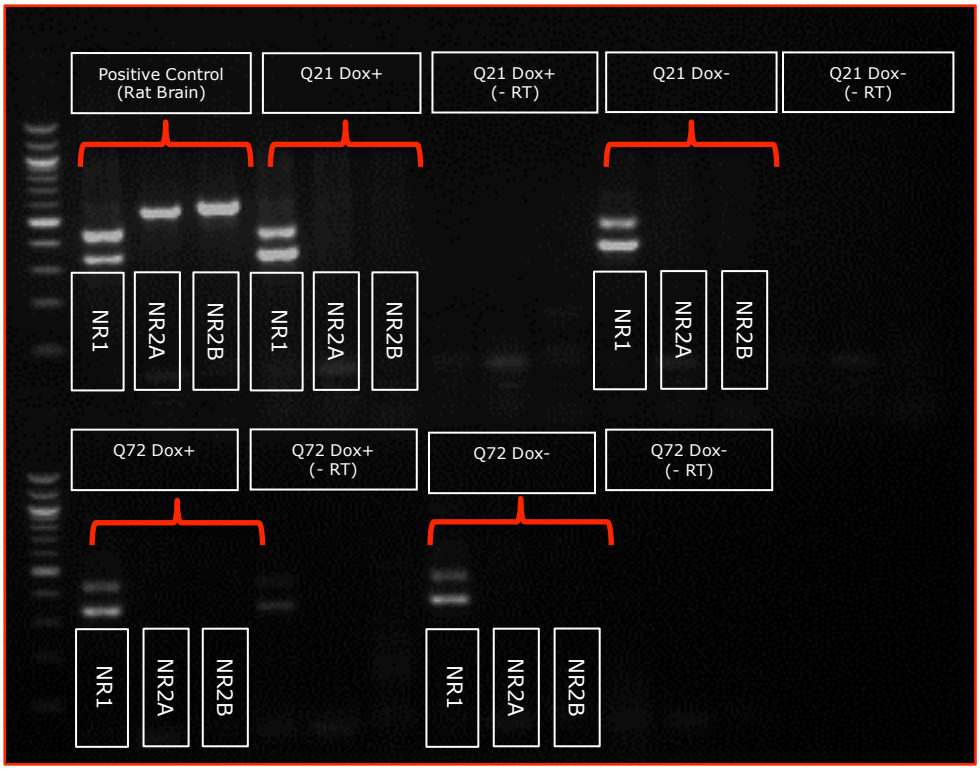


Figure 15: Expression of NMDARs subunits in Tet-On PC12 cells. Total RNA was isolated from brain tissue or Tet-On PC12 cells cultured for 7 days as described in the methods, cDNA was reverse transcribed using SuperScript™ II reverse transcriptase, and RT-PCR for NMDARs subunits was performed using REDTaq DNA Polymerase with 10 µM of the forward and reverse primers. While NMDARs NR1 subunit was expressed in Q21 and Q72 Tet-On PC12 cells; neither NMDARs NR2A nor NR2B subunits was expressed in any of these cells.

FK866/NA combination rescued Aβ -induced toxicity in cortical neuronal culture

Next, in view of the primary role of axon pathology in AD models (Hiruma et al. 2003; Molnar et al. 2004; Rosales-Corral et al. 2012), I investigated if FK866 neuroprotective properties also extend to an *in vitro* model of Aβ toxicity.

I studied whether 10 nM FK866/1 mM NA could also modulate Aβ-induced toxicity in cortical neuronal culture. Similar to our study in the HD model, I again compared this effect to that of memantine, with a focus on axonal damage. 100 nm - 5 µM Aβ had no effect on axonal viability of cortical neurons (Figure 16). In the other hand and consistent with previous studies (Rapoport et al. 2002; Song et al. 2008), 10 µM Aβ treatment for 48 hours significantly ($p < 0.01$) reduced cellular viability of cortical neurons (Figure 17A - C), by reducing axonal area and impairing nuclear morphology. 10 nM FK866/1 mM NA

significantly ($p < 0.01$) rescued axonal pathology and ameliorated nuclear morphology of cortical neurons treated with 10 µM Aβ, and made them not different from that of cortical neurons treated with vehicle (Figure 17A - C). Again 1 mM NMN added together with 10 µM Aβ and 10 nM FK866/1 mM NA significantly ($p < 0.01$) reverted the neuroprotective effects of FK866/NA combination at the axonal compartment but not at the cellular body compartment (data not shown).

On the other hand, 10 µM memantine significantly ($p < 0.01$) improved the nuclear morphology of these neurons only, with limited effect on their axons (Figure 17A - C). Also in this model, combining 10 µM memantine and 10 nM FK866/1 mM NA had no synergistic neuroprotective effects ($p > 0.05$) (Figure 17A - C).

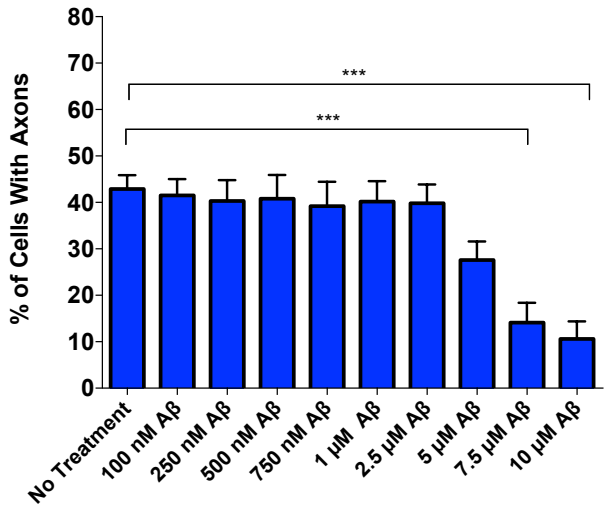
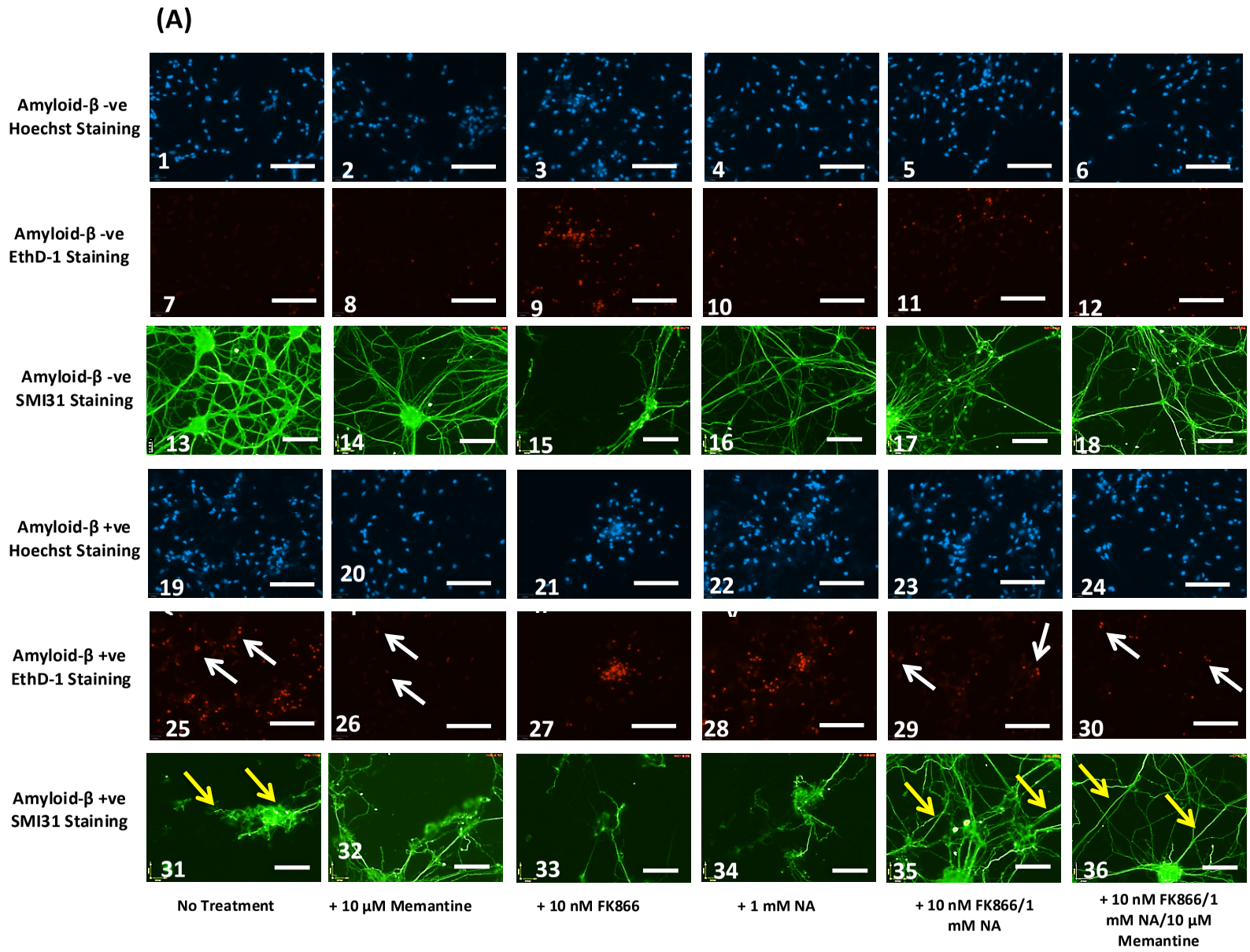
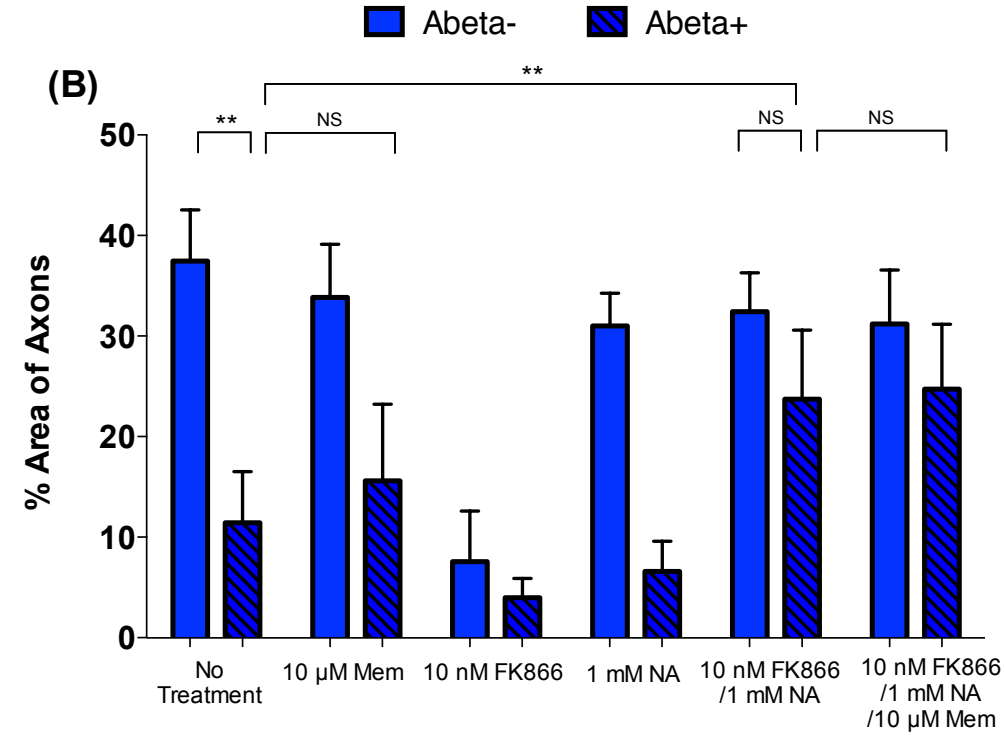


Figure 16: Effect of Aβ on axonal viability of primary cortical neurons. Primary cortical neurons were cultured for 6 days and then treated with different concentrations of Aβ as indicated for 48 hours. Quantification (%) of axonal area show that while 100 nm - 5 µM Aβ treatment for 48 hours had no effect on axonal viability of primary cortical neurons; 10 µM Aβ treatment for 48 hours significantly impaired axonal viability of these neurons. (n=4, mean ± SD, one-way ANOVA, ***, $p < 0.001$).


(A)
Amyloid-β -ve Hoechst Staining
Amyloid-β -ve EthD-1 Staining
Amyloid-β -ve SMI31 Staining
Amyloid-β +ve Hoechst Staining
Amyloid-β +ve EthD-1 Staining
Amyloid-β +ve SMI31 Staining
1
2
3
4
5
6
7
8
9
10
11
12
13
14
15
16
17
18
19
20
21
22
23
24
25
26
27
28
29
30
31
32
33
34
35
36
No Treatment
+ 10 µM Memantine
+ 10 nM FK866
+ 1 mM NA
+ 10 nM FK866/1 mM NA
+ 10 nM FK866/1 mM NA/10 µM Memantine


Abeta-
Abeta+
(B)
**
**
NS
NS
NS
% Area of Axons
50
40
30
20
10
0
No Treatment
10 μM Mem
10 nM FK866
1 mM NA
10 nM FK866 /1 mM NA
10 nM FK866 /1 mM NA /10 μM Mem

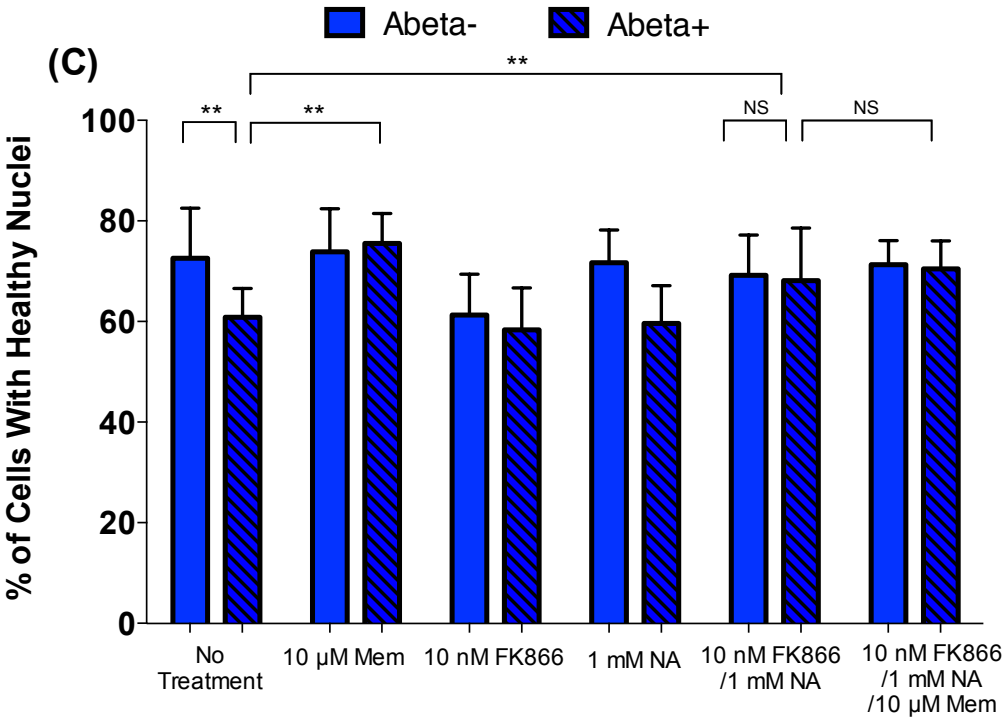

Abeta-
Abeta+
(C)
**
**
**
NS
NS
% of Cells With Healthy Nuclei
100
80
60
40
20
0
No Treatment
10 μM Mem
10 nM FK866
1 mM NA
10 nM FK866 /1 mM NA
10 nM FK866 /1 mM NA /10 μM Mem

Figure 17: FK866 co-administered with NA rescued Aβ -induced toxicity in cortical neuronal culture. (A) (1-6) and (19-24) DAPI-field images, (7-12) and (25-30) RED-field image, and (13-18) and (31-36) GFP-field images of primary cortical neurons cultured for 6 days and then treated with 10 μM Aβ, 10 nM FK866, 1 mM NA, and 10 μM memantine, as indicated, for 48 hours. 10 μM Aβ treatment for 48 hours significantly impaired axonal viability and nuclear morphology (yellow arrows in image 31; and white arrows in image 25). 10 nM FK866 co-administered with 1 mM NA significantly reduced axonal pathology and ameliorated nuclear morphology of cortical neurons treated with 10 μM Aβ (yellow arrows in image 35; and white arrows in image 29). 10 μM memantine significantly improved the nuclear morphology of these neurons only, with limited effect on their axons (white arrows in image 26). Combining 10 μM memantine and 10 nM FK866/1 mM NA had no synergistic neuroprotective effects (yellow arrows in image 36; and white arrows in image 30). (B) Quantification (%) of primary cortical neurons axonal area. (C) Quantification (%) of primary cortical neuronal cells with morphologically healthy nuclei. (n=4, mean ± SD, two-way ANOVA followed by Bonferroni post-hoc test, **, $p < 0.01$, NS, $p > 0.05$). Scale bar, 20 μm. Mem = Memantine.

2.5 Discussion

Among its biological functions, NAD metabolism regulates axon degeneration, which is an early and often causative event in a variety of neurodegenerative diseases including HD and AD. Our results show that the NAMPT inhibitor FK866 (in combination with NA) significantly improves axonal and nuclear morphologies in *in vitro* models of HD and Aβ toxicity. NAMPT product NMN overcomes this protection and restores toxicity, suggesting that FK866 acts by reducing its concentration. Since this compound has been recently shown to potently delay injury-induced axon degeneration, our data suggest similarities between axon pathology in injury and that in HD and Aβ toxicity models and identify a potential target for therapeutic intervention.

Different molecular pathways have been described to explain the mechanisms by which mHTT fragments and Aβ peptide promote neuronal dysfunction in HD and AD respectively. However, it is difficult to attribute the broad clinical picture of these neurodegenerative diseases to a single mechanism and unlikely that a single therapeutic regimen will be able to manage HD and AD patients, especially if started after symptom onset. Several studies indicate that axonal damage contributes to the pathogenesis of HD and AD (Li et al. 2001; Morfini et al. 2009; Rosales-Corral et al. 2012), and may be the earliest event in some models (Adalbert et al. 2009; Marangoni et al. 2014). Targeting this axon pathology by limiting the toxic action of mHTT fragments and Aβ peptide is therefore a promising therapeutic strategy that has not yet been addressed in the clinic. This could be due to the lack of information

about the molecular mechanisms that lead to this dysfunction, and therefore the lack of specific molecular targets.

Using Tet-On PC12 cells, I found that 10-100 nM FK866 significantly improved axonal and nuclear morphologies in Q72 dox+ PC12 cells. FK866 mechanism implies a gradual depletion of NAD levels and therefore significantly reduced cellular viability in both Q21 and Q72 PC12 cells. However, its combination with 1 mM NA completely restored cell viability in this model. This is important as combination with this nucleotide, (Figure 9), has already been proposed as strategy for clinical trials to limit the toxicity of FK866 due to NAD depletion while maintaining its therapeutic properties. I found that 1 mM NMN reverts the neuroprotective effect of 10 nM FK866/1 mM NA. These results are consistent with a model in which an increase of NMN, which could result by a reduced availability of NMNAT2 following impairment in axonal transport, activates a pro-axon death pathway that is delayed by modulation of NAD synthesis pathway with FK866 in *vitro* and *ex-vivo*. While NMN consistently reverted FK866-induced neuroprotection at the axonal compartment, it did not revert FK866-induced neuroprotection at the cellular body compartment, and this is important and probably indicates that the NAD synthesizing enzymes NMNATs are still converting NMN to NAD.

I found that memantine, which has been shown to reduce neurite beading (Takeuchi et al. 2005), has a protective effect on mHTT-induced toxicity in Q72 dox+ PC12 cells only at the cellular body compartment, while showing no effect at the axonal compartment. This limited neuroprotective effect could be due to the fact that Tet-On PC12 cells do not express a normal complement of NMDARs subunits, limiting the functional responses of these cells to glutamate-induced NMDARs activation. I found that while NMDARs NR1 subunit was expressed in Q21 and Q72 Tet-On PC12 cells, neither NMDARs NR2A nor NR2B subunits were expressed in any of these cell groups. Although NMDARs are the most memantine-sensitive ion channels, it can affect other ion channels as well, in particular blocking 5-hydroxytryptamine receptors and nicotinic acetylcholine receptors. Hence, I cannot exclude the possibility that memantine-induced protection at the cellular body compartment in these cells is attributed to another mechanism unrelated to NMDARs antagonism.

Similarly, I found that the neuroprotective effect of 10 nM FK866/1 mM NA extended to an *in vitro* model of Aβ toxicity. While low concentrations of Aβ had no effect neither on axonal viability nor on cellular viability of cortical neurons, 10 μM Aβ treatment for 48 hours and

consistent with previous studies (Rapoport et al. 2002; Song et al. 2008) significantly impaired cellular viability of these neurons. Moreover, 10 nM FK866/1 mM NA significantly rescued axonal pathology and ameliorated nuclear morphology of cortical neurons treated with Aβ. This FK866-induced axonal protection is also reverted by NMN, suggesting a similar role of NMN as a trigger of axonal degeneration in models of Aβ toxicity and a shared pathogenic mechanism between HD and Aβ toxicity. Again I found that memantine has a protective effect on Aβ-induced toxicity in cortical neuronal culture only at the cellular body compartment where it significantly improved nuclear morphology, while showing very limited effect at the axonal compartment.

Combining FK866/NA and memantine had no synergistic neuroprotective effects in both HD and Aβ toxicity *in vitro* models. This could be due to the limited effect of memantine only at the cellular body compartment while showing no effect at the axonal compartment.

In conclusion, our study indicates that an increase in NMN could initiate axon degeneration in *in vitro* models of HD and Aβ toxicity similar to acute injury models, reveal that FK866 could be a promising compound for the treatment of these neurodegenerative diseases and highlight the need of testing the efficacy of this compound *in vivo*.

Chapter 3:

FK866 restored some of the behavioural abnormalities in *in vivo* models of Huntington's disease (HD) and Alzheimer's disease (AD)

3.1 Introduction

Europe has the world's highest proportion of older persons, with 16% being over 65, and this is going to increase to 25% by 2030. There is a strong link between age and the incidence of neurodegenerative diseases, thus number of people suffering from these debilitating conditions is constantly on the increase, which makes treating them one of the leading medical and societal challenges. The costs of managing neurodegenerative diseases are estimated at £23bn a year at the UK while across Europe costs are in the order of €130bn a year, however there is currently no cure for these progressive unavoidably fatal age-associated diseases.

Targeting axon degeneration, which had been confirmed to be a critical event in the pathogenesis of HD, and AD (Conforti et al. 2014) could be a novel therapeutic strategy. Expression of WLD^S, which is a modified form of nuclear NAD-biosynthetic enzyme NMNAT1 with an N-terminal sequence that diverts some NMNAT1 to the axon (Conforti et al. 2000), delay axon degeneration after an injury by 10-fold (Lunn et al. 1989; Conforti et al. 2000; Mack et al. 2001). Blocking the synthesis of the NAD precursor NMN with the NMN-synthesizing enzyme NAMPT inhibitor FK866 (Hasmann and Schemainda, 2003) (Figure 9), strongly protects axons *in vitro, ex-vivo* and *in vivo* after acute injury (Di Stefano et al. 2014). Recently, I found that FK866 in combination with NA significantly improved axonal and nuclear morphologies in *in vitro* models of HD and Aβ toxicity, and NMN consistently reverted this protection (Chapter 2), suggesting similarities between axon pathology in injury and that in HD and Aβ toxicity. Here I asked whether FK866 neuroprotective effects could extend beyond the *in vitro* models and also modulate behavioural symptoms in HdhQ140 and APP_{swe}/PS1dE9 *in vivo* models of HD and AD respectively, and I compared that to the reported neuroprotective effects of the NMDARs antagonist memantine.

HdhQ140 is a knock-in mouse model of HD created by Scott Zeitlin's group by inserting a chimeric mouse/human exon 1 containing 140 CAG repeats into the murine *HTT* gene under the control of their endogenous PrP promoter (Menalled et al. 2003). HdhQ140 mice display striatal atrophy by 12 months of age, extensive loss of spines and reduction in dendrites complexity by 20-26 months of age (Lerner et al. 2012), and loss of striatal neurons at 2 years (Hickey et al. 2008). In addition, these mice show behavioural anomalies in a wide range of motor (climbing, vertical pole, rotarod, and running wheel performance) and non-motor functions (fear conditioning and anxiety), starting early at 1-4 months of age, followed by

progressive gliosis and decrease in dopamine and cyclic AMP-regulated phosphoprotein at 12 months of age (Hickey et al. 2008).

APP_{swe}/PS1dE9 is a double transgenic mouse model of AD created by David Borchelt's group by overexpressing chimeric mouse/human *APP* gene with the "Swedish" double mutation together with *PS1* gene deleted at exon 9, both under the control of their endogenous PrP promoter (Jankowsky et al. 2001). These double mutations cause age-related increase in soluble and insoluble $A\beta_{40}$ and its amyloidogenic variant $A\beta_{42}$ (Marutle et al. 2002; Wang et al. 2003), with cognitive impiarment during the reversal phase of left-right discrimination learning, passive avoidance learning, and nest building (Filali et al. 2011), as well as the Morris water maze (Liu et al. 2002). Aβ plaques deposition had been observed in these mice as early as 4-6 months of age, with a progressive increase in plaques number up to 12 months, and a similar increase in Aβ levels (Jankowsky et al. 2001).

3.2 Aims of The Study

This study aims to test the hypothesis that FK866 neuroprotective properties in *in vitro* models of HD and AD could extend beyond that and also modulate behavioural symptoms in HdhQ140 and APP_{swe}/PS1dE9 *in vivo* models of these neurodegenerative disease, and to compare this to the reported neuroprotective effects of memantine.

3.3 Materials and Methods

Mouse origins and breeding. HdhQ140 and APP_{swe}/PS1dE9 (Menalled LB et al. 2003; Jankowsky JL et al. 2001) and their controls were crossed with Thy1.2 yellow fluorescent protein (YFP)-H (Feng et al. 2000) to produce HdhQ140/YFP-H, APP_{swe}/PS1dE9/YFP-H and their YFP+ controls. This crossing made it possible labelling multiple neuronal subsets *in vivo* and also allows imaging of neuronal structures including axons (Beirowski et al. 2004; Coleman et al. 2005; Enright et al. 2007), and detection of axonal dystrophy (Bridge et al. 2009; Adalbert et al. 2009). All mice were obtained from The Jackson's laboratories (USA) and kept at The Bio Support Unit at The University of Nottingham. All breeding and procedures were performed as authorized under The Animals Scientific Procedures Act 1986 under project licence 40/3601.

Genotyping. Ear biopsies of 10-day old mice were collected under isoflurane anaesthesia. DNA was extracted from biopsies and genotyping was performed by RT-PCR using the following forward (for) and reverse (rev) primers according to The Jackson's laboratories protocols:

HdhQ140

For1: 5'-CATTCATTGCCTTGCTGCTAAG-3'

Rev1: 5'-CTGAAACGACTTGAGCGACTC-3'

For2: 5'-GATCGGCCATTGAACAAGATG-3'

Rev2: 5'-AGAGCAGCCGATTGTCTGTTG-3'

APP_{swe}/PS1dE9

For1 (APP_{swe}): 5'-GACTGACCACTCGACC AGGTTCTG-3'

Rev1 (APP_{swe}): 5'-CTTGTAAGTTGGATTCTCATATCC-3'

For2 (PS1dE9): 5'-AATAGAG AACGGCAGGAGCA-3'

Rev2 (PS1dE9): 5'-GCCATGAGGGCACTAATCAT-3'

For **YFP-H** genotyping, primers used were as follows:

For: 5'-CGAACTCCAGCAGGACCATGTGA-3'

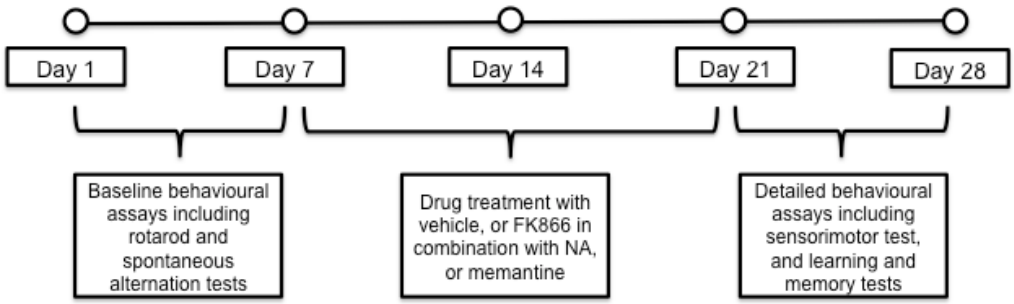
Rev: 5'-CTTCTTCAAGGACGACGGCAACT-3'

Treatments groups. Experiments were started at 5 months and 2 weeks age. Mice from each genotype (HdhQ140/YFP-H, APP_{swe}/PS1dE9/YFP-H and their YFP+ controls) were divided into 3 treatment groups (vehicle, FK866/NA, and memantine all injected), including both males and females (n=5-6 mice/genotype, treatment and gender conditions). From day 1 –

day 7, I performed a baseline set of behavioural assays including rotarod and spontaneous alternation tests. From day 8 – day 21, I injected the mice once/day at 9.00 am with vehicle, or FK866 (15 mg/kg/day i.p.) or memantine (20 mg/kg/day i.p.). NA was co-administered with FK866 in drinking water (50 mg/kg/day p.o.). From day 22 – day 28, I performed a more detailed set of behavioural assays (I continued drug treatments during this week), including sensorimotor (rotarod, open field, prepulse inhibition (PPI)), and learning and memory (elevated plus maze, spontaneous alternation).

While dose of (15 mg/kg/day i.p.) FK866 for 14 days caused no significant difference in brain NAD level, dose of (15 mg/kg twice a day i.p.) FK866 for 14 days significantly lowered brain NAD level. So we agreed to use 15 mg/kg twice a day dose in my *in vivo* study. However, this dose caused significant weight reduction (> 20%) that necessitates humane killing and even sudden death in some of FK866-treated APPswe/PS1dE9/YFP-H mice. So we decided to lower FK866 dose to 15 mg/kg/day and that was the dose we used in our *in vivo* study.

Behavioural assays. In order to evaluate the effect of drug treatments on motor and cognitive behavioural functions in HdhQ140/YFP-H knock-in mouse model of HD and APP_{swe}/PS1dE9/YFP-H transgenic mouse model of AD, mice were subjected to a battery of validated behavioural assays that were adapted from previous studies.



Rotarod. Mice were placed on a rotating rod of a Rotarod apparatus (Letica Scientific Instruments), facing the direction of movement. The latency to fall was recorded over a period of 10 min during which speed was set to increase from 5 to 35 RPM, as a measure of motor coordination with natural fear of falling response. Before drug treatment, the test was carried out over 3 consecutive days (day 1 – day 3). For each day, three trials were performed

with a 1 - 2 hours inter-trial interval, and each trial was repeated twice with a 5 min interval. After drug treatment, the test was carried out over 1 day. Again, for that day, three trials were performed with a 1 - 2 hours inter-trial time and each trial was repeated twice with a 5 min interval.

Spontaneous alternation. A Y-shaped maze comprised of three transparent Plexiglas® arms at a 120° angle from each other was used for this test. The start point was located in the center of the maze and the animal was allowed to freely explore the three arms over 5 min. Alternations rate of arm choice and total number of arm entries were measured as parameters of spatial working memory and locomotor activity, respectively. This test was conducted after the Rotarod once before drug treatment and again after drug treatment.

Open-field. Following the spontaneous alternation, mice were placed in the open-field arena (30 cm x 35 cm x 30 cm) and allowed to move freely for 30 min. Their behaviour was recorded using Ethovision Software (Noldus, Wageningen, Netherlands). The total distance moved and the percentage of time spent in the center of the arena was considered as index of locomotor activity and anxiety-related behaviour, respectively.

Prepulse inhibition (PPI). Following the open field, mice were placed into a Plexiglas cylinder inside a chamber (SR-LAB San Diego Instruments, USA), equipped with fan and light that prevents external noise or vibrations from interfering with the experiment. A speaker was producing acoustic stimuli and mouse movements were detected and recorded as measure of sensory gating. The test session was adapted from Brody et al. 2003 and consisted of 72 trials of different trial types: 40 ms-long of 120 dB stimuli (pulse alone trial); 20 ms-long of either 68, 72, 80 or 90 dB stimuli preceding the 120 dB (prepulse + pulse trial) and 65 dB background white noise (no stimulus trial). Trial types were presented in an irregular, counter-balanced order with around 15 sec inter-trial time and proceeded by 5 min acclimation period during which the background noise was presented alone. Startle magnitude was calculated as: the average response to the pulse alone trials and % of PPI was calculated as: [1 − (startle response to prepulse + pulse) ÷ (startle response to pulse alone)] × 100.

Elevated plus maze. On the last day of the behavioural assays, animals were placed in a plus-shaped apparatus with two open and two enclosed arms constructed from white opaque acrylic, each with an open roof and elevated around 80 cm from the floor. Mice were placed at the junction of the four arms of the maze and allowed to explore freely over 5 min. Their behaviour was recorded with Ethovision. The preference for being in open arms over closed arms (expressed as either as a percentage of entries and/or a percentage of time spent in the open arms) was calculated as measure of anxiety-like behaviour. This test relies upon rodents' tendency toward dark, enclosed spaces and an unconditioned fear of heights/open spaces.

Statistical analysis. Data were presented as mean ± SEM. Two- or Three-way ANOVA was used for statistical analysis followed by Bonferroni post-hoc test. Group comparison was considered statistically significant when p-value was < 0.05. Weight was considered as a covariate in rotarod and PPI, where it was shown to affect performance.

3.4 Results

Motor functions were impaired both in HdhQ140/YFP-H mice and in APP_{swe}/PS1dE9/YFP-H mice, while learning, memory and locomotor activity remained intact

Before investigating whether FK866/NA combination could modulate behavioural symptoms in *in vivo* models of HD and AD, I subjected HdhQ140/YFP-H and APP_{swe}/PS1dE9/YFP-H mice to a set of behavioural assays to check whether baseline performance was affected in these mice and compared it to their YFP+ controls. I used rotarod test to assess motor balance, learning and coordination, and spontaneous alternation test to assess cognitive functions and locomotor activity. I found that rotarod learning curve was significantly ($p < 0.01$) impaired in HdhQ140/YFP-H model of HD and also in APP_{swe}/PS1dE9/YFP-H model of AD in comparison to their YFP+ controls (Figure 18A - C). A significant effect of genotype on motor functions was particularly clear at day 3 of the rotarod learning curve when latency to fall was significantly ($p < 0.001$) reduced in both HdhQ140/YFP-H and APP_{swe}/PS1dE9/YFP-H mice in comparison to their YFP+ controls (Figure 18A - C).

Pre-Treatment Rotarod Performance Analysis Summary		
	F-value	**p-value**
Weight (gm)	107.02	< 0.001
Genotype	44.34	**< 0.001**
Sex	2.58	0.109
Genotype:Sex	6.59	**0.001**

Pre-treatment rotarod performance of HdhQ140/YFP-H and APP$_{swe}$/PS1dE9/YFP-H mice and their YFP+ controls

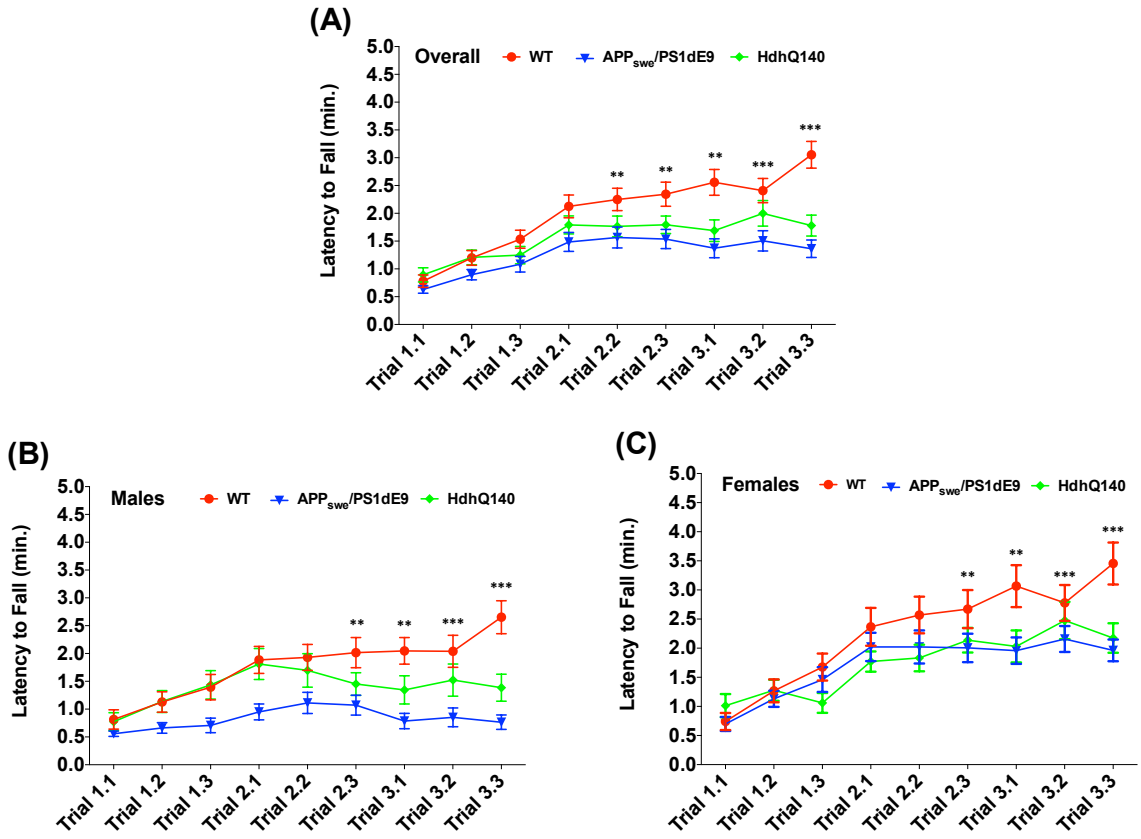


Figure 18: Rotarod performance was impaired in HdhQ140/YFP-H model of HD and in APP$_{swe}$/PS1dE9/YFP-H model of AD in comparison to their YFP+ controls. Latency to fall (min) was measured in three trials per day over three days of testing. A significant effect of genotype on motor functions was particularly clear at day 3 of the rotarod learning curve when latency to fall was significantly ($p < 0.001$) reduced in both HdhQ140/YFP-H and APP$_{swe}$/PS1dE9/YFP-H mice (A), males (B), and females (C) in comparison to their YFP+ controls (n=5-6 mice/genotype, treatment and gender conditions, mean ± SEM, two-way ANOVA followed by Bonferroni post-hoc test, ***, $p < 0.001$, **, $p < 0.01$).

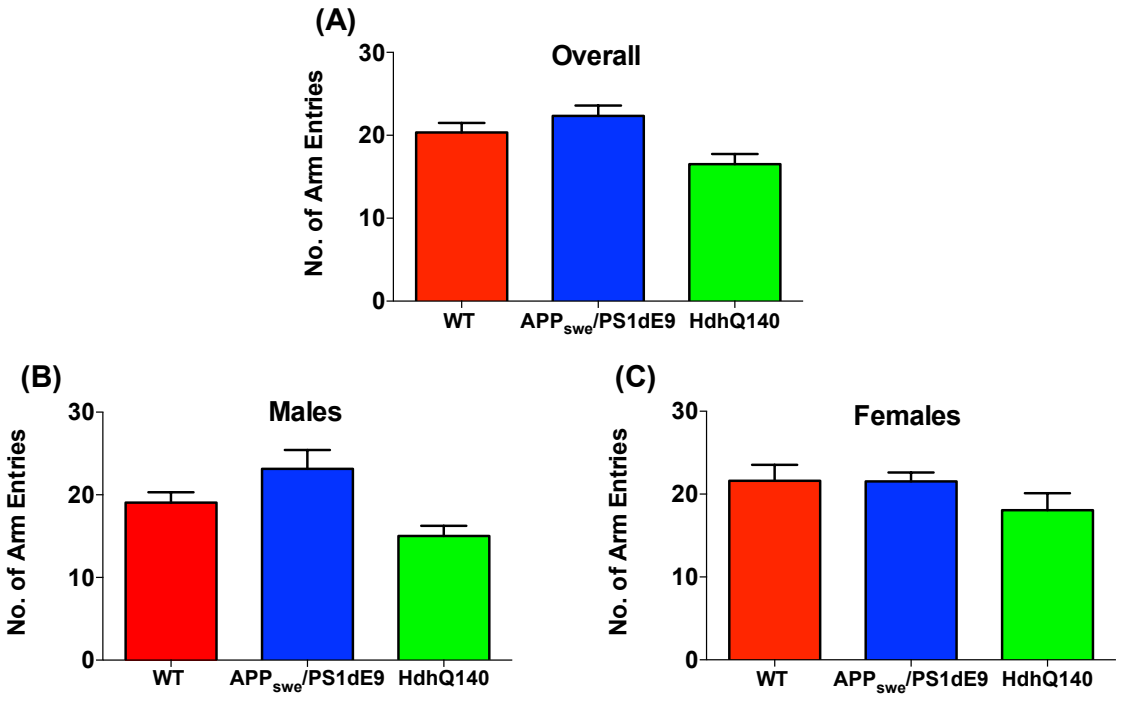
There was no significant difference ($p > 0.05$) in the total number of arm entries (Figure 19A - C), and in the percentage of alternations (Figure 19D - F) as measure by spontaneous

alternation test in both HdhQ140/YFP-H and APP_{swe}/PS1dE9/YFP-H mice in comparison to their YFP+ controls, and neither genotype nor gender effects were found, suggesting no deficits in both spatial working memory and locomotor activity.

Pre-Treatment Spontaneous Alternation Analysis Summary "Number of Arm Entries"		
	F-value	**p-value**
Genotype	4.65	0.012
Sex	1.80	0.184
Genotype:Sex	0.55	0.578

Pre-Treatment Spontaneous Alternation Analysis Summary "% of Alternations"		
	F-value	**p-value**
Genotype	2.10	0.129
Sex	0.07	0.790
Genotype:Sex	2.44	0.094

Pre-treatment spontanous alternation performance of HdhQ140/YFP-H and APP_{swe}/PS1dE9/YFP-H mice and their YFP+ controls



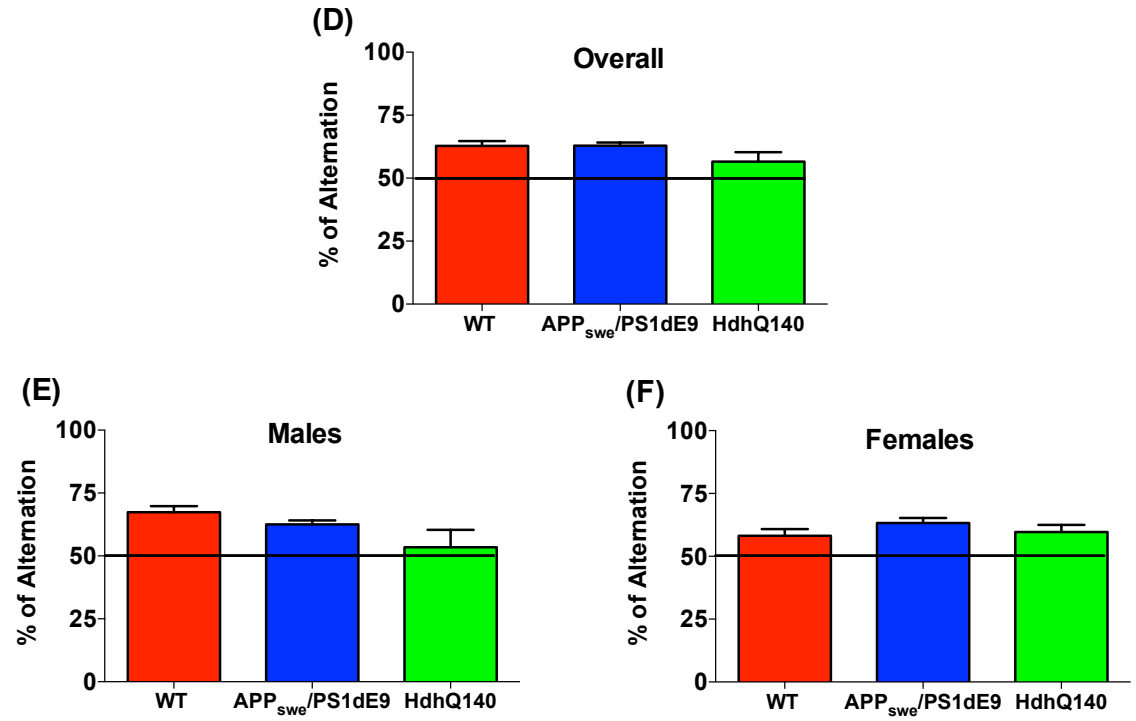


Figure 19: Spatial working memory and locomotor activity was not impaired both in HdhQ140/YFP-H model of HD and in APP_{swe}/PS1dE9/YFP-H model of AD. Mice were allowed to freely explore the spontaneous alternation maze over a period of 5 min and the number of arm entries and the percentage of alternations were measured. The spontaneous alternation rate was calculated as the ratio of alternations performed, out of the maximum number of possible alternations, by the total number of arm entries minus one. There was no significant difference ($p > 0.05$) in the total number of arm entries and also in the percentage of alternations in both HdhQ140/YFP-H and APP_{swe}/PS1dE9/YFP-H mice (A, and D), males (B, and E) and females (C, and F), suggesting no deficits in both spatial working memory and locomotor activity (n=5-6 mice/genotype, treatment and gender conditions, mean ± SEM, two-way ANOVA followed by Bonferroni post-hoc test).

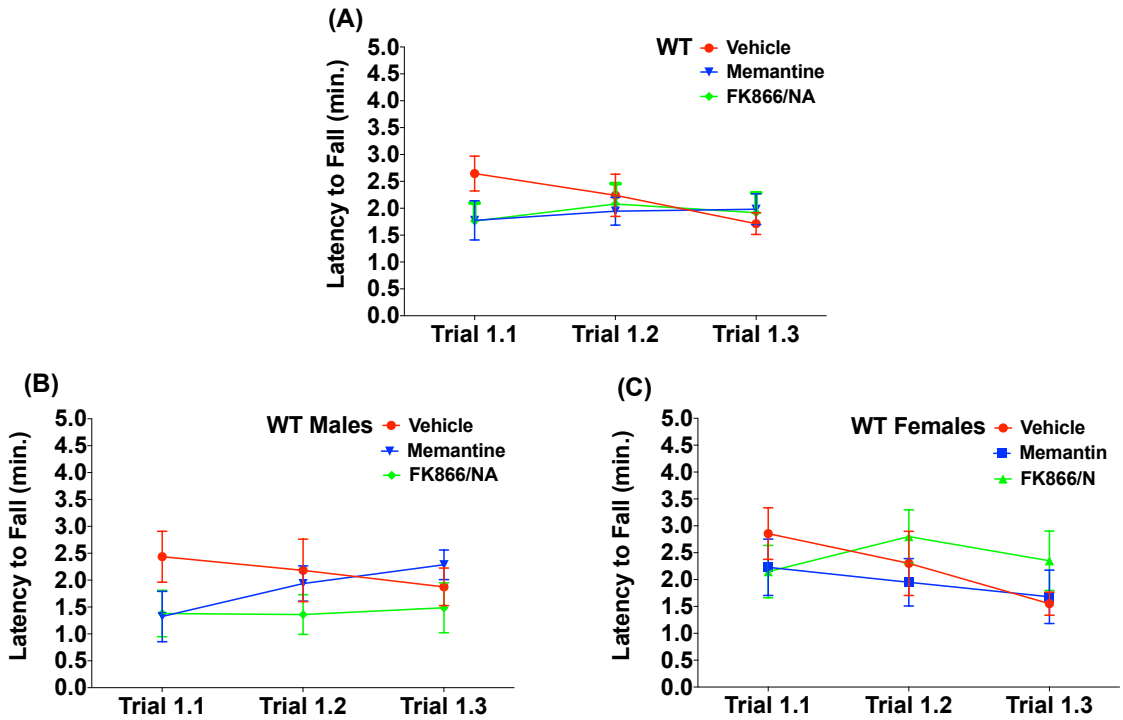
FK866/NA and memantine restored the locomotor abnormalities of APP_{swe}/PS1dE9/YFP-H mice and HdhQ140/YFP-H mice respectively

HdhQ140/YFP-H and APP_{swe}/PS1dE9/YFP-H mice received drug treatment for 2 weeks, and then subjected to a detailed set of behavioural assays, including tests for sensorimotor, learning, and memory functions. I continued drug treatment while doing the behavioural assays.

There was no significant difference ($p > 0.05$) in motor balance, learning and coordination as measured by rotarod test (Figure 20A - I), and also in spatial working memory as measured by spontaneous alternation test (Figure 21A - C) in HD and AD mice and their YFP+ controls treated/untreated with FK866/NA and memantine. In addition, there was no significant effect of treatments ($p > 0.05$) neither on the relative distance moved in the center of the open field arena (Figure 22A - C), nor on the percentage of time spent in the elevated plus maze open arms (Figure 22D - F), both used as an index of anxiety-like behaviour, in all mice groups.

Post-Treatment Rotarod Performance Analysis Summary		
	F-value	**p-value**
Weight (gm)	35.49	< 0.001
Genotype	3.97	0.020
Sex	4.00	0.046
Treatment	1.41	0.247
Genotype:Sex	5.68	0.004
Genotype:Treatment	0.97	0.422
Sex:Treatment	0.43	0.651
Genotype:Sex:Treatment	1.28	0.277

Post-treatment rotarod performance of HdhQ140/YFP-H and APP_{swe}/PS1dE9/YFP-H mice and their YFP+ controls



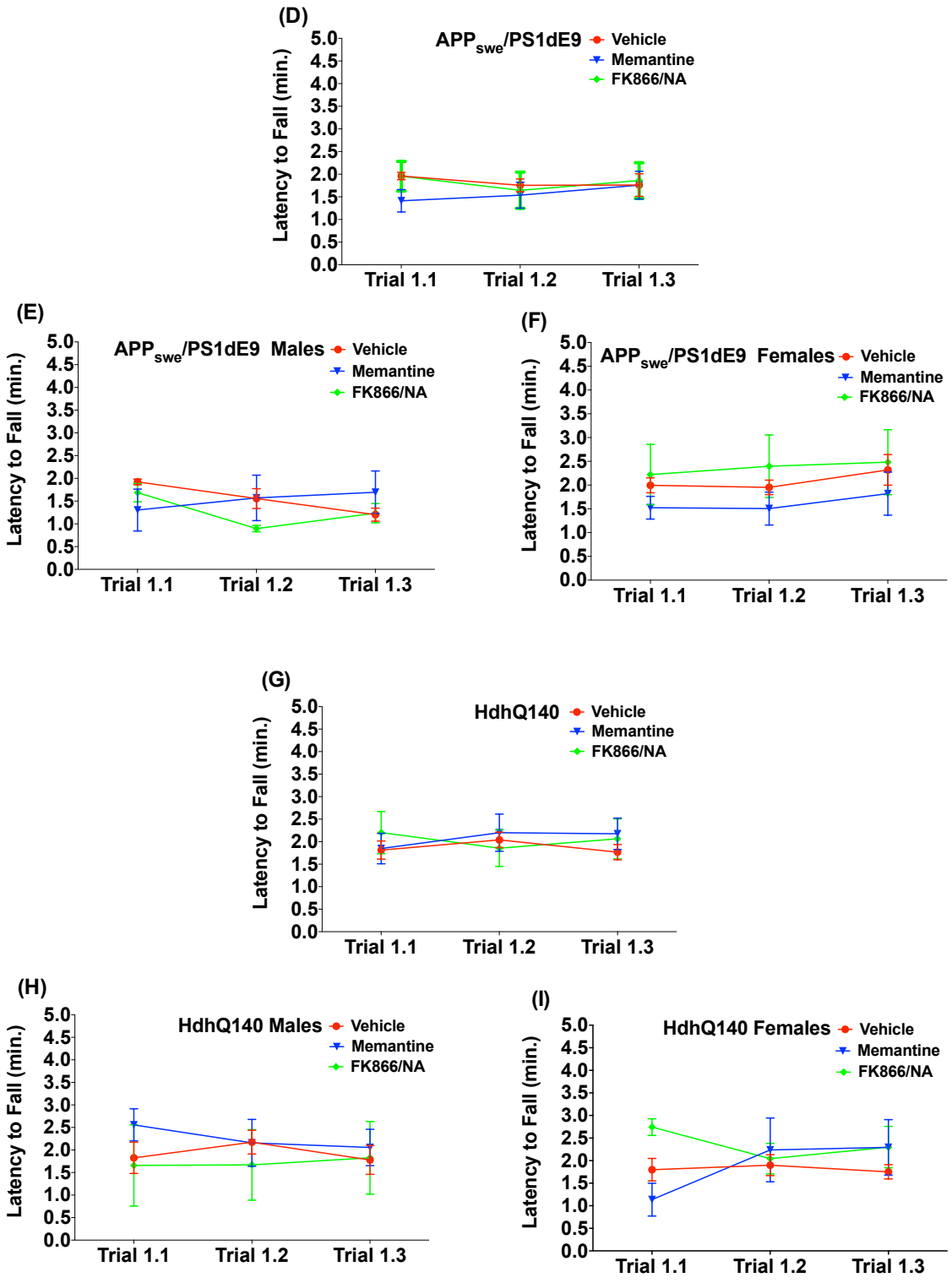


Figure 20: Post-treatment rotarod performance did not change both in HdhQ140/YFP-H model of HD and in APP_{swe}/PS1dE9/YFP-H model of AD. Latency to fall (min) was measured in three trials per day over one day of testing. There was no significant difference ($p > 0.05$) in motor balance, learning and coordination as measured by rotarod test (A – I) in HdhQ140/YFP-H mice, APP_{swe}/PS1dE9/YFP-H mice, and their YFP+ controls treated/untreated with FK866/NA and memantine (n=5-6 mice/genotype, treatment and gender conditions, mean ± SEM, two-way ANOVA followed by Bonferroni post-hoc test).

Post-Treatment Spontaneous Alternation Analysis Summary "% of Alternations"		
	F-value	**p-value**
Genotype	4.45	0.015
Sex	12.90	< 0.001
Treatment	6.66	0.002
Genotype:Sex	0.02	0.983
Genotype:Treatment	0.27	0.897
Sex:Treatment	0.76	0.472
Genotype:Sex:Treatment	1.13	0.352

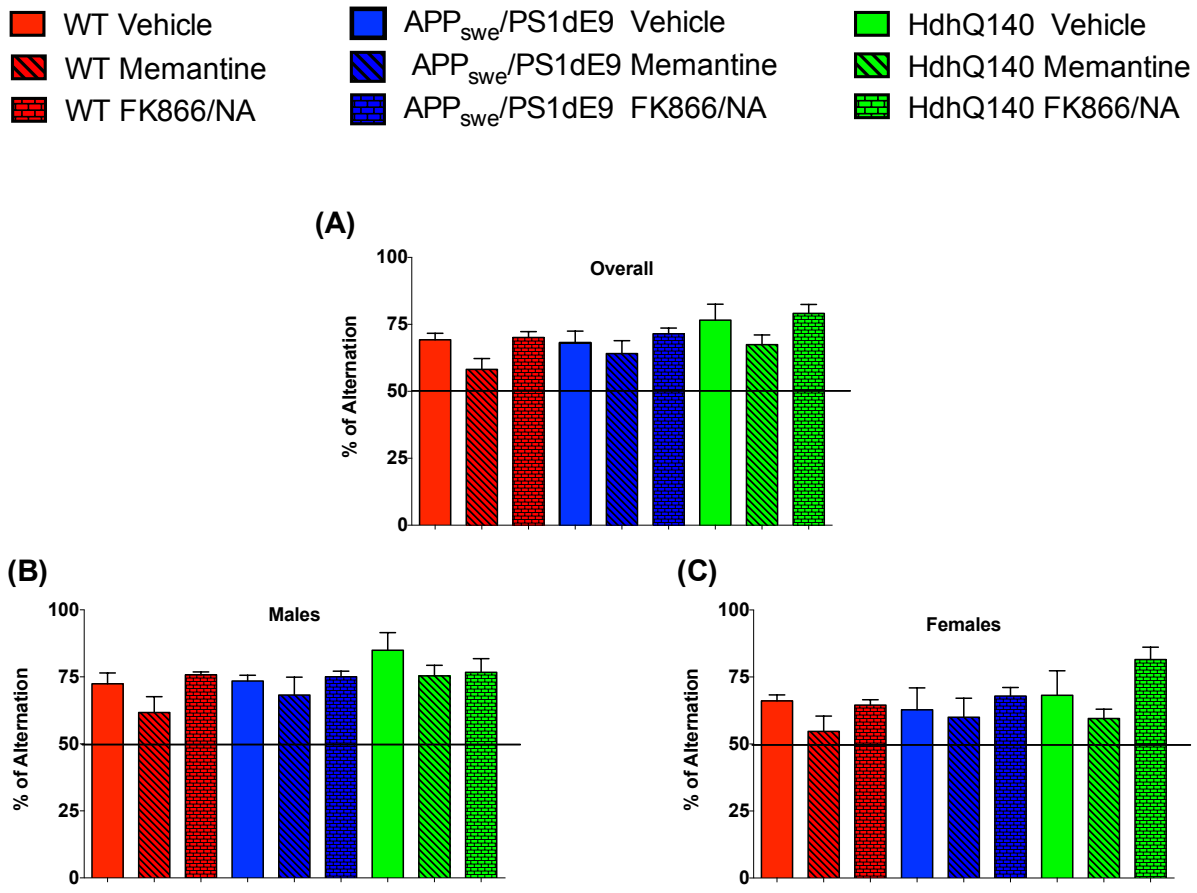
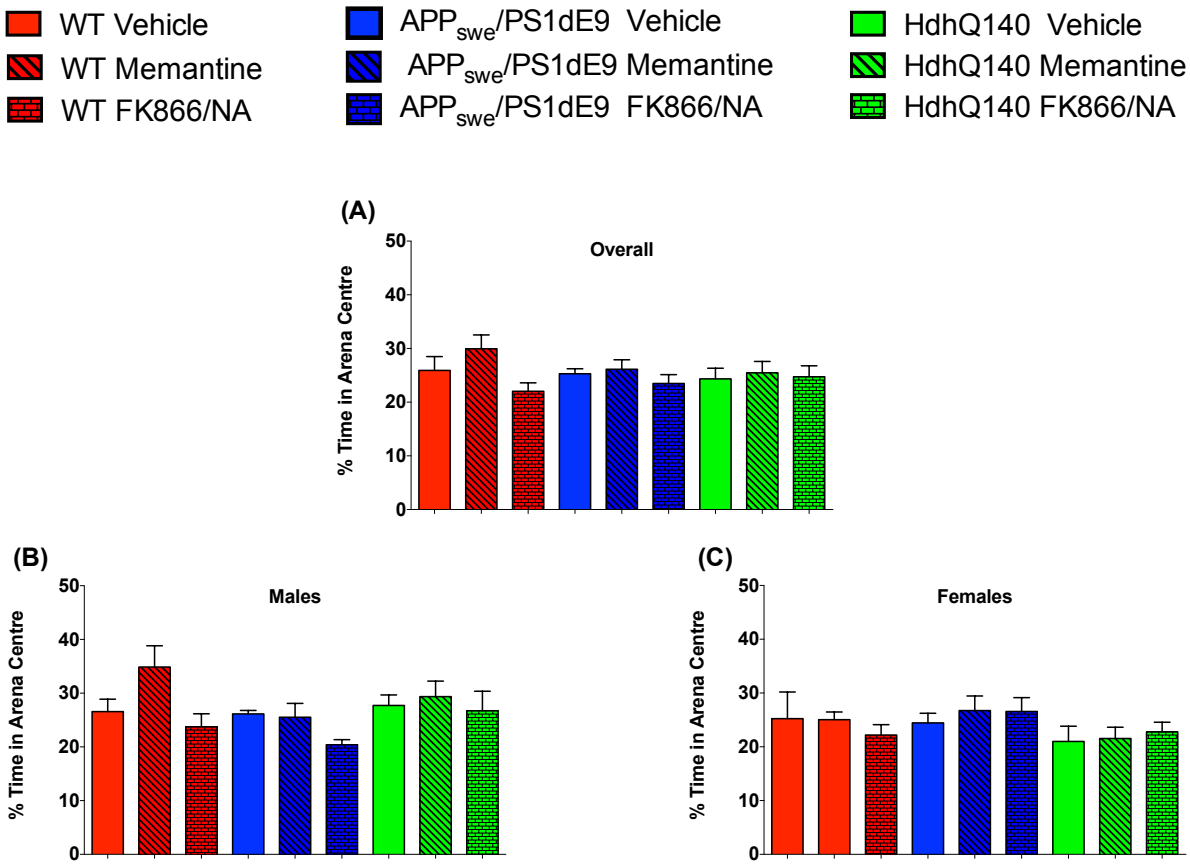


Figure 21: Post-treatment spatial working memory was preserved both in HdhQ140/YFP-H model of HD and in APP_{swe}/PS1dE9/YFP-H model of AD. Mice were allowed to freely explore the Y-shaped maze over a period of 5 min and the percentage of alternations was measured as the ratio of alternations performed, out of the maximum number of alternations possible, by the total number of arm entries minus one. There was no significant difference ($p > 0.05$) in spatial working memory as measured by spontaneous alternation test in both HdhQ140/YFP-H and APP_{swe}/PS1dE9/YFP-H mice (A), males (B) and females (C), and their YFP+ controls treated/untreated with FK866/NA and memantine (n=5-6 mice/genotype, treatment and gender conditions, mean ± SEM, two-way ANOVA followed by Bonferroni post-hoc test).

Post-Treatment Open Field Analysis Summary "% Time in Arena Centre"		
	F-value	p-value
Genotype	0.55	0.581
Sex	5.28	0.025
Treatment	2.63	0.079
Genotype:Sex	3.87	0.025
Genotype:Treatment	0.79	0.533
Sex:Treatment	1.80	0.172
Genotype:Sex:Treatment	0.67	0.615

Post-Treatment Elevated Plus Maze Analysis Summary "% Time in Open Arms"		
	F-value	p-value
Genotype	1.48	0.234
Sex	0.02	0.884
Treatment	2.22	0.115
Genotype:Sex	0.79	0.459
Genotype:Treatment	0.71	0.588
Sex:Treatment	0.71	0.495
Genotype:Sex:Treatment	1.18	0.327



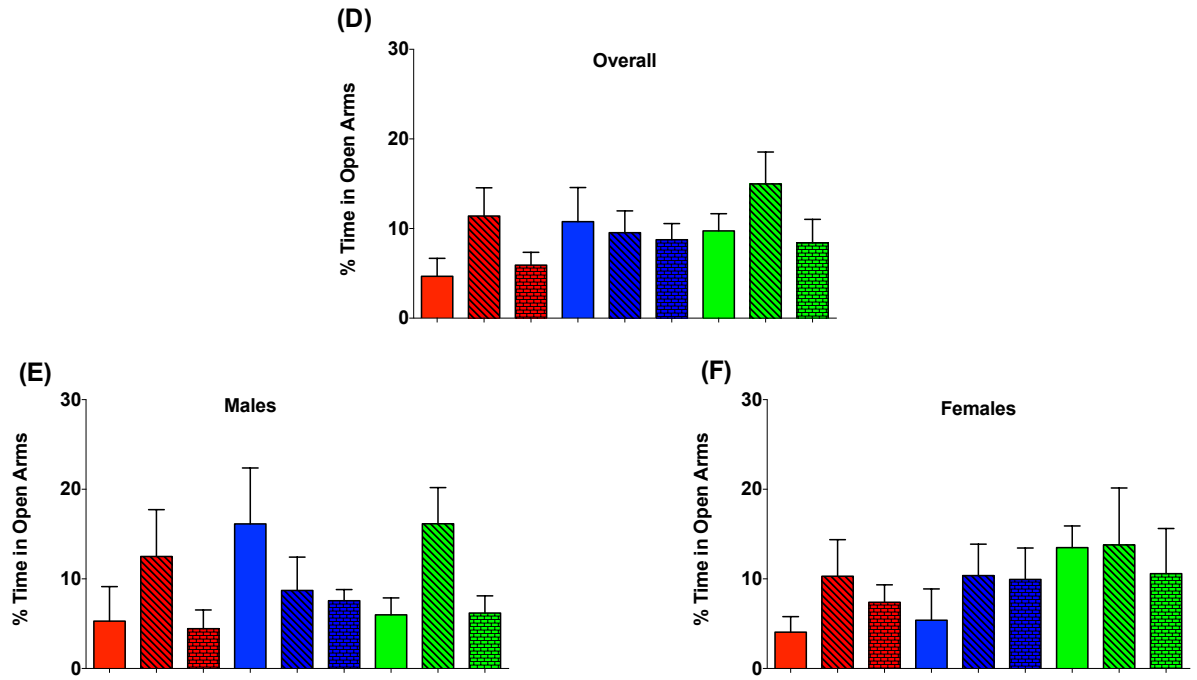


Figure 22: Post-treatment anxiety-like behaviour did not change both in HdhQ140/YFP-H model of HD and in APP_{swe}/PS1dE9/YFP-H model of AD. Mice were placed in the open-field arena and allowed to move freely for 30 min., and the percentage of time spent in the center of the arena was considered as index of anxiety-related behaviour. In the next day, mice were placed in a plus-shaped apparatus with two open and two enclosed arms and allowed to explore freely over 5 min., and the preference of time spent in the open arms was measured as index of anxiety-like behaviour. There was no significant difference ($p > 0.05$) neither on the percentage of time spent in the center of the open field arena (A - C), nor on the percentage of time spent in the elevated plus maze open arms (D - F), both used as an index of anxiety-like behaviour, in all mice groups treated/untreated with FK866/NA and memantine (n=5-6 mice/genotype, treatment and gender conditions, mean ± SEM, two-way ANOVA followed by Bonferroni post-hoc test).

Effect of drug treatment on the locomotor activity of HdhQ140/YFP-H mice, APP_{swe}/PS1dE9/YFP-H mice, and their YFP+ controls was measured using different behavioural assays. I used total number of arm entries as measured by spontaneous alternation test and elevated plus maze test in addition to total distance moved in the open field arena as measured by open field test as an index of locomotor activity in these mice.

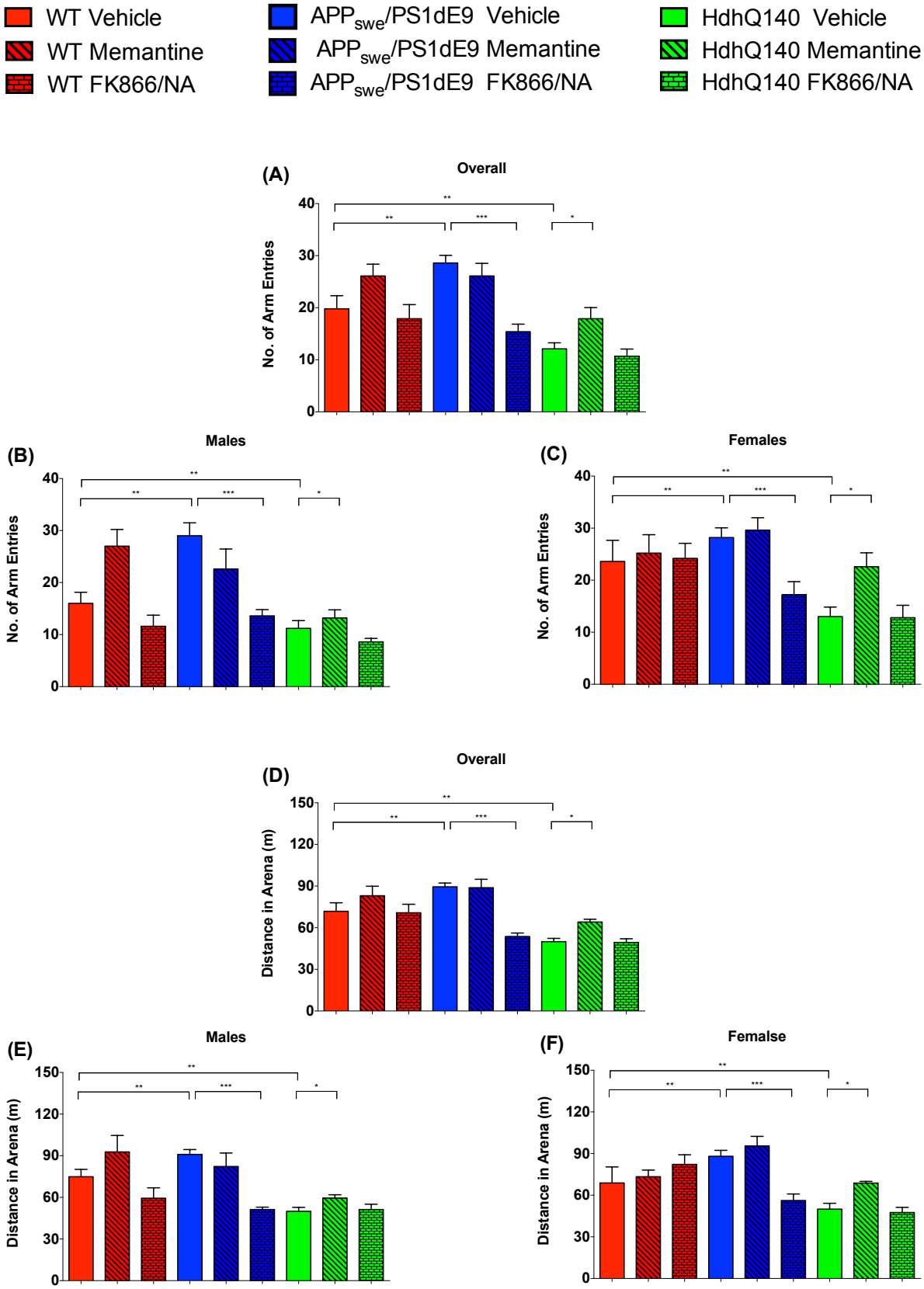
I found that FK866/NA significantly ($p < 0.001$) reduced APP_{swe}/PS1dE9/YFP-H mice hyperactivity to levels similar to those of their YFP+ vehicle-treated controls (Figure 23A - I). In addition, I found that memantine significantly ($p < 0.05$) restored the reduction in the

locomotor activity of HdhQ140/YFP-H mice to levels similar to those of their YFP+ vehicle-treated controls (Figure 23A - F).

Post-Treatment Spontaneous Alternation Analysis Summary "Number of Arm Entries"		
	F-value	**p-value**
Genotype	24.79	< 0.001
Sex	16.39	< 0.001
Treatment	18.03	< 0.001
Genotype:Sex	0.49	0.613
Genotype:Treatment	3.73	**0.008**
Sex:Treatment	0.90	0.411
Genotype:Sex:Treatment	2.80	0.032

Post-Treatment Open Field Analysis Summary "Distance in Arena"		
	F-value	**p-value**
Genotype	24.83	< 0.001
Sex	0.47	0.497
Treatment	16.92	< 0.001
Genotype:Sex	0.34	0.710
Genotype:Treatment	5.43	**< 0.001**
Sex:Treatment	1.21	0.304
Genotype:Sex:Treatment	24.83	0.020

Post-Treatment Elevated Plus Maze Analysis Summary "Entry Frequency in All Arms"		
	F-value	**p-value**
Genotype	15.31	< 0.001
Sex	1.58	0.213
Treatment	2.94	0.059
Genotype:Sex	0.47	0.629
Genotype:Treatment	5.60	**< 0.001**
Sex:Treatment	2.74	0.072
Genotype:Sex:Treatment	0.74	0.566


WT Vehicle
WT Memantine
WT FK866/NA
APPswe/PS1dE9 Vehicle
APPswe/PS1dE9 Memantine
APPswe/PS1dE9 FK866/NA
HdhQ140 Vehicle
HdhQ140 Memantine
HdhQ140 FK866/NA
(A)
Overall
No. of Arm Entries
(B)
Males
No. of Arm Entries
(C)
Females
No. of Arm Entries
(D)
Overall
Distance in Arena (m)
(E)
Males
Distance in Arena (m)
(F)
Femalse
Distance in Arena (m)

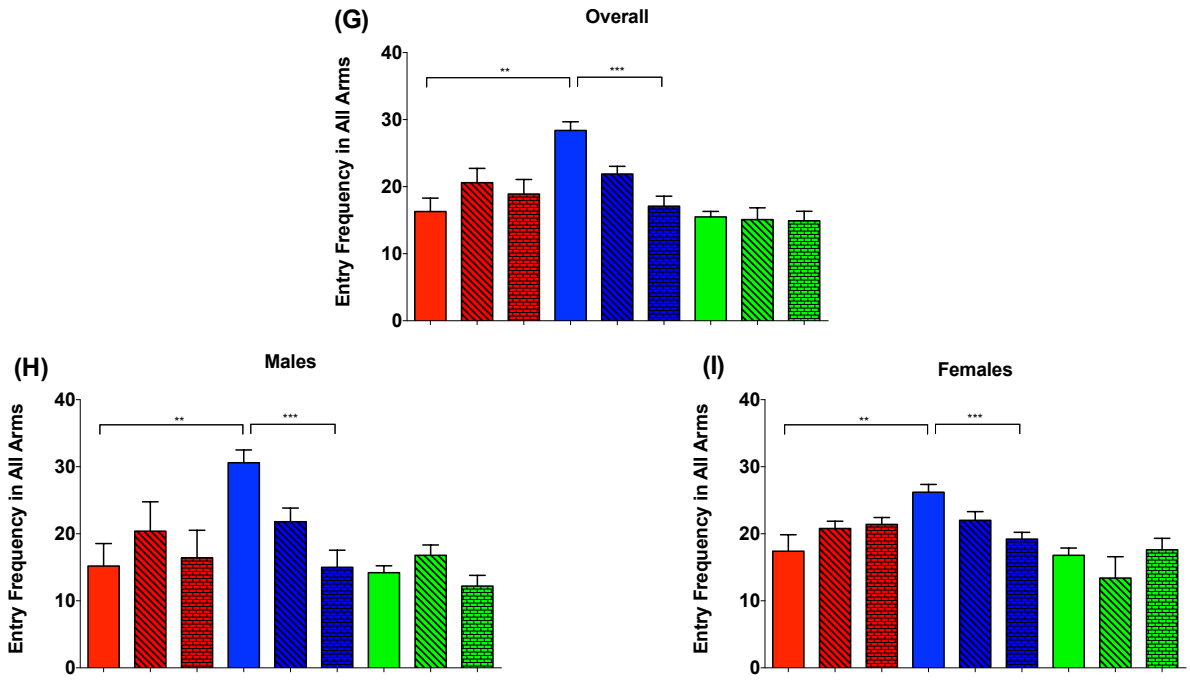


Figure 23: FK866/NA and memantine improved the locomotor activity of APP_{swe}/PS1dE9/YFP-H mice and HdhQ140/YFP-H mice respectively. Effect of drug treatment on locomotor activity of HdhQ140/YFP-H mice, APP_{swe}/PS1dE9/YFP-H mice, and their YFP+ controls was measured using different behavioural assays. I used total number of arm entries as measured by spontaneous alternation test and elevated plus maze test in addition to total distance moved in the open field arena as an index of locomotor activity in these mice. I found that FK866/NA significantly ($p < 0.001$) reduced APP_{swe}/PS1dE9/YFP-H vehicle-treated mice hyperactivity to levels similar to those of their YFP+ vehicle-treated controls (A - I). In addition, I found that memantine significantly ($p < 0.05$) restored the reduction in the locomotor activity of HdhQ140/YFP-H vehicle-treated mice to levels similar to those of their YFP+ vehicle-treated controls (A - F) (n=5-6 mice/genotype, treatment and gender conditions, mean ± SEM, two-way ANOVA followed by Bonferroni post-hoc test, ***, $p < 0.001$, **, $p < 0.01$, *, $p < 0.05$).

Memantine and FK866/NA improved the sensorimotor gating abnormalities of APP_{swe}/PS1dE9/YFP-H mice

Several studies reported impairment in sensorimotor gating (Davis, 1980) in many psychiatric disorders and also in HD and AD, both in patients and in mouse models of these neurodegenerative diseases, where disruption of corticostriatal circuits and limbic system occur (Swerdlow et al. 1995; Carter et al. 1999; Pillay et al. 2008; Wang et al. 2012). I used PPI test to assess sensorimotor processes in HdhQ140/YFP-H, APP_{swe}/PS1dE9/YFP-H mice and their YFP+ controls, and also to investigate if FK866/NA and memantine could modulate

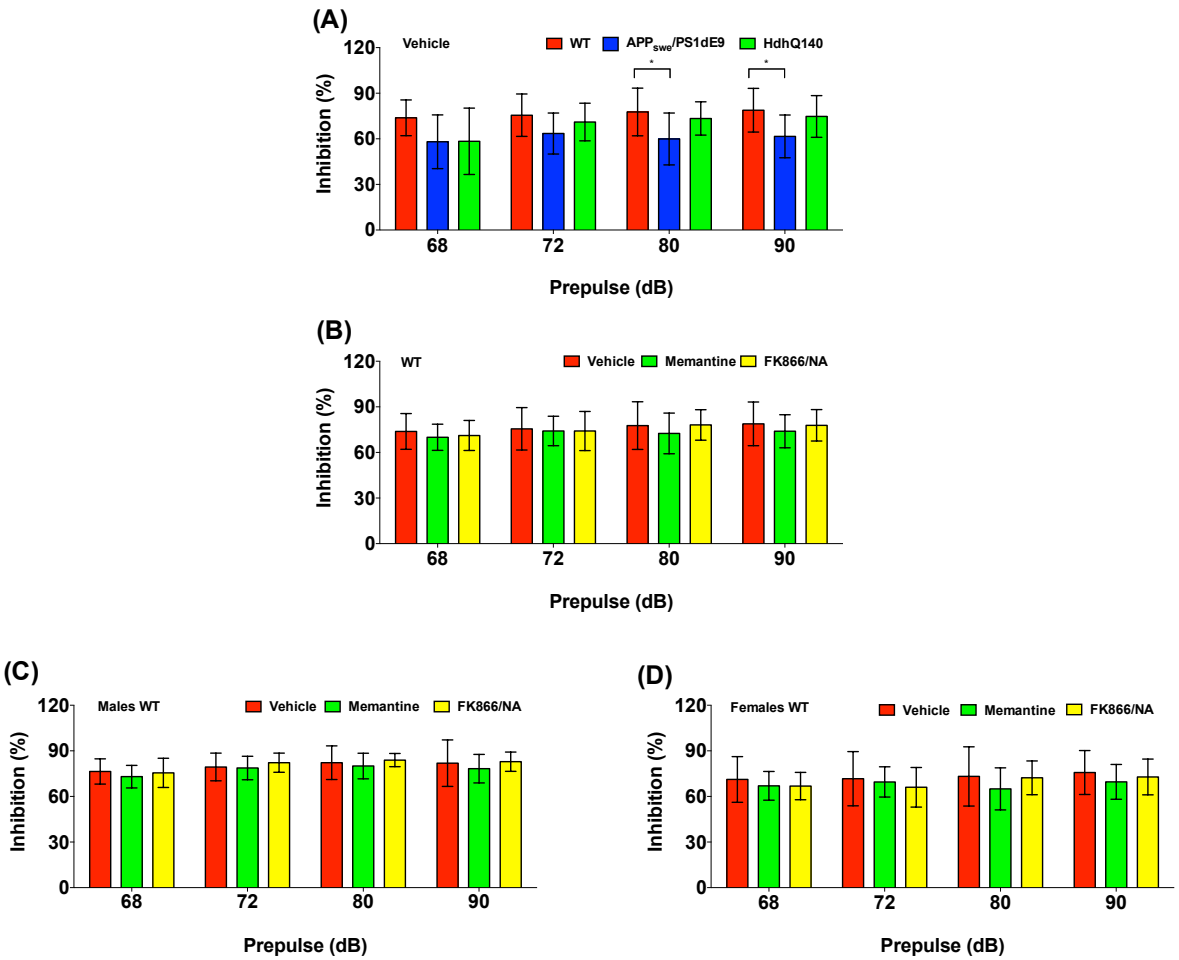
any impairment in PPI% or peak startle amplitude/latency of these mice as an index of sensorimotor gating abnormality. While there was no impairment ($p > 0.05$) of PPI parameters in HdhQ140/YFP-H mice treated/untreated with FK866/NA and memantine (Figure 24A, H - J, and K - P), PPI% at 80 and 90 dB were significantly ($p < 0.05$) reduced in APPswe/PS1dE9/YFP-H vehicle-treated mice in comparison to their YFP+ vehicle-treated controls (Figure 24A), with a significant gender effect. In addition, I found that peak startle amplitude was significantly ($p < 0.05$) lower in the AD vehicle-treated mice compared to the control vehicle-treated mice (Figure 24K - M), suggesting impairment in sensorimotor gating of these transgenic mice. Peak startle latency however was comparable ($p > 0.05$) between APPswe/PS1dE9/YFP-H vehicle-treated mice and their YFP+ vehicle-treated controls (Figure 24N - P). Our drug treatment results showed that memantine significantly ($p < 0.05$) improved the sensorimotor gating abnormalities of APPswe/PS1dE9/YFP-H vehicle-treated mice to levels similar to those of their YFP+ vehicle-treated controls (Figure 24E, F, and K - M). FK866/NA had a similar effect, although it was not that significant ($p > 0.05$) (Figure 24E, F, and K - M).

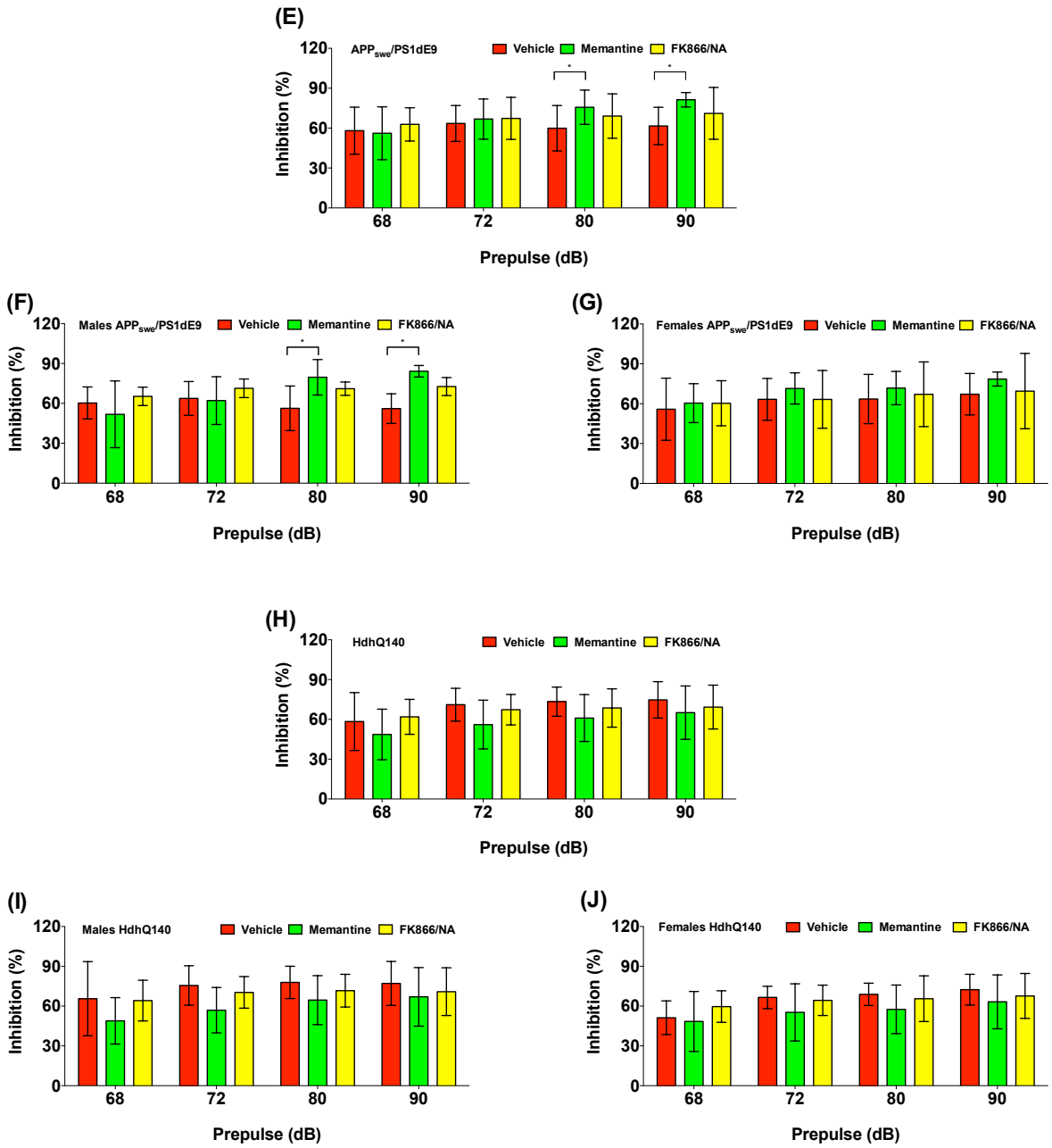
Post-Treatment PPI Analysis Summary "PPI%"		
	F-value	**p-value**
Weight (gm)	0.27	0.606
Genotype	15.86	< 0.001
Prepulse	7.73	< 0.001
Sex	6.34	0.012
Treatment	0.95	0.388
Genotype:Prepulse	0.49	0.819
Genotype:Sex	2.39	0.094
Genotype:Treatment	5.51	**< 0.001**
Prepulse:Sex	0.17	0.914
Prepulse:Treatment	0.42	0.865
Sex:Treatment	0.52	0.593
Genotype:Prepulse:Sex	0.07	0.999
Genotype:Prepulse:Treatment	0.50	0.911
Genotype:Sex:Treatment	0.59	0.667

Post-Treatment PPI Analysis Summary "Startle Amplitude"		
	F-value	**p-value**
Weight (gm)	0.87	0.354
Genotype	0.84	0.435
Sex	1.26	0.265

Treatment	1.48	0.234
Genotype:Sex	0.58	0.561
Genotype:Treatment	3.07	**0.022**
Sex:Treatment	1.16	0.321
Genotype:Sex:Treatment	1.31	0.276

Post-Treatment PPI Analysis Summary "Startle Latency"		
	F-value	**p-value**
Weight (gm)	0.14	0.713
Genotype	1.03	0.363
Sex	0.19	0.664
Treatment	0.04	0.964
Genotype:Sex	0.23	0.794
Genotype:Treatment	1.70	0.160
Sex:Treatment	0.11	0.896
Genotype:Sex:Treatment	1.10	0.365




(E)
APPswe/PS1dE9
Vehicle
Memantine
FK866/NA
Inhibition (%)
120
90
60
30
0
68
72
80
90
Prepulse (dB)
(F)
Males APPswe/PS1dE9
Vehicle
Memantine
FK866/NA
Inhibition (%)
Prepulse (dB)
(G)
Females APPswe/PS1dE9
Vehicle
Memantine
FK866/NA
Inhibition (%)
Prepulse (dB)
(H)
HdhQ140
Vehicle
Memantine
FK866/NA
Inhibition (%)
Prepulse (dB)
(I)
Males HdhQ140
Vehicle
Memantine
FK866/NA
Inhibition (%)
Prepulse (dB)
(J)
Females HdhQ140
Vehicle
Memantine
FK866/NA
Inhibition (%)
Prepulse (dB)

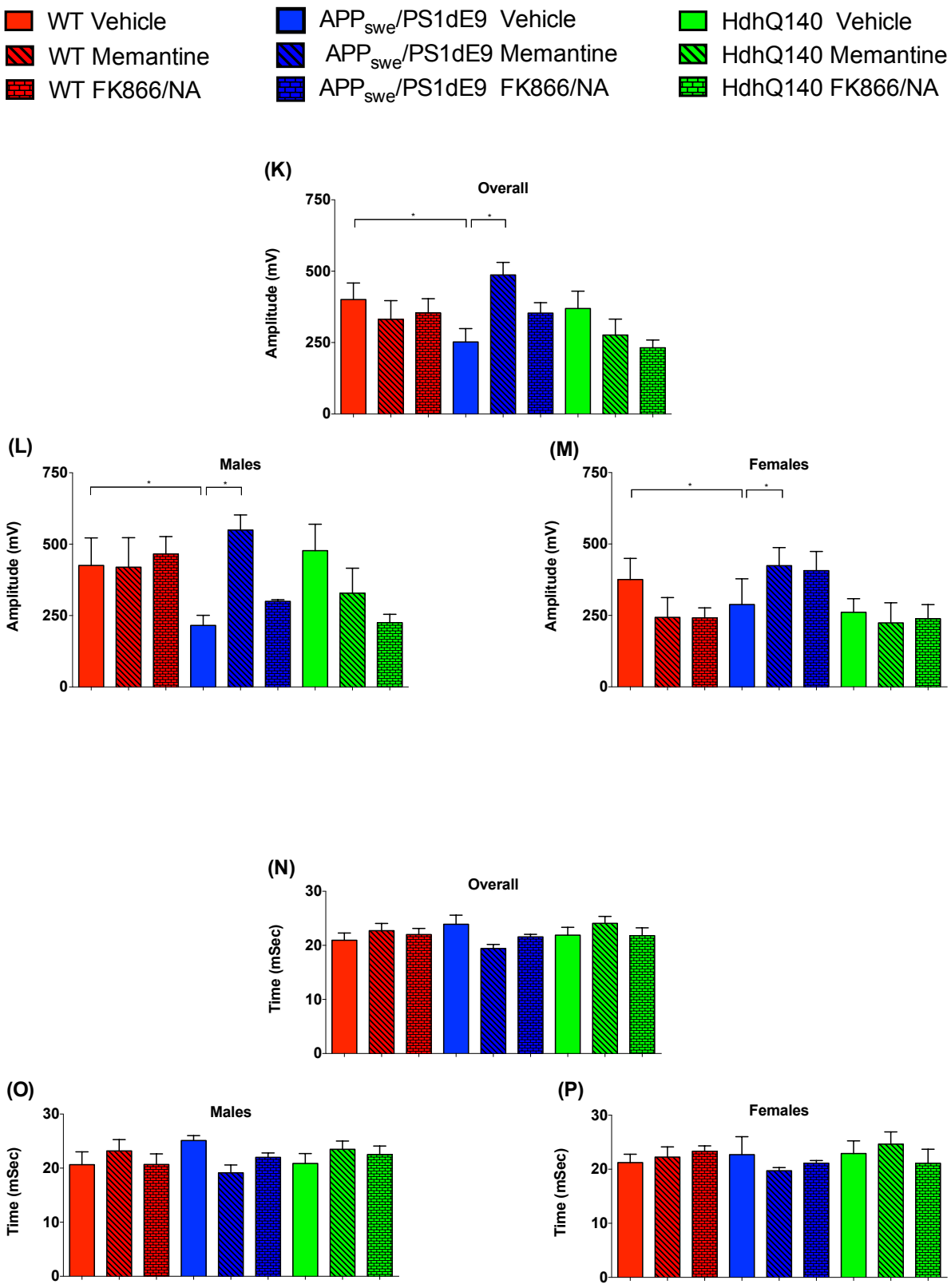

WT Vehicle
WT Memantine
WT FK866/NA
APPswe/PS1dE9 Vehicle
APPswe/PS1dE9 Memantine
APPswe/PS1dE9 FK866/NA
HdhQ140 Vehicle
HdhQ140 Memantine
HdhQ140 FK866/NA
(K)
Overall
Amplitude (mV)
750
500
250
0
(L)
Males
Amplitude (mV)
(M)
Females
Amplitude (mV)
(N)
Overall
Time (mSec)
30
20
10
0
(O)
Males
Time (mSec)
(P)
Females
Time (mSec)

Figure 24: Memantine and FK866/NA improved the sensorimotor gating abnormalities of APP_{swe}/PS1dE9/YFP-H mice. Drug treatment did not alter PPI parameters in HdhQ140/YFP-H mice. Mice were placed into a Plexiglas cylinder inside a chamber, a speaker was producing acoustic stimuli, and PPI parameters were detected and recorded as measure of sensory gating. While there was no change ($p > 0.05$) in PPI parameters of HdhQ140/YFP-H treated/untreated mice (A, H - J, and K - P), PPI% at 80 and 90 dB were significantly ($p < 0.05$) reduced in APPswe/PS1dE9/YFP-H vehicle-treated mice in comparison to their YFP+ vehicle-treated controls (A). In addition, peak startle amplitude was significantly ($p < 0.05$) lower in APPswe/PS1dE9/YFP-H vehicle-treated mice in comparison to their YFP+ vehicle-treated controls (K - M), suggesting impairment in sensorimotor gating of these transgenic mice. Peak startle latency however was comparable between APPswe/PS1dE9/YFP-H vehicle-treated mice and their YFP+ vehicle-treated controls (N - P). Our drug treatment results showed that memantine significantly ($p < 0.05$) improved sensorimotor gating abnormalities of APPswe/PS1dE9/YFP-H mice to levels similar to those of their YFP+ vehicle-treated controls, with a significant gender effect. (E, F, and K - M). (n=5-6 mice/genotype, treatment and gender conditions, mean ± SEM, two-way ANOVA followed by Bonferroni post-hoc test, *, $p < 0.05$).

3.5 Discussion

The majority of the treatments for neurodegenerative diseases, including HD and AD focused only on cellular compartment and with limited or no success, while axonal compartment had been neglected and left untreated despite its importance. This could be due to the lack of information about the pathogenesis of axon degeneration, and therefore the lack of specific molecular targets. Our results show that the NAMPT inhibitor FK866 (in combination with NA) and the NMDARs antagonist memantine significantly restored the locomotor abnormalities of APPswe/PS1dE9/YFP-H mice and HdhQ140/YFP-H mice respectively to levels similar to those of their YFP+ vehicle-treated controls, with no effect on motor balance, learning and coordination, spatial working memory, and anxiety-like behaviour. In addition, I found that memantine improved the sensorimotor gating abnormalities of APPswe/PS1dE9/YFP-H mice to levels similar to those of their YFP+ vehicle-treated controls.

Before characterizing the effect of drug treatment on HD and AD *in vivo* models, I subjected our mice to a baseline set of behavioural assays to check their general activity and compare it to their YFP+ controls. I found that motor balance, learning and coordination was significantly impaired in HdhQ140/YFP-H model of HD in comparison to their YFP+ controls, and the effect was particularly clear at day 3 of the rotarod learning curve. This could be explained by increased apathy and lack of motivation in these mice that are in line

with findings in human HD patients (Paulsen et al. 2011; Rosas et al. 2008). Motor functions were significantly impaired also in APPswe/PS1dE9/YFP-H model of AD in comparison to their YFP+ controls, and again the effect was particularly clear at day 3 of the rotarod learning curve. This could be explained by the well-documented hyperactivity of APPswe/PS1dE9/YFP-H mice (Hooijmans et al. 2004; Cheng et al. 2013), and was also noticed by the tendency of these mice to quickly jump off the rod. Regarding the spatial working memory and locomotor activity, I found no significant difference in the total number of arm entries, and also in the percentage of alternations in all mice, and neither genotype nor gender effects were found.

Immediately after baseline behavioural assays, I injected HdhQ140/YFP-H and APPswe/PS1dE9/YFP-H mice with vehicle, or FK866 in combination with NA, or memantine for 2 weeks, and then I performed a more detailed set of behavioural assays including sensorimotor, learning and memory assays. I continued drug treatment while doing these detailed behavioural assays to exclude the possibility that these drugs may be washed out and affect on the reliability of the results. However, I have to bear in my mind the limitations of doing the behavioural assays while the mice are still receiving drug treatment. These drugs may act on a target other than the axon, and so may consequently modulate the behavioural phenotype of these mice.

Locomotor abnormalities were the main behavioural disturbances detected in HD and AD mice whose age post-treatment were 6 months. In line with previous findings (Hooijmans et al. 2004; Cheng et al. 2013), APPswe/PS1dE9/YFP-H vehicle-treated mice showed significant increase in locomotor activity or hyperactivity in comparison to their YFP+ vehicle-treated controls. Other studies however reported no alteration in locomotion of APPswe/PS1dE9/YFP-H mice (Melnikova et al. 2006; Reiserer et al. 2007). In the other hand, HdhQ140/YFP-H vehicle-treated mice showed significant decrease in locomotor activity in comparison to their YFP+ vehicle-treated controls that is consistent with the well-documented reports of increased apathy and lack of motivation in human HD patients (Paulsen et al. 2011; Rosas et al. 2008). Drug treatment results showed that FK866/NA and memantine significantly restored the impairment in locomotor activity of AD and HD mice respectively to levels similar to those of their YFP+ vehicle-treated controls. This interesting finding was consistent in the three behavioural assays used for the assessment of locomotor activity in these mice.

Sensorimotor gating abnormalities were also detected in APPswe/PS1dE9/YFP-H vehicle-treated mice in comparison to their YFP+ vehicle-treated controls, especially in APPswe/PS1dE9/YFP-H male mice. This is consistent with several studies, which reported impairment in sensorimotor gating both in patients and in mouse models of AD, and can be directly correlated with Aβ burden (Jessen et al. 2001; Cancelli et al. 2006; Pillay et al. 2008; Wang et al. 2012). Reduced PPI% was found at 80 and 90 dB, together with alternation in peak startle amplitude, which was significantly lower in the AD mice compared to the control mice. Peak startle latency however was comparable between APPswe/PS1dE9/YFP-H mice and their YFP+ controls. Drug treatment results showed that memantine significantly improved the sensorimotor gating abnormalities of APPswe/PS1dE9/YFP-H vehicle-treated mice to levels similar to those of their YFP+ vehicle-treated controls. In the other hand, I found no impairment in PPI parameters of HdhQ140/YFP-H vehicle-treated mice in comparison to their YFP+ vehicle-treated controls at the time-points considered.

Finally, cognitive function tests used in this *in vivo* study recorded no difference in motor balance, learning and coordination as measured by rotarod test, in spatial working memory as measured by spontaneous alternation test, and also in anxiety-like behaviour as measured by open field test and elevated plus maze test in all mice groups treated/untreated with FK866/NA and memantine.

It is very important to emphasize that some of the reported behavioural manifestations in APP_{swe}/PS1dE9/YFP-H mice were inconsistent across different laboratories. This could be due to the characteristics of the particular APP_{swe}/PS1dE9/YFP-H mouse model tested, i.e. number of backcrosses onto C57BL/6J background, sex of the test animals, and methodology used to analyze the behavioural assay, for example test duration and the level of stress caused by test apparatus.

While memantine had not been tested before in HdhQ140/YFP-H knock-in mouse model of HD, many studies had characterized the effect of this NMDARs antagonist in APPswe/PS1dE9/YFP-H transgenic mouse model of AD. Minkeviciene et al. 2004 found that 30 mg/kg/day p.o. memantine for 2-3 weeks significantly improved the acquisition of Morris water maze in APP_{swe}/PS1dE9/YFP-H mice without affecting swimming speed, locomotor activity or aggressive behaviour. Another study by Filali et al. 2011 found that 10 mg/kg/day i.p. memantine for 3 weeks was better than placebo during the reversal phase of left-right discrimination, though equivalent to saline for Morris water maze and passive avoidance

learning in APP_{swe}/PS1dE9/YFP-H mice with no effect on non-learned behaviours in elevated plus-maze exploration and nest building.

In conclusion, our *in vivo* study found that locomotor impairment is the major behavioural abnormality detected in 6 months old APPswe/PS1dE9/YFP-H mice and HdhQ140/YFP-H mice, and FK866/NA and memantine respectively restored this impairment to levels similar to those of their YFP+ vehicle-treated controls. Sensorimotor impairment is another behavioural abnormality detected in 6 months old APPswe/PS1dE9/YFP-H mice, and it is corrected with memantine. Cognitive function assays used in this study revealed no abnormality in all mice groups treated/untreated with FK866/NA and memantine at the time-point considered.

Chapter 4:

FK866 ameliorated axonal swelling and dystrophy abnormalities in *in vivo* models of Huntington's disease (HD) and Alzheimer's disease (AD) respectively

4.1 Introduction

Inhibiting the synthesis of the NAD precursor NMN with the NMN-synthesizing enzyme NAMPT inhibitor FK866 (Hasmann and Schemainda, 2003) (Figure 9), strongly protects axons *in vitro, ex-vivo* and *in vivo* after acute injury (Di Stefano et al. 2014). FK866 in combination with NA also significantly improved axonal morphology in *in vitro* models of HD and Aβ toxicity, an effect that is consistently reverted with NMN (chapter 2). In addition, FK866/NA restored some of the behavioural abnormalities in *in vivo* models of HD and AD (chapter 3). Here I wanted to analyse whether FK866-mediated behavioural improvement is accompanied by a beneficial effects on a number of neuropathological hallmarks of HdhQ140/YFP-H *in vivo* model of HD and APP_{swe}/PS1dE9/YFP-H *in vivo* model of AD, and I compared it to the reported neuroprotective effects of the NMDARs antagonist memantine. Expression of YFP protein in these *in vivo* models makes it possible labelling multiple neuronal subsets *in vivo* and also allows imaging of neuronal structures including axons (Beirowski et al. 2004; Coleman et al. 2005; Enright et al. 2007), and detection of axonal dystrophy (Bridge et al. 2009; Adalbert et al. 2009).

The YFP-H transgenic mice were first generated in 2000 by Feng and collaborators, together with other mice lines (25 lines) in which red (RFP), green (GFP), yellow (YFP), or cyan (CFP) fluorescent proteins (together termed XFPs) were selectively labelled neurons in their entirety, including axons, nerve terminals, dendrites, and dendritic spines under the control of the modified neuron-specific promoter Thy-1.2 (Feng et al. 2000). The generation of the XFP mice have several advantages over the classical techniques used for visualizing neurons and their compartments, like immunohistochemistry, electron microscopy, and Golgi staining. XFPs could label axons over centimetre-long distances and dendrites over millimetre-long distances, even when they are not fused to peptides that facilitate their transport (Feng et al. 2000). In addition, expression of XFPs for up to 9 months had no detectable *in vivo* toxicity and also had no effect on synaptic structure (Feng et al. 2000). Another study however reported significant increase in axonal swelling in gracile tract, gracile nucleus and dorsal roots but not in lateral columns, olfactory bulb, motor cortex, ventral roots or peripheral nerve in YFP-H transgenic mice aged 8 months or over compared with their YFP- controls (Bridge et al. 2009). Thus, long-term expression of YFP protein may accelerates age-related axonal swelling in some axons and data reliant on the presence of YFP protein in these CNS regions in older animals needs to be interpreted carefully (Bridge et al. 2009). Another feature of the XFP transgenic mice is that XFP expression varies significantly among the 25

lines generated from the same construct, and it is most prominent in those neurons that are Thy1 positive (Feng et al. 2000). For example, Thy1 is present at high levels on all motoneurons and sensory neurons, and XFP fluorescent proteins are expressed by many or all such neurons in 21/25 lines. In the other hand, Thy1 is hardly detectable on cortical and cerebellar neurons, and XFP fluorescent proteins are expressed on a minority of these neurons in most lines (Feng et al 2000). A comprehensive mapping of labeled cell types throughout CNS in adult and postnatal (P0–P30) YFP-H transgenic mice has been provided (Porrero et al. 2010). The YFP transgene is selectively expressed in layers 5 and 6 neocortical pyramidal neurons in addition to large populations of hippocampal, subicular and amygdaloid projection neurons (Porrero et al. 2010).

The YFP-H transgenic mice were extensively used to assess neurodegeneration both in CNS and PNS. Crossing this line with *Wld*^{S} transgenic mice have been used for quantitative and qualitative analysis of Wallerian degeneration *in vivo* (Beirowski et al. 2004), and also to study axonal and dendritic damage induced by ischemic damage (Zhang et al. 2005; Enright et al. 2007). In another study, YFP-H line was crossed with TgCRND8 transgenic mouse model of AD to trace dystrophic axons and dendrites back to their cell bodies and see if they are precursors of irreversible neuron damage (Adalbert et al. 2009). Adalbert and his colleagues found that almost all TgCRND8 axons retain continuity throughout the disease course even across highly dystrophic regions up to 6 months and most for up to 1 year, and the corresponding cell bodies were morphologically normal and metabolically active and remain capable of supporting their processes, raising the prospect of a therapeutic window for functional rescue of individual neurons after their axons become highly dystrophic (Adalbert et al. 2009). YFP-H line was also crossed with 5xFAD transgenic mouse model of AD in order to analyse the structural changes that occur in these AD mice longitudinally and link it to Aβ plaques (Crowe et al. 2013). Results revealed that simple dystrophies were transient in nature and not directly associated with Aβ plaques, while Rosette dystrophies were more complex structures and always surrounded an Aβ plaque (Crowe et al. 2013). In another study, YFP-H line was crossed with HdhQ140 knock-in mouse model of HD to investigate axon degeneration in this model, and to assess whether this occurs early in and contributes to the course of pathology (Marangoni et al. 2014). Axonal morphology in HdhQ140/YFP-H mice was strikingly abnormal is some brain areas where axonal swellings were detected at 6 months and at 12 months of age in stria terminalis and striatum (Marangoni et al. 2014). In

the other hand, cell bodies, dendrites and synapses appeared normal suggesting that axonal pathology is the main feature of the disease in this model (Marangoni et al. 2014).

In our study, I characterized axonal swellings and dystrophies in addition to nuclear and dendritic morphology in HdhQ140/YFP-H and APP_{swe}/PS1dE9/YFP-H *in vivo* models of HD and AD respectively in comparison to their YFP+ controls, and examined whether FK866/NA treatment for 3 weeks could modulate any structural abnormality in these mice and compared it to the reported neuroprotective effects of memantine.

4.2 Aims of The Study

This study aims to test the hypothesis that FK866 neuroprotective properties in *in vitro* and *in vivo* models of HD and AD could extend beyond that and also modulate axonal damage in HdhQ140/YFP-H and APP_{swe}/PS1dE9/YFP-H *in vivo* models of these neurodegenerative disease, and to compare this to the reported neuroprotective effects of memantine.

4.3 Materials and Methods

Tissue preparation and sectioning. After finishing the detailed behavioural assays, HdhQ140/YFP-H and APP_{swe}/PS1dE9/YFP-H mice, together with their corresponding YFP+ controls, were perfused transcardially with 4% phosphate buffered PFA and their brains were dissected and processed. Brain samples were post-fixed by overnight immersion in the same fixative and then cryoprotected in 30% sucrose at 4°C for at least 48 h before processing. Each brain sample was cut into 2 halves, one stored in -80°C for future works and the other sectioned into 50 µm slices using a Leica CM1850 cryostat.

Immunohistochemistry. After cryostat sectioning, slices were rehydrated for at least 40 min. in PBS, then mounted on slides (super frost slides™). For characterizing the co-localization of axonal and dendritic dystrophies and Aβ plaques in APP_{swe}/PS1dE9/YFP-H mice, slices were blocked with 5% normal gout serum (Sigma-Aldrich™) in PBS (blocking buffer) at room temperature for 1 hour, incubated with 1:1000 monoclonal anti-β-amyloid primary antibody (produced in mouse) (Sigma-Aldrich™) at 4°C overnight, washed 3 times for 5

min. with PBS, incubated with 1:200 goat anti-mouse Alexa Fluor 568 secondary antibody (Invitrogen™) at room temperature for 1 hour, and then washed 3 times for 5 min. with PBS. For characterizing nuclear morphology, slices were incubated with 1:500 Hoechst stain (Invitrogen™) at room temperature for 10 min., and then washed 3 times for 5 min. with PBS. Lastly, few drops of Vectashield mounting media (Vector Laboratories) were added and slides were covered with coverslips. Negative controls in which slices were incubated with PBS and not with anti-β-amyloid antibody were used to test the specificity of this primary antibody. Images were acquired using the DMIRB fluorescent microscope or the Zeiss LSM 710 confocal microscope at 1 Airy Unit (AU) with the following excitation/emission filters: DAPI/Hoechst: 405 nm/420 – 480 nm, YFP: 488 nm/505 – 550 nm, Alexa Fluor 568: 561 nm/575 – 615 nm.

Imaging and quantitative analysis. All quantitative analyses were performed using ImageJ.

- For morphological characterization of YFP+ neurons, images were acquired with a 10X air-objective and number of axonal swellings/dystrophies in cortex, striatum dorsal, striatum ventral, and stria terminalis (Figure 25) were quantified within 5 sagittal sections/mouse (n = 5-6 mice/genotype, treatment and gender conditions). A cut-off of approximately 5 μm was used for swellings quantification.

- For morphological characterization of nuclei, images were acquired with a 40X oil-objective and nuclear area in cortex and amygdala were quantified within 4 sagittal sections/mouse (n = 5-6 mice/genotype, treatment and gender conditions).

- For morphological characterization of dendrites, images were acquired with a 40X oil-objective and proximal and distal dendrites diameter and spines number in cortex were quantified within 4 sagittal sections/mouse (n = 5-6 mice/genotype, treatment and gender conditions).

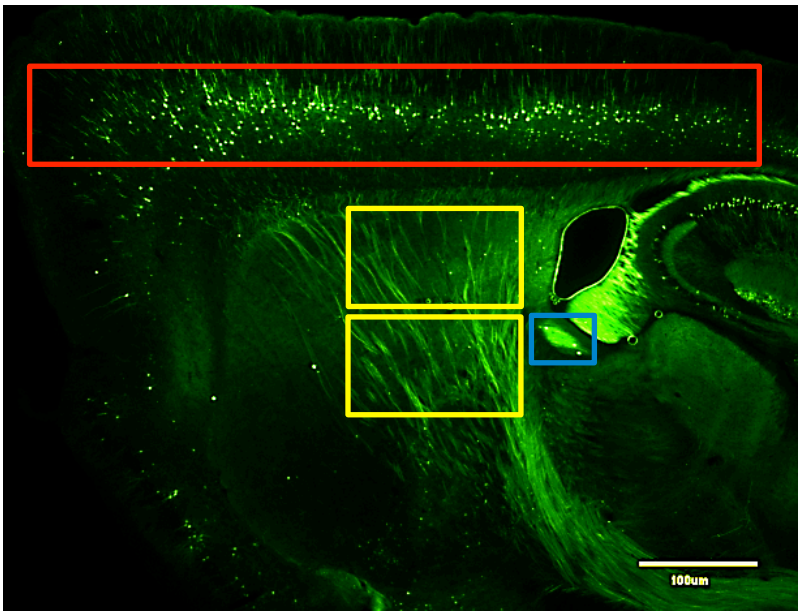


Figure 25: Fluorescent microscopy image (2.5X) of sagittal brain section (50 µm) of 6-months old WT/YFP-H mouse. The red box indicates the brain area of cortex, the upper yellow box indicates the brain area of striatum dorsal, the lower yellow box indicates the brain area of striatum ventral, and the blue box indicates the brain area of stria terminalis. Scale bar, 100 µm.

Statistical analysis. Data were presented as mean ± SEM. Two- or Three-way ANOVA was used for statistical analysis followed by Bonferroni post-hoc test. Group comparison was considered statistically significant when p-value was < 0.05.

4.4 Results

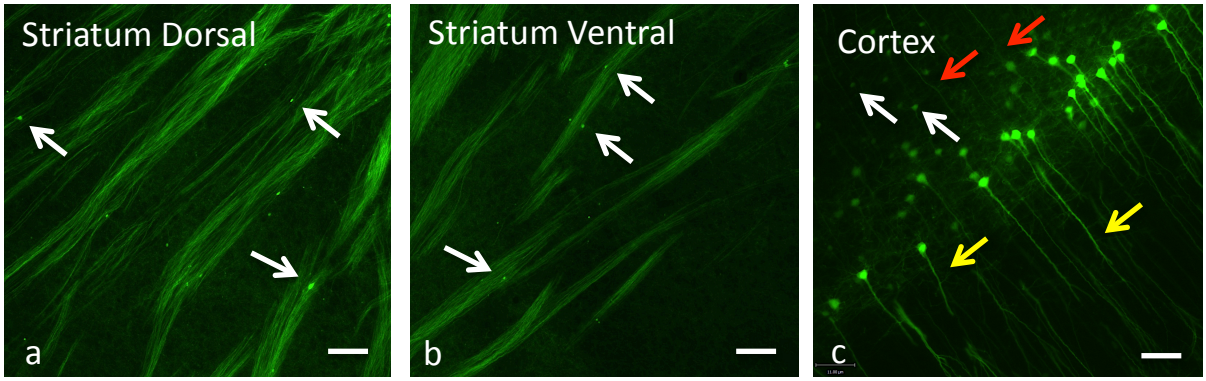
Axonal swellings in stria terminalis were an early feature of HdhQ140/YFP-H mice, while cortical dystrophies were a characteristic phenomenon of APP_{swe}/PS1dE9/YFP-H mice

Crossing HdhQ140 knock-in mouse model of HD and APP_{swe}/PS1dE9 transgenic moue model of AD with YFP-H line allows tracing individual neurons running from cortical layer V toward striatum dorsal and striatum ventral passing through corpus callosum, and therefore enables visualization of neuronal structures in detail with no detectable *in vivo* toxicity (Adalbert et al. 2009; Marangoni et al. 2014).

At 6 months old and as recently reported (Marangoni et al. 2014), there was no significant difference ($p > 0.05$) in the number of axonal swellings in striatum dorsal (Figure 26A(a), 26B(a - c)), striatum ventral (Figure 26A(b), 26B(d – f)), and cortex (Figure 26A(c), 26B(g – i)) in all mice, and neither genotype nor gender effects were found. However, a striking increase in swellings was detected in HdhQ140/YFP-H mice axons running through stria terminalis (Figure 27A(c), 27B(a – c)), a limbic forebrain structure located in the proximity of striatum and lateral ventricle. Quantification revealed a significant ($p < 0.001$) increase in axonal swellings number in stria terminalis of HD mice in comparison to their YFP+ controls (Figure 27B(a - c)). These findings are consistent with Marangoni et al. 2014 study, which reported a significant increase in the number of axonal swellings in stria terminalis of 6-months old HdhQ140/YFP-H, and the effect was even greater at 12-months old (Marangoni et al. 2014). In the other hand, there was no significant difference ($p > 0.05$) in the number of axonal swellings in stria terminalis of APP_{swe}/PS1dE9/YFP-H mice in comparison to their YFP+ controls (Figure 27B(a - c)).

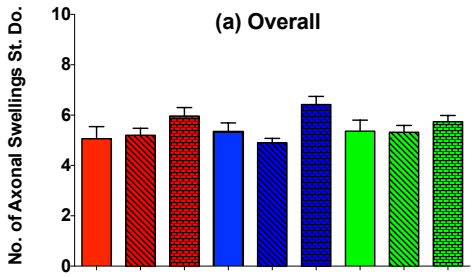
Consistent with previous reports (Jankowsky et al. 2004), quantification of the number of cortical dystrophies in APP_{swe}/PS1dE9/YFP-H mice revealed a big increase in cortical dystrophies in these transgenic mice at 6-months old (Figure 28A(a)) in comparison to their YFP+ controls, which show morphologically intact cortical neurons and projections. In addition, I found that these dystrophies co-localized with the deposition of Aβ plaques (Figure 29(d)), and axons retain their continuity and remain morphologically normal even at the most severely dystrophic plagues (Figure 29(a-d)). Interestingly and consist with previous studies (Wang et al. 2003), APP_{swe}/PS1dE9/YFP-H female mice developed higher cortical dystrophies number and bigger Aβ plaques deposits compared to APP_{swe}/PS1dE9/YFP-H male mice of the same age. Quantification revealed a significant ($p < 0.001$) gender difference in the number of cortical dystrophies in 6-months old APP_{swe}/PS1dE9/YFP-H mice (Figure 28B). Number of cortical dystrophies was significantly ($p < 0.001$) higher in APP_{swe}/PS1dE9/YFP-H female mice than in APP_{swe}/PS1dE9/YFP-H male mice (Figure 28B).

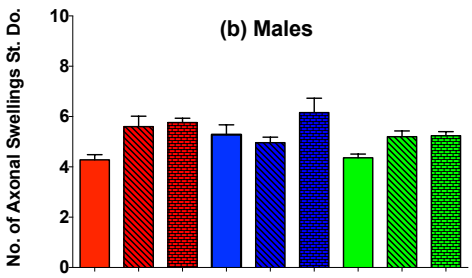
(A)

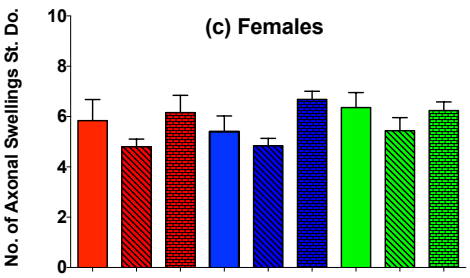


(B)

WT Vehicle
WT Memantine
WT FK866/NA
APP_{swe}/PS1dE9 Vehicle
APP_{swe}/PS1dE9 Memantine
APP_{swe}/PS1dE9 FK866/NA
HdhQ140 Vehicle
HdhQ140 Memantine
HdhQ140 FK866/NA







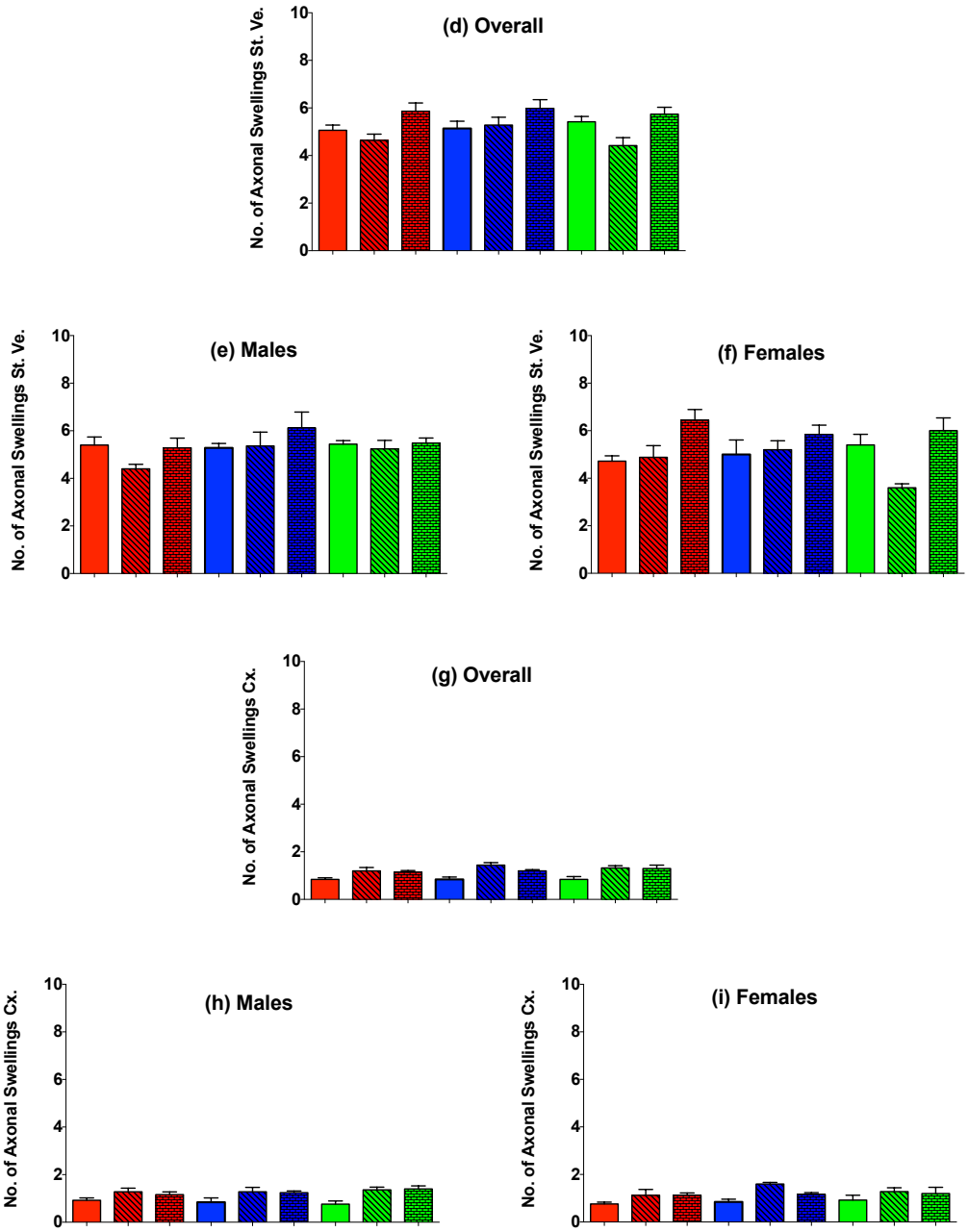


Figure 26: Corticostriatal neurons show no change in axonal swellings both in HdhQ140/YFP-H model of HD and in APP$_{swe}$/PS1dE9/YFP-H model of AD at 6-months old. (A) Fluorescent microscopy images (10X) of sagittal brain sections (50 µm) of 6-months old WT/YFP-H mouse show axonal swellings in striatum dorsal (white arrows, a), striatum ventral (white arrows, b), and cortex (white arrows, c, yellow arrows represent the dendrites, while red arrows represent the axons). (B) Quantification of axonal swellings shows no significant difference ($p > 0.05$) in their number in striatum dorsal (a - c), striatum ventral (d - f), and cortex (g - i) in all mice treated/untreated with FK866/NA and memantine, and neither genotype nor gender effects were found. Interestingly, number of axonal swellings was significantly higher in striatum than that in cortex in all mice groups (n=5-6 mice/genotype, treatment and gender conditions, mean ± SEM, two-way ANOVA followed by Bonferroni post-hoc test). Green = YFP, St. Do. = Striatum Dorsal, St. Ve. = Striatum Ventral, Cx. = Cortex. Scale bar, 50 µm.

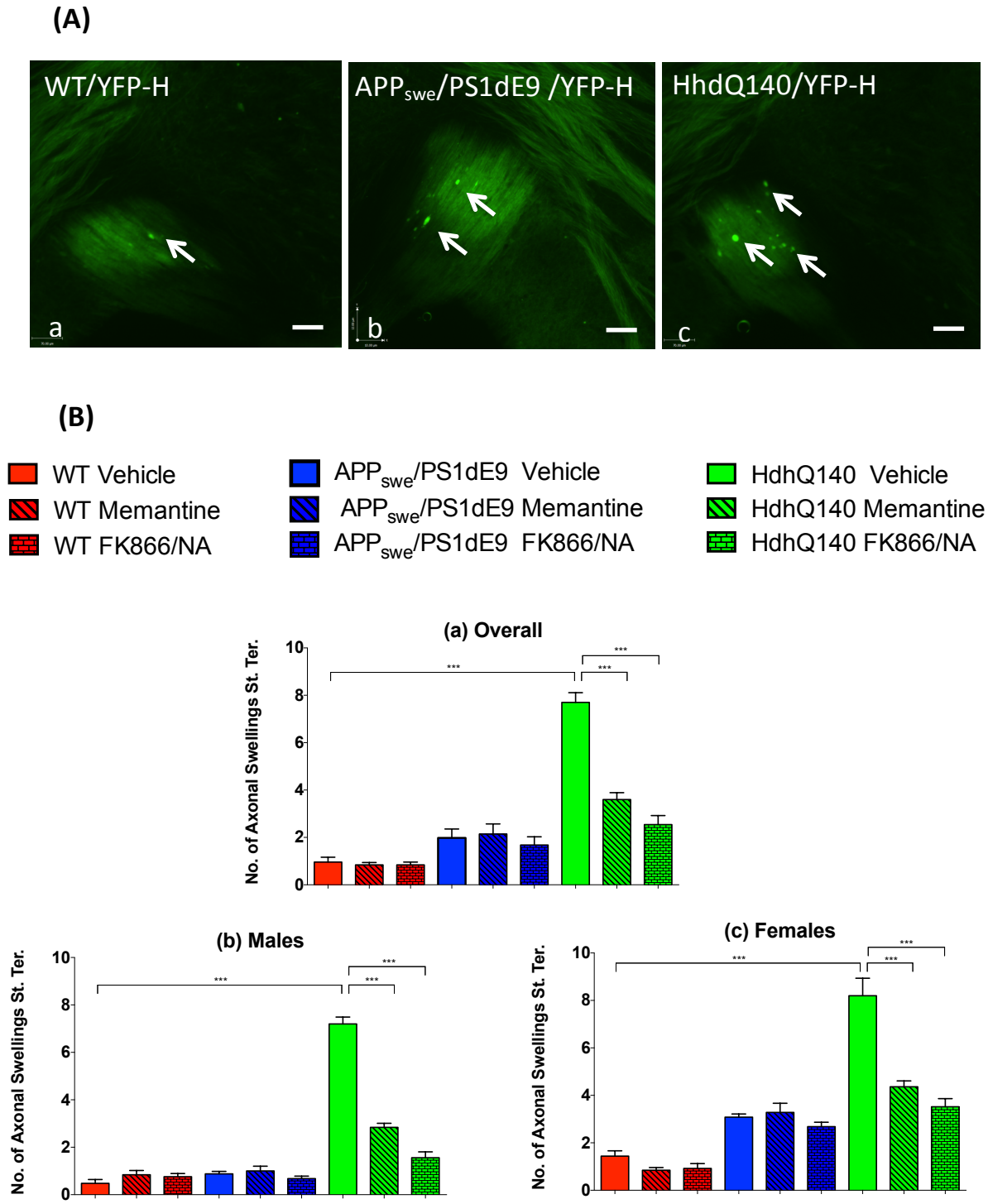


Figure 27: Axonal swellings in stria terminalis of HdhQ140/YFP-H mice are ameliorated with FK866/NA and memantine. (A) Fluorescent microscopy images (10X) of sagittal brain sections (50 µm) of 6-months old WT/YFP-H (a), APP_{swe}/PS1dE9 /YFP-H (b), and HdhQ140/YFP-H (c) mice, show swellings in axons running through stria terminalis (white arrows, a, b, and c). (B) Morphological characterization of axons running through stria terminalis show a significant increase ($p < 0.001$) in the number of axonal swellings in stria terminalis of HdhQ140/YFP-H mice (a - c) in comparison to their YFP+ controls. Interestingly, both FK866/NA and memantine significantly ($p < 0.001$) reduced the number of these swellings in this area, and the reduction was

consistent in both males and females (a - c). In the other hand, there was no significant difference ($p > 0.05$) in the number of axonal swellings in stria terminalis of APP_{swe}/PS1dE9/YFP-H mice (a - c) in comparison to their YFP+ controls. (n=5-6 mice/genotype, treatment and gender conditions, mean ± SEM, two-way ANOVA followed by Bonferroni post-hoc test, ***, $p < 0.001$). Green = YFP, St. Ter. = Stria Terminalis. Scale bar, 50 µm.

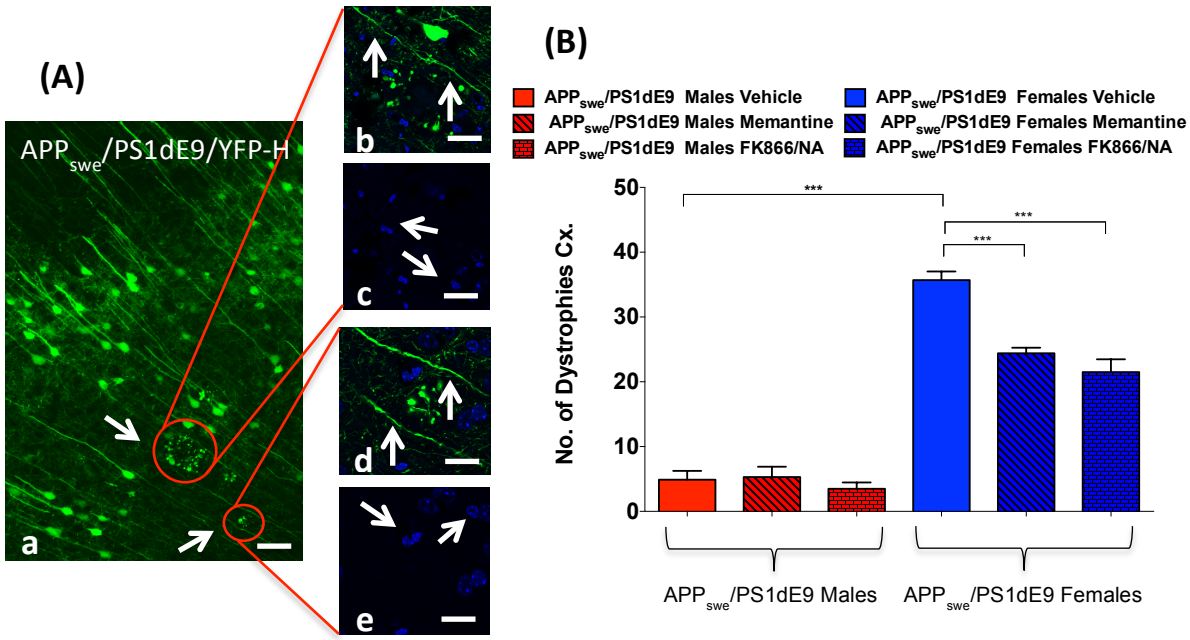


Figure 28: Cortical dystrophies in APP_{swe}/PS1dE9/YFP-H mice are decreased with FK866/NA and memantine. (A) Confocal microscopy images (10X) of sagittal brain sections (50 µm) of 6-months old APP_{swe}/PS1dE9/YFP-H mouse (a) show cortical neurons with severe, proximal axonal dystrophies (white arrows, a). Enlarged images (40X, left) show axons retain their continuity and remain morphologically normal around the dystrophies (white arrows, b and d). Nuclei (stained with blue Hoechst dye) also retain normal size, location, and morphology (white arrows, c and e). (B) Number of cortical dystrophies was significantly ($p < 0.001$) higher in APP_{swe}/PS1dE9/YFP-H vehicle-treated female mice than in APP_{swe}/PS1dE9/YFP-H vehicle-treated male mice. Interestingly, both FK866/NA and memantine significantly ($p < 0.001$) reduced the number of cortical dystrophies in APP_{swe}/PS1dE9/YFP-H female mice. (n=5-6 mice/genotype, treatment and gender conditions, mean ± SEM, two-way ANOVA followed by Bonferroni post-hoc test, ***, $p < 0.001$). Green = YFP, Blue = Hoechst, Cx. = Cortex. Scale bar (a), 50 µm; Scale bar (b - e), 20 µm.

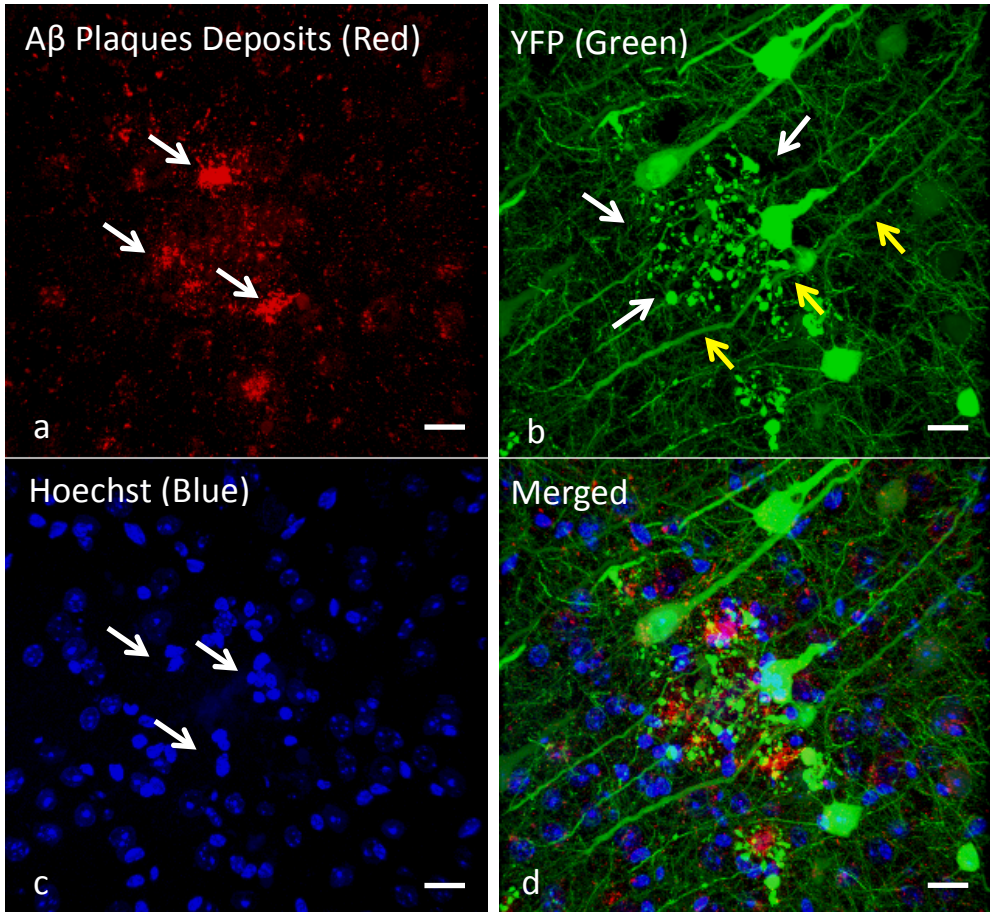
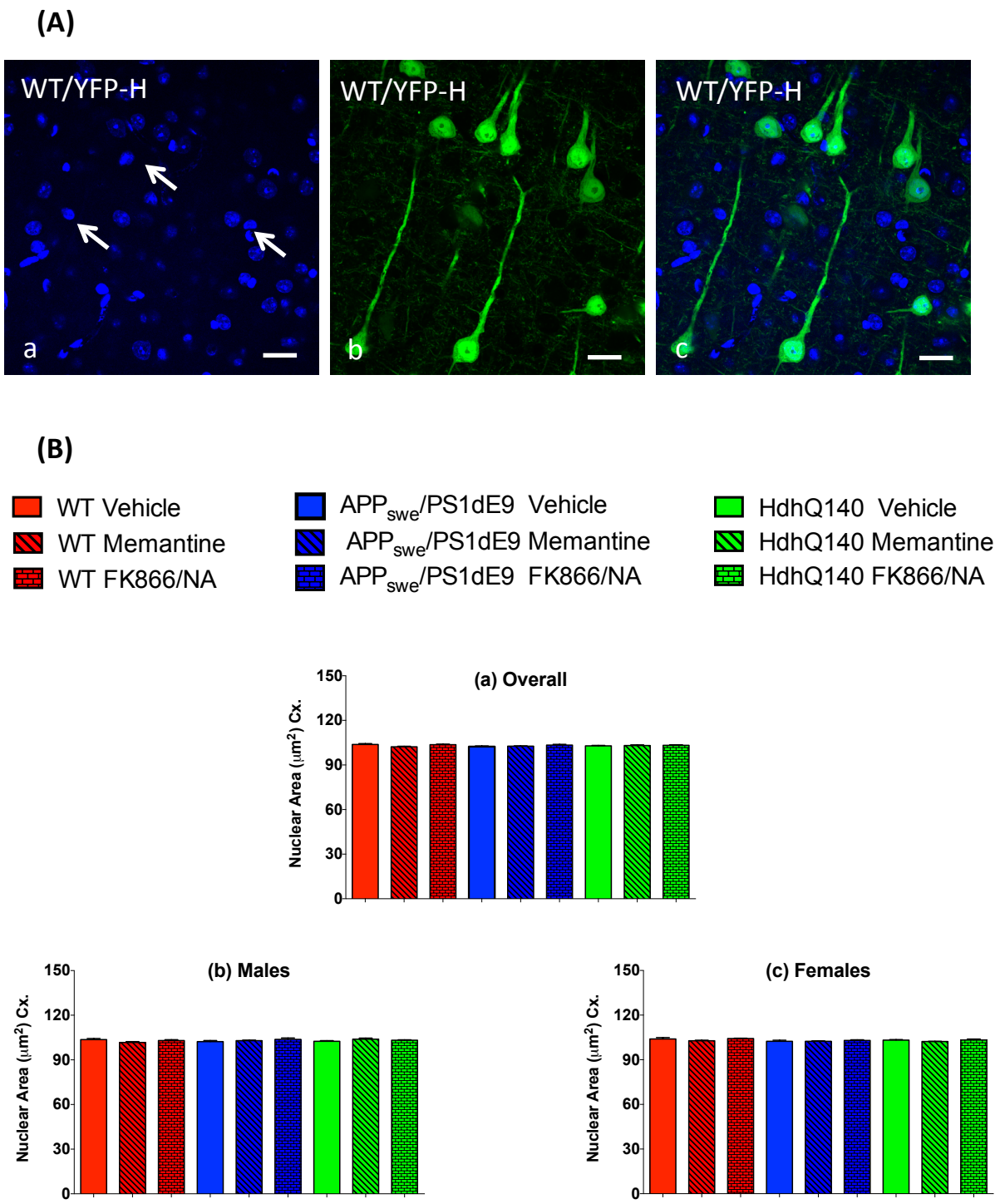


Figure 29: Cortical dystrophies in APP_{swe}/PS1dE9/YFP-H mice co-localized with the deposition of Aβ plaques. Confocal microscopy images (40X) of sagittal brain sections (20 µm) of 6-months old APP_{swe}/PS1dE9/YFP-H mouse show cortical neurons with severe, proximal axonal dystrophies (white arrows, b), co-localized with Aβ plaques deposits (white arrows, a). Axons retain their continuity and remain morphologically normal around the dystrophies (yellow arrows, b). Nuclei (stained with blue Hoechst dye) also retain normal size, location, and morphology (white arrows, c). Green = YFP, Blue = Hoechst, Red = Aβ plaques deposits. Scale bar, 20 µm.

Next, I asked whether swelling and dystrophy abnormalities detected in HD and AD mice correlate with any impairment in their corresponding cell bodies. For this, I analysed nuclear morphology in amygdala, an area that contains the cell bodies of the axons running in stria terminalis (Marangoni et al. 2014), and also nuclear morphology in cortex. Results revealed normal cell bodies morphology and no alteration in nuclear size both in cortex (Figure 30A(a), 30B(a - c)) and in amygdala (Figure 30B(d - f)) in all mice, and neither genotype nor gender effects were found. Moreover, there was no difference in gross dendritic morphology,

and neither dendrite diameter (Figure 31A(a), 31B(a - f)) nor spines number (Figure 31A(b), 31B(g – i)) was altered in all mice groups.



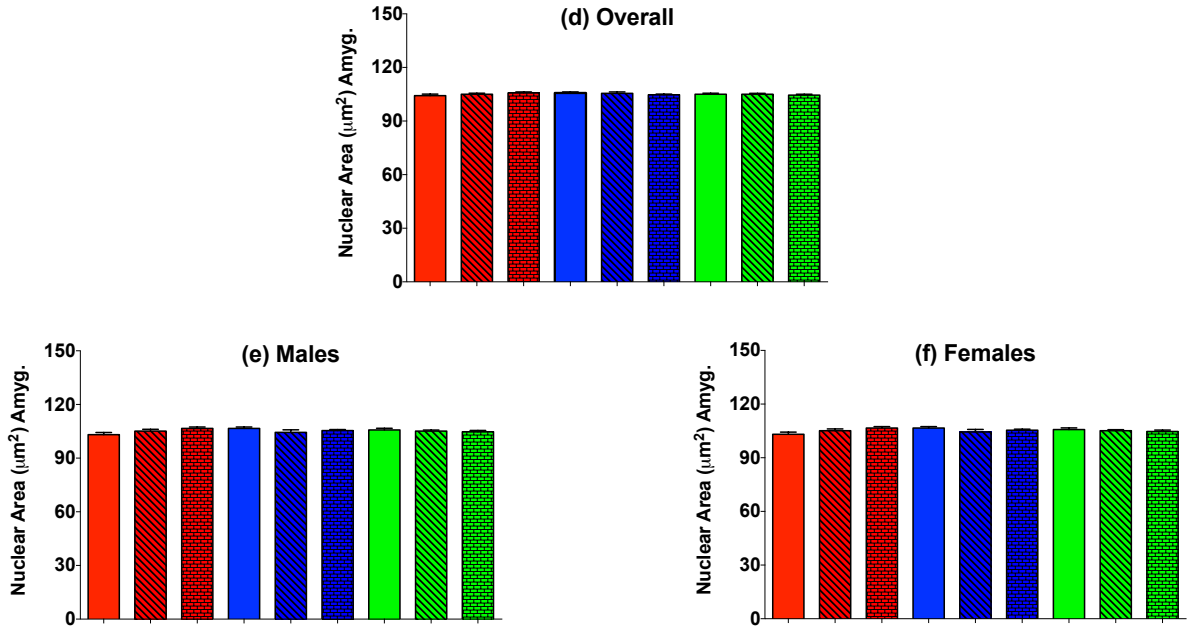
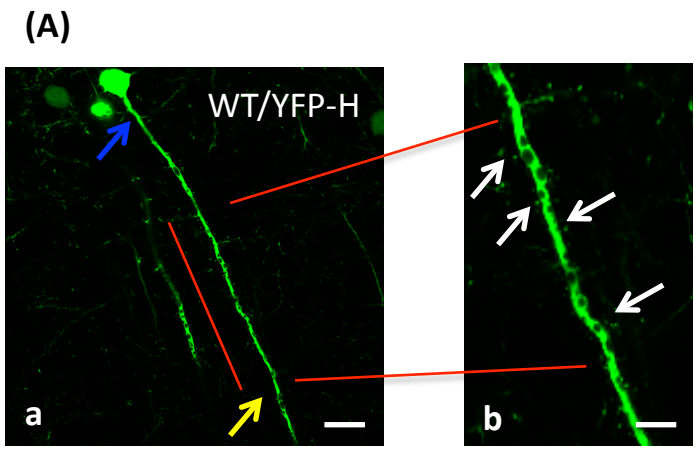
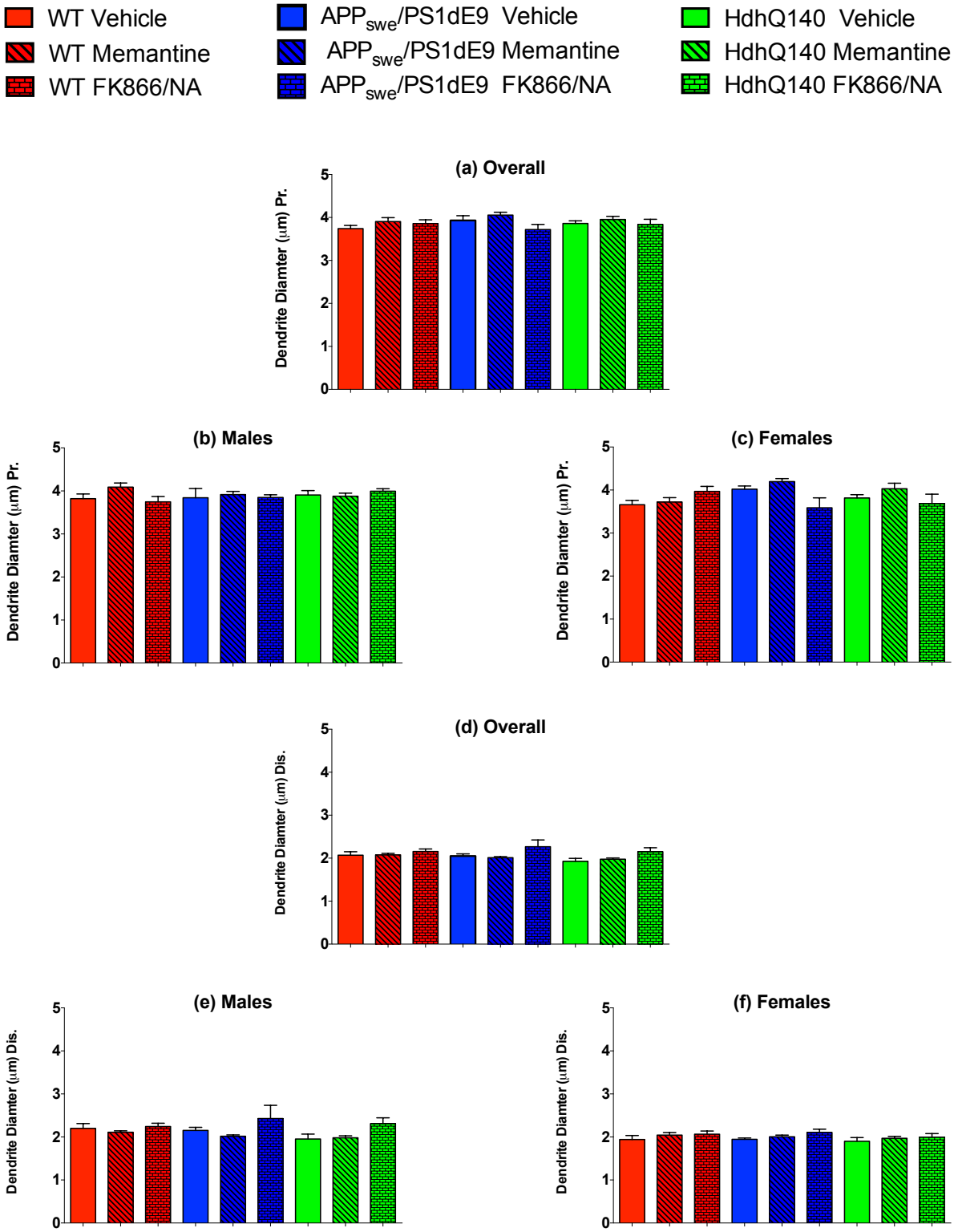


Figure 30: Nuclear morphology did not change both in HdhQ140/YFP-H model of HD and in APP_{swe}/PS1dE9/YFP-H model of AD at 6-months old. (A) Confocal microscopy images (40X) of sagittal brain sections (50 µm) of 6-months old WT/YFP-H (a - c) show nuclei (stained with blue Hoechst dye) retain their normal size, location, and morphology (white arrows, a). (B) Characterization of nuclear morphology show no significant difference ($p > 0.05$) in nuclear area neither in the cortex (a - c), nor in the amygdala (d - f) in all mice treated/untreated with FK866/NA and memantine, and neither genotype nor gender effects were found. (n=5-6 mice/genotype, treatment and gender conditions, mean ± SEM, two-way ANOVA followed by Bonferroni post-hoc test). Green = YFP, Blue = Hoechst, Cx. = Cortex, Amyg. = Amygdala. Scale bar, 20 µm.



(B)


WT Vehicle
WT Memantine
WT FK866/NA
APPswe/PS1dE9 Vehicle
APPswe/PS1dE9 Memantine
APPswe/PS1dE9 FK866/NA
HdhQ140 Vehicle
HdhQ140 Memantine
HdhQ140 FK866/NA
(a) Overall
Dendrite Diamter (μm) Pr.
(b) Males
(c) Females
(d) Overall
Dendrite Diamter (μm) Dis.
(e) Males
(f) Females
0
1
2
3
4
5

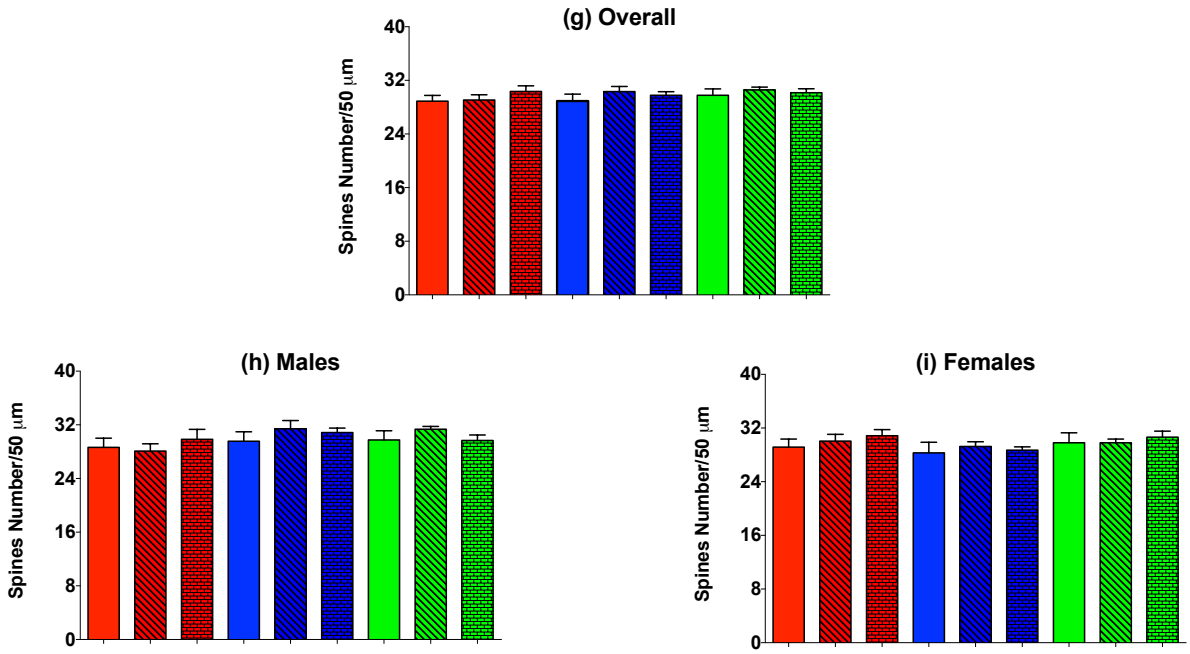


Figure 31: Gross dendritic morphology was preserved both in HdhQ140/YFP-H model of HD and in APP_{swe}/PS1dE9/YFP-H model of AD at 6-months old. (A) Confocal microscopy images (40X) of sagittal brain sections (50 µm) of 6-months old WT/YFP-H (a, and b) show dendrites retain their structural integrity, and no alteration in proximal diameter (blue arrows, a), distal diameter (yellow arrows, a), or spines number (white arrows, b). (B) Characterization of dendritic morphology show no significant difference ($p > 0.05$) neither in dendrite diameter (proximal: a - c, distal: d - f), nor in spines number (g –i) in all mice treated/untreated with FK866/NA and memantine, and neither genotype nor gender effects were found. (n=5-6 mice/genotype, treatment and gender conditions, mean ± SEM, two-way ANOVA followed by Bonferroni post-hoc test). Green = YFP, Pr. = Proximal, Dis. = Distal. Scale bar, 20 µm.

FK866/NA and memantine improved swelling and dystrophy abnormalities detected in HdhQ140/YFP-H mice and APP_{swe}/PS1dE9 mice respectively

HdhQ140 and APP_{swe}/PS1dE9 mice crossed with YFP-H mice and their corresponding YFP+ controls received treatment of vehicle, or FK866/NA, or memantine for 3 weeks, and then their brains were dissected, sectioned, stained, and imaged as previously described in materials and methods section. Aims were to test whether these drugs could modulate any structural impairment in HD and AD mice in comparison to their corresponding YFP+ vehicle-treated controls.

I found that both FK866/NA and memantine significantly ($p < 0.001$) reduced the number of axonal swellings in stria terminalis of HdhQ140/YFP-H mice (Figure 27B(a - c)).

Interestingly, there was no gender difference in the effect of these drugs, and the reduction in HD mice was consistent in both males and females (Figure 27B(a - c)).

In addition, our results revealed that both FK866/NA and memantine significantly ($p < 0.001$) reduced the number of cortical dystrophies in APP_{swe}/PS1dE9/YFP-H female mice (Figure 28B), while the effect was not that noticeable in APP_{swe}/PS1dE9/YFP-H male mice (Figure 28B).

In the other hand, there was no significant difference ($p > 0.05$) in the number of axonal swellings in striatum dorsal (Figure 26B(a - c)), striatum ventral (Figure 26B(d - f)), and cortex (Figure 26B(g - i)) in both HD and AD mice and their corresponding YFP+ controls treated/untreated with FK866/NA and memantine.

Similarly, there was no change ($p > 0.05$) in nuclear size both in cortex (Figure 30B(a - c)) and in amygdala (Figure 30B(d - f), and also no alteration in dendrites diameter (Figure 31B(a - f)) and spines number (Figure 31B(g -i)) in both HD and AD mice and their corresponding YFP+ controls treated/untreated with FK866/NA and memantine.

4.5 Discussion

Inhibition of NMN synthesis with the NAMPT inhibitor FK866 strongly protects axons *in vitro, ex-vivo* and *in vivo* after acute injury (Di Stefano et al. 2014). Our results show that FK866/NA combination significantly improve swelling abnormalities in HdhQ140/YFP-H *in vivo* model of HD and dystrophy abnormalities in APP_{swe}/PS1dE9/YFP-H *in vivo* model of AD, without altering gross nuclear and dendritic morphology of these mice.

As previously reported (Adalbert et al. 2009; Marangoni et al. 2014), our study revealed how crossing neurodegenerative disease models with YFP-H line (Feng et al. 2000) could be used as a powerful tool to assess axon pathology in these models, and also to test the activity of novel neuroprotective drugs. However, due to the limited pattern of YFP expression in YFP-H line, one limitation of using these transgenic mice for visualizing neurons is we cannot exclude the possibility that axon degeneration could occur in neurons that are not labelled with YFP fluorescent protein. To circumvent this limitation, Gatto et al. 2015 crossed R6/2 transgenic mouse model of HD with YFP-J16 line, to directly evaluate early axonal abnormalities in the context of HD *in vivo*. YFP-J16 transgenic mice display a much wider

patter of YFP expression compared to YFP-H line, from layer III – VI of the cerebral cortex including the corpus callosum, which is largely composed of axons emanating from cortical projection neurons (Gatto et al. 2015). Using diffusion tensor imaging and fluorescence microscopy, Gatto et al. 2015 reported a marked degeneration of callosal axons long before the onset of motor symptoms that progressively worsened with age and was influenced by PolyQ tract length in mHTT protein (Gatto et al. 2015).

Consistent with recent study by Marangoni et al. 2014, a striking increase in swellings was detected in HdhQ140/YFP-H mice axons running through stria terminalis, a brain area located in the proximity of striatum and lateral ventricle which is part of the limbic system and plays a role in fear and anxiety-related behaviour. In the other hand, while YFP+ controls showed morphologically intact cortical neurons and projections, APP_{swe}/PS1dE9/YFP-H mice and consistent with previous reports (Jankowsky et al. 2004) developed characteristic cortical dystrophies co-localized with the deposition of Aβ plaques, with a significant gender effect. APP_{swe}/PS1dE9/YFP-H female mice developed higher cortical dystrophies number and bigger Aβ plaques deposits compared to APP_{swe}/PS1dE9/YFP-H male mice of the same age. This is consistent with data from human studies (Letenneur et al. 1994; Brayne et al. 1995; Fratiglioni et al. 1997), and reports from animal models (Callahan et al. 2001; Wang et al. 2003), which reported an increase in the prevalence of AD in females. The mechanisms that underlie this gender distinction in AD are not clear, but the disparity in estrogen level between males and females, together with the dramatic decline in estrogen level with menopause, has been shown to enhance the generation of Aβ and consequently increase the prevalence rate of this neurodegenerative disease in females, although the physiological basis for this effect is still unclear (Wang et al. 2003). 3D confocal imaging showed that APP_{swe}/PS1dE9/YFP-H axons at these dystrophies retained their continuity and remained morphologically normal, not only across the most severe dystrophic regions and plaques deposits, but also distally and proximally where they connected to morphologically normal nuclei. This is consistent with a study in TgCRND8 transgenic mouse model of AD, and suggests the presence of both a metabolically active cell body and bidirectional axonal transport through a continuous axon in the cortical dystrophy region, since impairment of either mechanism is likely to cause Wallerian degeneration (Ferri et al. 2003; Coleman, 2005; Adalbert et al. 2009). In the other hand, no alternation in the morphology of striatal neurons and also no sign of degeneration in nuclear, dendritic and synaptic compartments were detected both in HdhQ140/YFP-H mice and in APP_{swe}/PS1dE9/YFP-H mice. In addition,

cognitive function tests used in this *in vivo* study recorded no difference in motor functions, spatial working memory, and anxiety-like behaviour in both models and their YFP+ controls (chapter 3). These findings are in agreement with studies on HD and AD mouse models where axon pathology preceded death of other neuronal compartments and correlates with symptom onset and progression (Conforti et al. 2014).

The present study revealed, for the first time, that inhibiting NMN synthesis with FK866 (15 mg/kg/day i.p.) while salvaging NAD levels with NA (50 mg/kg/day p.o.) for 3 weeks significantly reduced axonal swellings in stria terminalis of HdhQ140/YFP-H mice, and cortical dystrophies of APP_{swe}/PS1dE9/YFP-H mice, without causing any alteration in gross nuclear and dendritic morphology of these mice. FK866 was well tolerated in phase I cancer trials and has shown some effect in cases of cutaneous T-cell lymphoma. Hence our findings are opening the prospect of using FK866 as a promising therapeutic strategy for neurodegenerative disease models that has not been addressed in the clinic. However how inhibiting the NMN-synthesizing enzyme NAMPT with FK866 alleviated axonal pathology in *in vivo* models of HD and AD is not clear, and additional studies are required to better understand FK866 neuroprotective mechanism.

Memantine is an open-channel blocker, acting predominantly via a mechanism characterized by uncompetitive inhibition with a fast 'off-rate' (designated UFO drug action) (Okamoto et al. 2009). Low micromolar concentrations of memantine preferentially inhibit extrasynaptic stimulation of NMDARs but relatively preserve synaptic NMDARs whose activation is essential for physiological synaptic transmission (Lipton 2006; Lipton 2007). In contrast, higher concentrations of this drug loose this selectivity and inhibit both NMDARs-mediated extrasynaptic and synaptic activities like other NMDARs antagonists. Memantine is now widely prescribed for the treatment of moderate-to-severe AD, and shown to be effective in in cellular and mouse models of HD. I found that inhibiting NMDARs with memantine (20 mg/kg/day i.p.) for 3 weeks significantly reduced axonal swellings in stria terminalis of HdhQ140/YFP-H mice, and cortical dystrophies of APP_{swe}/PS1dE9/YFP-H mice, without causing any alteration in gross nuclear and dendritic morphology of these mice. In addition, memantine treatment significantly restored the locomotor impairment in 6 months old HdhQ140/YFP-H mice, and also corrected the sensorimotor abnormalities in 6 months old APPswe/PS1dE9/YFP-H mice (chapter 3). Many *in vitro* and *in vivo* studies had confirmed the effectiveness of memantine in models of HD and AD (chapter 1). Okamoto et al. 2009 found that 10 months treatment of low dose memantine (1 mg/kg/day i.p.) blocked

extrasynaptic (but not synaptic) NMDARs and significantly improved striatal volume and motor functions as measured by rotarod test in 12 months old YAC128 transgenic mouse model of HD (Okamoto et al. 2009). In contrast, high dose memantine (30 mg/kg/day i.p.) blocked both synaptic and extrasynaptic NMDARs and worsened the outcomes of these mice, suggesting that the balance between synaptic and extrasynaptic NMDARs activity may be crucial in determining neuronal survival in HD (Okamoto et al. 2009). Dong et al. 2008 found that 6 months treatment of 5 mg/kg/day p.o. memantine was associated with a significant decrease in Aβ plaques number and plaques burden, and a significant increase in synaptic density in the molecular layer of the dentate gyrus in 9 months old Tg2576 transgenic mouse model of AD (Dong et al. 2008). 10 and 20 mg/kg/day p.o. memantine had similar beneficial effects on Aβ plaques and synaptic density but was associated with marked increase in degenerating axons identified by a variety of pathologic features including myelin degradation products, disorganization of the axoplasm, and disintegration of the internal part of the myelin, suggesting that chronic memantine administration may have both neuroprotective and neurotoxic effects in a mouse model of AD (Dong et al. 2008).

In conclusion, our study show that selective inhibition of the rate limiting enzyme in NAD biosynthesis NAMPP with FK866 alleviated swelling and dystrophy abnormalities in *in vivo* models of HD and AD respectively without causing any unwanted change in nuclear or dendritic morphology of these mice.

Chapter 5:

General Discussion

In this thesis I aimed to answer whether the axon protective properties of the NMN-synthesizing enzyme NAMPT inhibitor FK866 *in vitro, ex-vivo* and *in vivo* after acute injury could extend beyond that and also modulate axonal damage and behavioural symptoms in *in vitro* and in *in vivo* models of HD and AD. I compared FK866 effect to that of the reported neuroprotective and axon protective NMDAR antagonist memantine.

I found that inhibiting NMN synthesis with FK866 while salvaging NAD levels with NA significantly rescued axonal pathology and ameliorated nuclear morphology in *in vitro* cellular models of HD and Aβ toxicity, while co-administering NMN consistently reverted FK866-mediated axonal protection. In addition, I found that FK866/NA neuroprotective properties extended to *in vivo* models and attenuated some of the behavioural abnormalities and improved axonal pathology in HdhQ140/YFP-H mice, a model of HD, and in APPswe/PS1dE9/YFP-H mice, a model of AD.

How WLD^S preserve severed axons for days *in vitro* and weeks *in vivo* is debatable. Exogenous addition of NAD itself and its precursors as well as overexpression of its biosynthetic enzymes delays Wallerian degeneration (Araki et al. 2004; Wang et al. 2005; Sasaki et al. 2006). This has led to the widely held assumption that increased NMNAT activity and NAD supply is central to WLD^S-mediated neuroprotective mechanism. Despite reinforcing the importance of NMNAT enzymatic activity for protection, recent studies fail to confirm its dependence on NAD (Conforti et al. 2007; Conforti et al. 2009; Sasaki et al. 2009). In contrast, our research group recently showed that the NMNAT substrate and the NAD precursor NMN accumulates before injured nerves degenerate, that exogenous NMN promotes axon degeneration when NMNAT is absent, and that reducing NMN levels pharmacologically with the NAMPT inhibitor FK866 or genetically by expressing the bacterial enzyme NMN deamidase remarkably delays axon degeneration after acute injury (Di Stefano et al. 2014). The rise in NMN after acute injury is likely a consequence of the depletion of the endogenous labile axonal NMNAT2 (its half life is under 1 hour), whose enzymatic activity is essential for axon survival and growth. WLD^S, due to its higher stability, rescues depletion of NMNAT2 both in primary culture and *in vivo* by directly substituting its NMNAT function in axons and prevents NMN accumulation (Gilley and Coleman, 2010; Gilley et al. 2013; Di Stefano et al. 2014). In addition, depletion of NAD causes no overt hard to axons within the timescale of Wallerian degeneration. These findings indicate that the mechanism by which WLD^S and other related NMNATs preserve axon

survival is by limiting NMN accumulation and not by increasing NAD production (Di Stefano et al. 2014), and that NMN could be one of the first events in axon degeneration.

Although many reports showed that modulation of NAD metabolism by WLD^S or other related NMNATs have strong protective effect in some disease models (defined as significant axon preservation and alleviation of symptoms) (Conforti et al. 2014), our study is novel in that it revealed, for the first time, a protective effect of a pharmacological treatment. In addition, while WLD^S preserves human axons (Kitay et al. 2013), its application in human disease is challenging. On the other hand, inhibiting NAMPT with FK866 could be translated for targeting human disease, since it involves a well-known drug that can be administered easily and has already shown promising effect in cancer trials (Conforti et al. 2014). However, owing to FK866 short half-life in circulation, prolonged treatment regimens are required and toxicity from long-term NAD depletion could arise. In fact, significant weight reduction (> 20%) that necessitates humane killing and even sudden death was reported in some of our FK866-treated APPswe/PS1dE9/YFP-H mice, and it is probably attributed to long-term NAD depletion. Hence, systemic blocking of NMN synthesis may not be a very good long-term strategy and the need to identify more targets within the same pathway that could be modulated more safely remains.

As I said, injury-induced NMNAT2 depletion and NMN accumulation could be one of the first events in axon degeneration, but what is downstream of NMN???

Sterile alpha and TIR motif–containing 1 (SARM1, dSarm in *D. melanogaster*) protein (Figure 32) is one of five intracellular adaptors for Toll-like receptor (TLR) signalling (Conforti et al. 2014), and it is an essential mediator of axon degeneration, and shown to be required for rapid Wallerian degeneration in mice (Osterloh et al. 2012; Gerdts et al. 2013). SARM1 involvement emerged from genetic screening for loss of function mutations that delay axon degeneration following antennal ablation in *D. melanogaster* (Osterloh et al. 2012). Deletions of dSarm1 in *D. melanogaster* or its mouse orthologue SARM1 remarkably delay injury-induced axon degeneration tenfold for over 2 weeks both *in vivo* and *in vitro*, comparable to the effect of WLD^S, identifying dSarm/Sarm1 as a member of an ancient axon death signaling pathway (Osterloh et al. 2012).



Figure 32: Structure-activity relationship of SARM1 (Conforti et al. 2014). SARM1 is a modular protein comprising an N-terminal Heat/Armadillo (ARM) domain, two central sterile α-motif (SAM) domains and a carboxy-terminal Toll interleukin-1 receptor (TIR) domain in common with other TLR signalling molecules. Several studies indicate a mitochondrial-interacting sequence at the extreme N-terminal, but this seems to be unnecessary for axon degeneration (Gerdts et al. 2013). The SAM and TIR sequences are both essential for rapid axon degeneration, probably acting as sites for homodimerization and signalling respectively (Gerdts et al. 2013). The N-terminal ARM domain appears to inhibit the pro-degenerative function, as its removal seems to generate a constitutively active protein (Gerdts et al. 2013).

Since SARM1 loss of function does not lead to any evident toxic effect, pharmacologically interfering with SARM1 activity may represent a promising therapeutic target, especially if shown that SARM1 deletion confers protection in models of neurodegenerative disorders. However, its exact role and position in Wallerian degeneration pathway remains unclear (Conforti et al. 2014). Nerve insult seems to be critical for SARM1-dependent axon degeneration, since overexpression of wild-type SARM1 in the absence of injury did not induce axon degeneration (Gerdts et al. 2015). These findings suggest that additional signal is required after nerve insult to promote SARM1-dependent axon degeneration, which could be degradation of the endogenous labile NMNAT2 and the consequent accumulation of NMN. A recent study shows that SARM1 deletion corrects axon outgrowth and prevent perinatal lethality in mice lacking NMNAT2 (Gilley et al. 2015). Another very recent study from our laboratory shows that NMN requires SARM1 presence to induce axon degeneration after injury (Loreto et al. in press). These findings suggest that SARM1 may be acting downstream of NMNAT2 depletion and NMN accumulation. Using engineered protease-sensitized SARM1, Gerdts et al. 2015 recently reported that a constitutive active SARM1 initiates a local destruction program involving rapid breakdown of NAD, even in the absence of an injury (Gerdts et al. 2015). It would be interesting to understand whether endogenous SARM1 follow a similar activation, and whether NMN can regulate this activation and the following NAD depletion. This would help to clarify some of the previous contradiction in the field. Further studies are required to determine the exact relationship of SARM1 to the

NAD precursor NMN and the NAD-biosynthetic enzymes NMNATs, and modulation of SARM1 activity may be used as an alternative or synergistic therapeutic strategy.

Additionally, Loreto et al. shows that NMN induces axon degeneration after injury by stimulating a SARM1-dependent influx of Ca^{2+}, mainly arising from the extracellular environment. However, while supporting a crucial role for extracellular Ca^{2+} in the late execution stages of Wallerian degeneration, this study shows that Ca^{2+} increase shortly precedes axonal fragmentation. Therefore, Ca^{2+} regulated steps might be at a point where morphologically protecting axons may not restore their function and upstream mediators of axon death pathway may prove therapeutically more useful targets (Loreto et al. in press).

Our *in vitro* data are consistent with FK866 acting as specific inhibitor of NAMPT. In support of this, co-administering NMN with FK866/NA consistently reverted FK866-mediated axonal protection. However, off-target effect of this drug cannot be completely ruled out is the absence of a genetic evidence to confirm our pharmacological findings. On the other hand, how FK866/NA reduced axon pathology and also attenuated some of the behavioural abnormalities in *in vivo* model of HD and AD needs further investigation. First, NAD and NMN levels in the brain areas most sensitive to the treatment remain to be determined. Second, the availability of NMN deamidase transgenic mouse model that express the bacterial enzyme NMN deamidase and shown to prevent NMN accumulation and delay Wallerian degeneration could be used as a genetic evidence to confirm our *in vivo* data. In addition, specific inhibition of NAMPT with FK866 was shown to reduce the secondary inflammatory injury and permanent damage in an experimental compression model of spinal cord injury (Esposito et al. 2012). Hence, assessment of activated neutrophils, microglia and astrocytes in addition to pro-inflammatory mediators like tumor necrosis factor (TNF)-α and interleukin (IL)-1β and IL-6 in HdhQ140/YFP-H mice and APPswe/PS1dE9/YFP-H mice treated with FK866/NA is important to better understand our *in vivo* results.

Chapter 6:

Conclusive Remarks and Future Directions

In conclusion and in agreement with our hypothesis, this thesis suggests that axonal abnormalities induced by mHTT and Aβ in *in vitro* and in *in vivo* models of neurodegeneration could follow the activation of an axon death pathway similar to that activated after acute injury. In addition, we identify a key role of the NMN-synthesizing enzyme NAMPT as a novel therapeutic target in models of neurodegenerative diseases that had not been addressed in the clinic. However, additional studies are required to better understand FK866 neuroprotective mechanisms and the feasibility and safety of long-term systemic NAMPT pharmacological inhibition.

- In order to refine our data obtained in HD and Aβ toxicity *in vitro* models where we have identified changes associated with mHTT and Aβ modulated with FK866 treatment, future studies may include:

    1. Measuring the level of NAD and its precursor NMN in HD and Aβ toxicity *in vitro* models before and after FK866 treatment,

    2. Characterizing the expression of NAMPT and NMNATs to assess any change associated with mHTT and Aβ and whether it is modulated with FK866 treatment,

    3. Investigating axonal transport of NMNAT2 to assess any impairment associated with mHTT and Aβ and whether it is improved with FK866 treatment.

- For HdhQ140/YFP-H *in vivo* model of HD and APPswe/PS1dE9/YFP-H *in vivo* model of AD and to better understand our *in vivo* results, future studies may include:

    1. Crossing these *in vivo* models with NMN deamidase transgenic mouse model to see whether expressing the bacterial enzyme NMN deamidase in these neurodegenerative disease models could prevent NMN accumulation and alleviate pathology in these mice.

    2. Characterizing behavioural symptoms in particular those related to cognition and memory, and neuronal morphology in particular axonal morphology in these mice at a later time-point, to see if there are abnormalities other than the ones detected at 6-months of age, and if it is corrected with FK866 treatment.

    3. Additional tests for cognition, memory, and anxiety-related behaviour like avoidance tests, object discrimination, Morris water maze, and contextual fear

conditioning would also be useful to better understand axonal and other neuronal abnormalities which may be detected in these mice at older age.

4. Investigating potential anti-inflammatory actions of FK866 including assessment of activated neutrophils, microglia and astrocytes, in addition to pro-inflammatory mediators like TNF-α, IL-1β and IL-6, and neurotrophic factors BDNF and GDNF, and whether it is modified with FK866 treatment.

References

Adalbert R, Nogradi A, Babetto E, Janeckova L, Walker SA, et al. (2009) Severely dystrophic axons at amyloid plaques remain continuous and connected to viable cell bodies. Brain 132: 402-416.

Andra K, Abramowski D, Duke M, Probst A, Wiederhold KH, et al. (1996) Expression of APP in transgenic mice: a comparison of neuron-specific promoters. Neurobiol Aging 17: 183-190.

Andrew SE, Goldberg YP, Theilmann J, Zeisler J, Hayden MR (1994) A CCG repeat polymorphism adjacent to the CAG repeat in the Huntington disease gene: implications for diagnostic accuracy and predictive testing. Hum Mol Genet 3: 65-67.

Araki T, Sasaki Y, Milbrandt J (2004) Increased nuclear NAD biosynthesis and SIRT1 activation prevent axonal degeneration. Science 305: 1010-1013.

Arrasate M, Mitra S, Schweitzer ES, Segal MR, Finkbeiner S (2004) Inclusion body formation reduces levels of mutant huntingtin and the risk of neuronal death. Nature 431: 805-810.

Arzberger T, Krampfl K, Leimgruber S, Weindl A (1997) Changes of NMDA receptor subunit (NR1, NR2B) and glutamate transporter (GLT1) mRNA expression in Huntington's disease--an in situ hybridization study. J Neuropathol Exp Neurol 56: 440-454.

Ashizawa T, Wong LJ, Richards CS, Caskey CT, Jankovic J (1994) CAG repeat size and clinical presentation in Huntington's disease. Neurology 44: 1137-1143.

Augood SJ, Faull RL, Emson PC (1997) Dopamine D1 and D2 receptor gene expression in the striatum in Huntington's disease. Ann Neurol 42: 215-221.

Augood SJ, Faull RL, Love DR, Emson PC (1996) Reduction in enkephalin and substance P messenger RNA in the striatum of early grade Huntington's disease: a detailed cellular in situ hybridization study. Neuroscience 72: 1023-1036.

Bae BI, Xu H, Igarashi S, Fujimuro M, Agrawal N, et al. (2005) p53 mediates cellular dysfunction and behavioral abnormalities in Huntington's disease. Neuron 47: 29-41.

Beal MF, Brouillet E, Jenkins BG, Ferrante RJ, Kowall NW, et al. (1993) Neurochemical and histologic characterization of striatal excitotoxic lesions produced by the mitochondrial toxin 3-nitropropionic acid. J Neurosci 13: 4181-4192.

Beal MF, Ferrante RJ, Swartz KJ, Kowall NW (1991) Chronic quinolinic acid lesions in rats closely resemble Huntington's disease. J Neurosci 11: 1649-1659.

Beal MF, Kowall NW, Ellison DW, Mazurek MF, Swartz KJ, et al. (1986) Replication of the neurochemical characteristics of Huntington's disease by quinolinic acid. Nature 321: 168-171.

Beirowski B, Berek L, Adalbert R, Wagner D, Grumme DS, et al. (2004) Quantitative and qualitative analysis of Wallerian degeneration using restricted axonal labelling in YFP-H mice. J Neurosci Methods 134: 23-35.

Bennett EJ, Shaler TA, Woodman B, Ryu KY, Zaitseva TS, et al. (2007) Global changes to the ubiquitin system in Huntington's disease. Nature 448: 704-708.

Blanpied TA, Boeckman FA, Aizenman E, Johnson JW (1997) Trapping channel block of NMDA-activated responses by amantadine and memantine. J Neurophysiol 77: 309-323.

Blennow K, de Leon MJ, Zetterberg H (2006) Alzheimer's disease. Lancet 368: 387-403.

Block-Galarza J, Chase KO, Sapp E, Vaughn KT, Vallee RB, et al. (1997) Fast transport and retrograde movement of huntingtin and HAP 1 in axons. Neuroreport 8: 2247-2251.

Borchelt DR, Ratovitski T, van Lare J, Lee MK, Gonzales V, et al. (1997) Accelerated amyloid deposition in the brains of transgenic mice coexpressing mutant presenilin 1 and amyloid precursor proteins. Neuron 19: 939-945.

Borchelt DR, Thinakaran G, Eckman CB, Lee MK, Davenport F, et al. (1996) Familial Alzheimer's disease-linked presenilin 1 variants elevate Abeta1-42/1-40 ratio in vitro and in vivo. Neuron 17: 1005-1013.

Bormann J (1989) Memantine is a potent blocker of N-methyl-D-aspartate (NMDA) receptor channels. Eur J Pharmacol 166: 591-592.

Braak H, Braak E, Strothjohann M (1994) Abnormally phosphorylated tau protein related to the formation of neurofibrillary tangles and neuropil threads in the cerebral cortex of sheep and goat. Neurosci Lett 171: 1-4.

Brayne C, Gill C, Huppert FA, Barkley C, Gehlhaar E, et al. (1995) Incidence of clinically diagnosed subtypes of dementia in an elderly population. Cambridge Project for Later Life. Br J Psychiatry 167: 255-262.

Bresink I, Benke TA, Collett VJ, Seal AJ, Parsons CG, et al. (1996) Effects of memantine on recombinant rat NMDA receptors expressed in HEK 293 cells. Br J Pharmacol 119: 195-204.

Bridge KE, Berg N, Adalbert R, Babetto E, Dias T, et al. (2009) Late onset distal axonal swelling in YFP-H transgenic mice. Neurobiol Aging 30: 309-321.

Brignull HR, Morley JF, Garcia SM, Morimoto RI (2006) Modeling polyglutamine pathogenesis in C. elegans. Methods Enzymol 412: 256-282.

Brinkman RR, Mezei MM, Theilmann J, Almqvist E, Hayden MR (1997) The likelihood of being affected with Huntington disease by a particular age, for a specific CAG size. Am J Hum Genet 60: 1202-1210.

Brion JP (1998) The role of neurofibrillary tangles in Alzheimer disease. Acta Neurol Belg 98: 165-174.

Bruzzone S, Fruscione F, Morando S, Ferrando T, Poggi A, et al. (2009) Catastrophic NAD+ depletion in activated T lymphocytes through Nampt inhibition reduces demyelination and disability in EAE. PLoS One 4: e7897.

Busso N, Karababa M, Nobile M, Rolaz A, Van Gool F, et al. (2008) Pharmacological inhibition of nicotinamide phosphoribosyltransferase/visfatin enzymatic activity identifies a new inflammatory pathway linked to NAD. PLoS One 3: e2267.

Buxbaum JD, Christensen JL, Ruefli AA, Greengard P, Loring JF (1993) Expression of APP in brains of transgenic mice containing the entire human APP gene. Biochem Biophys Res Commun 197: 639-645.

Cabrejo L, Guyant-Marechal L, Laquerriere A, Vercelletto M, De la Fourniere F, et al. (2006) Phenotype associated with APP duplication in five families. Brain 129: 2966-2976.

Cacabelos R, Takeda M, Winblad B (1999) The glutamatergic system and neurodegeneration in dementia: preventive strategies in Alzheimer's disease. Int J Geriatr Psychiatry 14: 3-47.

Cai H, Wang Y, McCarthy D, Wen H, Borchelt DR, et al. (2001) BACE1 is the major beta-secretase for generation of Abeta peptides by neurons. Nat Neurosci 4: 233-234.

Caine D, Breen N, Patterson K (2009) Emergence and progression of 'non-semantic' deficits in semantic dementia. Cortex 45: 483-494.

Callahan MJ, Lipinski WJ, Bian F, Durham RA, Pack A, et al. (2001) Augmented senile plaque load in aged female beta-amyloid precursor protein-transgenic mice. Am J Pathol 158: 1173-1177.

Cancelli I, Cadore IP, Merlino G, Valentinis L, Moratti U, et al. (2006) Sensory gating deficit assessed by P50/Pb middle latency event related potential in Alzheimer's disease. J Clin Neurophysiol 23: 421-425.

Cangemi CF, Jr., Miller RJ (1998) Huntington's disease: review and anesthetic case management. Anesth Prog 45: 150-153.

Capodanno D, Milazzo G, Vitale L, Di Stefano D, Di Salvo M, et al. (2014) Updating the evidence on patent foramen ovale closure versus medical therapy in patients with cryptogenic stroke: a systematic review and comprehensive meta-analysis of 2,303 patients from three randomised trials and 2,231 patients from 11 observational studies. EuroIntervention 9: 1342-1349.

Carter RJ, Lione LA, Humby T, Mangiarini L, Mahal A, et al. (1999) Characterization of progressive motor deficits in mice transgenic for the human Huntington's disease mutation. J Neurosci 19: 3248-3257.

Cavallucci V, D'Amelio M, Cecconi F (2012) Abeta toxicity in Alzheimer's disease. Mol Neurobiol 45: 366-378.

Cepeda C, Cummings DM, Andre VM, Holley SM, Levine MS (2010) Genetic mouse models of Huntington's disease: focus on electrophysiological mechanisms. ASN Neuro 2: e00033.

Cha JH (2007) Transcriptional signatures in Huntington's disease. Prog Neurobiol 83: 228-248.

Chan EY, Luthi-Carter R, Strand A, Solano SM, Hanson SA, et al. (2002) Increased huntingtin protein length reduces the number of polyglutamine-induced gene expression changes in mouse models of Huntington's disease. Hum Mol Genet 11: 1939-1951.

Chen HS, Lipton SA (1997) Mechanism of memantine block of NMDA-activated channels in rat retinal ganglion cells: uncompetitive antagonism. J Physiol 499 (Pt 1): 27-46.

Chen HS, Lipton SA (2006) The chemical biology of clinically tolerated NMDA receptor antagonists. J Neurochem 97: 1611-1626.

Chen HS, Pellegrini JW, Aggarwal SK, Lei SZ, Warach S, et al. (1992) Open-channel block of N-methyl-D-aspartate (NMDA) responses by memantine: therapeutic advantage against NMDA receptor-mediated neurotoxicity. J Neurosci 12: 4427-4436.

Chen N, Luo T, Wellington C, Metzler M, McCutcheon K, et al. (1999) Subtype-specific enhancement of NMDA receptor currents by mutant huntingtin. J Neurochem 72: 1890-1898.

Cheng D, Logge W, Low JK, Garner B, Karl T (2013) Novel behavioural characteristics of the APP(Swe)/PS1DeltaE9 transgenic mouse model of Alzheimer's disease. Behav Brain Res 245: 120-127.

Chishti MA, Yang DS, Janus C, Phinney AL, Horne P, et al. (2001) Early-onset amyloid deposition and cognitive deficits in transgenic mice expressing a double mutant form of amyloid precursor protein 695. J Biol Chem 276: 21562-21570.

Chui DH, Tanahashi H, Ozawa K, Ikeda S, Checler F, et al. (1999) Transgenic mice with Alzheimer presenilin 1 mutations show accelerated neurodegeneration without amyloid plaque formation. Nat Med 5: 560-564.

Citron M (2010) Alzheimer's disease: strategies for disease modification. Nat Rev Drug Discov 9: 387-398.

Citron M, Oltersdorf T, Haass C, McConlogue L, Hung AY, et al. (1992) Mutation of the beta-amyloid precursor protein in familial Alzheimer's disease increases beta-protein production. Nature 360: 672-674.

Citron M, Westaway D, Xia W, Carlson G, Diehl T, et al. (1997) Mutant presenilins of Alzheimer's disease increase production of 42-residue amyloid beta-protein in both transfected cells and transgenic mice. Nat Med 3: 67-72.

Coleman M (2005) Axon degeneration mechanisms: commonality amid diversity. Nat Rev Neurosci 6: 889-898.

Coleman MP, Conforti L, Buckmaster EA, Tarlton A, Ewing RM, et al. (1998) An 85-kb tandem triplication in the slow Wallerian degeneration (Wlds) mouse. Proc Natl Acad Sci U S A 95: 9985-9990.

Colin E, Zala D, Liot G, Rangone H, Borrell-Pages M, et al. (2008) Huntingtin phosphorylation acts as a molecular switch for anterograde/retrograde transport in neurons. EMBO J 27: 2124-2134.

Conforti L, Fang G, Beirowski B, Wang MS, Sorci L, et al. (2007) NAD(+) and axon degeneration revisited: Nmnat1 cannot substitute for Wld(S) to delay Wallerian degeneration. Cell Death Differ 14: 116-127.

Conforti L, Gilley J, Coleman MP (2014) Wallerian degeneration: an emerging axon death pathway linking injury and disease. Nat Rev Neurosci 15: 394-409.

Conforti L, Tarlton A, Mack TG, Mi W, Buckmaster EA, et al. (2000) A Ufd2/D4Cole1e chimeric protein and overexpression of Rbp7 in the slow Wallerian degeneration (WldS) mouse. Proc Natl Acad Sci U S A 97: 11377-11382.

Conforti L, Wilbrey A, Morreale G, Janeckova L, Beirowski B, et al. (2009) Wld S protein requires Nmnat activity and a short N-terminal sequence to protect axons in mice. J Cell Biol 184: 491-500.

Cordaro M, Impellizzeri D, Paterniti I, Bruschetta G, Siracusa R, et al. (2014) Neuroprotective effects of Co-ultraPEALut on secondary inflammatory process and autophagy involved in traumatic brain injury. J Neurotrauma.

Cowan CM, Fan MM, Fan J, Shehadeh J, Zhang LY, et al. (2008) Polyglutamine-modulated striatal calpain activity in YAC transgenic huntington disease mouse model: impact on NMDA receptor function and toxicity. J Neurosci 28: 12725-12735.

Coyle JT (1979) An animal model for Huntington's disease. Biol Psychiatry 14: 251-276.

Crowe SE, Ellis-Davies GC (2013) In vivo characterization of a bigenic fluorescent mouse model of Alzheimer's disease with neurodegeneration. J Comp Neurol 521: 2181-2194.

Cui L, Jeong H, Borovecki F, Parkhurst CN, Tanese N, et al. (2006) Transcriptional repression of PGC-1alpha by mutant huntingtin leads to mitochondrial dysfunction and neurodegeneration. Cell 127: 59-69.

Dau A, Gladding CM, Sepers MD, Raymond LA (2014) Chronic blockade of extrasynaptic NMDA receptors ameliorates synaptic dysfunction and pro-death signaling in Huntington disease transgenic mice. Neurobiol Dis 62: 533-542.

Davies SW, Turmaine M, Cozens BA, DiFiglia M, Sharp AH, et al. (1997) Formation of neuronal intranuclear inclusions underlies the neurological dysfunction in mice transgenic for the HD mutation. Cell 90: 537-548.

Davis M, Strachan DI, Kass E (1980) Excitatory and inhibitory effects of serotonin on sensorimotor reactivity measured with acoustic startle. Science 209: 521-523.

De Felice FG, Velasco PT, Lambert MP, Viola K, Fernandez SJ, et al. (2007) Abeta oligomers induce neuronal oxidative stress through an N-methyl-D-aspartate receptor-dependent mechanism that is blocked by the Alzheimer drug memantine. J Biol Chem 282: 11590-11601.

De Filippis D, Russo A, De Stefano D, Cipriano M, Esposito D, et al. (2014) Palmitoylethanolamide inhibits rMCP-5 expression by regulating MITF activation in rat chronic granulomatous inflammation. Eur J Pharmacol 725: 64-69.

Decker H, Lo KY, Unger SM, Ferreira ST, Silverman MA (2010) Amyloid-beta peptide oligomers disrupt axonal transport through an NMDA receptor-dependent mechanism that is mediated by glycogen synthase kinase 3beta in primary cultured hippocampal neurons. J Neurosci 30: 9166-9171.

Dewachter I, Van Dorpe J, Smeijers L, Gilis M, Kuiperi C, et al. (2000) Aging increased amyloid peptide and caused amyloid plaques in brain of old APP/V717I transgenic mice by a different mechanism than mutant presenilin1. J Neurosci 20: 6452-6458.

Di Stefano M, Nascimento-Ferreira I, Orsomando G, Mori V, Gilley J, et al. (2014) A rise in NAD precursor nicotinamide mononucleotide (NMN) after injury promotes axon degeneration. Cell Death Differ.

DiFiglia M, Sapp E, Chase K, Schwarz C, Meloni A, et al. (1995) Huntingtin is a cytoplasmic protein associated with vesicles in human and rat brain neurons. Neuron 14: 1075-1081.

DiFiglia M, Sapp E, Chase KO, Davies SW, Bates GP, et al. (1997) Aggregation of huntingtin in neuronal intranuclear inclusions and dystrophic neurites in brain. Science 277: 1990-1993.

Dingledine R, Borges K, Bowie D, Traynelis SF (1999) The glutamate receptor ion channels. Pharmacol Rev 51: 7-61.

Dodart JC, Meziane H, Mathis C, Bales KR, Paul SM, et al. (1999) Behavioral disturbances in transgenic mice overexpressing the V717F beta-amyloid precursor protein. Behav Neurosci 113: 982-990.

Domingues A, Almeida S, da Cruz e Silva EF, Oliveira CR, Rego AC (2007) Toxicity of beta-amyloid in HEK293 cells expressing NR1/NR2A or NR1/NR2B N-methyl-D-aspartate receptor subunits. Neurochem Int 50: 872-880.

Dompierre JP, Godin JD, Charrin BC, Cordelieres FP, King SJ, et al. (2007) Histone deacetylase 6 inhibition compensates for the transport deficit in Huntington's disease by increasing tubulin acetylation. J Neurosci 27: 3571-3583.

Dong H, Yuede CM, Coughlan C, Lewis B, Csernansky JG (2008) Effects of memantine on neuronal structure and conditioned fear in the Tg2576 mouse model of Alzheimer's disease. Neuropsychopharmacology 33: 3226-3236.

Dragatsis I, Levine MS, Zeitlin S (2000) Inactivation of Hdh in the brain and testis results in progressive neurodegeneration and sterility in mice. Nat Genet 26: 300-306.

Duff K, Eckman C, Zehr C, Yu X, Prada CM, et al. (1996) Increased amyloid-beta42(43) in brains of mice expressing mutant presenilin 1. Nature 383: 710-713.

Eidelberg D, Surmeier DJ (2011) Brain networks in Huntington disease. J Clin Invest 121: 484-492.

Enright LE, Zhang S, Murphy TH (2007) Fine mapping of the spatial relationship between acute ischemia and dendritic structure indicates selective vulnerability of layer V neuron dendritic tufts within single neurons in vivo. J Cereb Blood Flow Metab 27: 1185-1200.

Esposito E, Impellizzeri D, Mazzon E, Fakhfouri G, Rahimian R, et al. (2012) The NAMPT inhibitor FK866 reverts the damage in spinal cord injury. J Neuroinflammation 9: 66.

Feng G, Mellor RH, Bernstein M, Keller-Peck C, Nguyen QT, et al. (2000) Imaging neuronal subsets in transgenic mice expressing multiple spectral variants of GFP. Neuron 28: 41-51.

Ferguson B, Matyszak MK, Esiri MM, Perry VH (1997) Axonal damage in acute multiple sclerosis lesions. Brain 120 (Pt 3): 393-399.

Fernandes HB, Raymond LA (2009) NMDA Receptors and Huntington's Disease. In: Van Dongen AM, editor. Biology of the NMDA Receptor. Boca Raton (FL).

Ferrante RJ, Kowall NW, Beal MF, Richardson EP, Jr., Bird ED, et al. (1985) Selective sparing of a class of striatal neurons in Huntington's disease. Science 230: 561-563.

Ferrante RJ, Kowall NW, Richardson EP, Jr. (1991) Proliferative and degenerative changes in striatal spiny neurons in Huntington's disease: a combined study using the section-Golgi method and calbindin D28k immunocytochemistry. J Neurosci 11: 3877-3887.

Ferri A, Sanes JR, Coleman MP, Cunningham JM, Kato AC (2003) Inhibiting axon degeneration and synapse loss attenuates apoptosis and disease progression in a mouse model of motoneuron disease. Curr Biol 13: 669-673.

Ferri CP, Prince M, Brayne C, Brodaty H, Fratiglioni L, et al. (2005) Global prevalence of dementia: a Delphi consensus study. Lancet 366: 2112-2117.

Filali M, Lalonde R, Rivest S (2011) Subchronic memantine administration on spatial learning, exploratory activity, and nest-building in an APP/PS1 mouse model of Alzheimer's disease. Neuropharmacology 60: 930-936.

Fischer LR, Glass JD (2007) Axonal degeneration in motor neuron disease. Neurodegener Dis 4: 431-442.

Francis PT (2003) Glutamatergic systems in Alzheimer's disease. Int J Geriatr Psychiatry 18: S15-21.

Fratiglioni L, Viitanen M, von Strauss E, Tontodonati V, Herlitz A, et al. (1997) Very old women at highest risk of dementia and Alzheimer's disease: incidence data from the Kungsholmen Project, Stockholm. Neurology 48: 132-138.

Gafni J, Ellerby LM (2002) Calpain activation in Huntington's disease. J Neurosci 22: 4842-4849.

Galvin JE, Uryu K, Lee VM, Trojanowski JQ (1999) Axon pathology in Parkinson's disease and Lewy body dementia hippocampus contains alpha-, beta-, and gamma-synuclein. Proc Natl Acad Sci U S A 96: 13450-13455.

Games D, Adams D, Alessandrini R, Barbour R, Berthelette P, et al. (1995) Alzheimer-type neuropathology in transgenic mice overexpressing V717F beta-amyloid precursor protein. Nature 373: 523-527.

Garcia-Alloza M, Robbins EM, Zhang-Nunes SX, Purcell SM, Betensky RA, et al. (2006) Characterization of amyloid deposition in the APPswe/PS1dE9 mouse model of Alzheimer disease. Neurobiol Dis 24: 516-524.

Garten A, Petzold S, Korner A, Imai S, Kiess W (2009) Nampt: linking NAD biology, metabolism and cancer. Trends Endocrinol Metab 20: 130-138.

Gatto RG, Chu Y, Ye AQ, Price SD, Tavassoli E, et al. (2015) Analysis of YFP(J16)-R6/2 reporter mice and postmortem brains reveals early pathology and increased vulnerability of callosal axons in Huntington's disease. Hum Mol Genet 24: 5285-5298.

Gauthier LR, Charrin BC, Borrell-Pages M, Dompierre JP, Rangone H, et al. (2004) Huntingtin controls neurotrophic support and survival of neurons by enhancing BDNF vesicular transport along microtubules. Cell 118: 127-138.

Gerdts J, Brace EJ, Sasaki Y, DiAntonio A, Milbrandt J (2015) SARM1 activation triggers axon degeneration locally via NAD(+) destruction. Science 348: 453-457.

Gerdts J, Summers DW, Sasaki Y, DiAntonio A, Milbrandt J (2013) Sarm1-mediated axon degeneration requires both SAM and TIR interactions. J Neurosci 33: 13569-13580.

Gerfen CR (1988) Synaptic organization of the striatum. J Electron Microsc Tech 10: 265-281.

Gerzon K, Krumkalns EV, Brindle RL, Marshall FJ, Root MA (1963) The Adamantyl Group in Medicinal Agents. I. Hypoglycemic N-Arylsulfonyl-N' -Adamantylureas. J Med Chem 6: 760-763.

Gilley J, Adalbert R, Yu G, Coleman MP (2013) Rescue of peripheral and CNS axon defects in mice lacking NMNAT2. J Neurosci 33: 13410-13424.

Gilley J, Coleman MP (2010) Endogenous Nmnat2 is an essential survival factor for maintenance of healthy axons. PLoS Biol 8: e1000300.

Gilley J, Orsomando G, Nascimento-Ferreira I, Coleman MP (2015) Absence of SARM1 rescues development and survival of NMNAT2-deficient axons. Cell Rep 10: 1974-1981.

Goate A, Chartier-Harlin MC, Mullan M, Brown J, Crawford F, et al. (1991) Segregation of a missense mutation in the amyloid precursor protein gene with familial Alzheimer's disease. Nature 349: 704-706.

Goedert M (1993) Tau protein and the neurofibrillary pathology of Alzheimer's disease. Trends Neurosci 16: 460-465.

Goedert M, Klug A, Crowther RA (2006) Tau protein, the paired helical filament and Alzheimer's disease. J Alzheimers Dis 9: 195-207.

Goldblum MC, Gomez CM, Dalla Barba G, Boller F, Deweer B, et al. (1998) The influence of semantic and perceptual encoding on recognition memory in Alzheimer's disease. Neuropsychologia 36: 717-729.

Gossen M, Freundlieb S, Bender G, Muller G, Hillen W, et al. (1995) Transcriptional activation by tetracyclines in mammalian cells. Science 268: 1766-1769.

Gotz J, Schild A, Hoerndli F, Pennanen L (2004) Amyloid-induced neurofibrillary tangle formation in Alzheimer's disease: insight from transgenic mouse and tissue-culture models. Int J Dev Neurosci 22: 453-465.

Goudie F. Problems of Aging. In: Stokes G, Goudie F, eds. Working with dementia. Oxford: Winslow Press, 1993: 29-43.

Graeber MB, Kosel S, Grasbon-Frodl E, Moller HJ, Mehraein P (1998) Histopathology and APOE genotype of the first Alzheimer disease patient, Auguste D. Neurogenetics 1: 223-228.

Graveland GA, Williams RS, DiFiglia M (1985) Evidence for degenerative and regenerative changes in neostriatal spiny neurons in Huntington's disease. Science 227: 770-773.

Gray CW, Patel AJ (1995) Neurodegeneration mediated by glutamate and beta-amyloid peptide: a comparison and possible interaction. Brain Res 691: 169-179.

Gray M, Shirasaki DI, Cepeda C, Andre VM, Wilburn B, et al. (2008) Full-length human mutant huntingtin with a stable polyglutamine repeat can elicit progressive and selective neuropathogenesis in BACHD mice. J Neurosci 28: 6182-6195.

Green HA, Patterson K (2009) Jigsaws-a preserved ability in semantic dementia. Neuropsychologia 47: 569-576.

Greenamyre JT, Young AB (1989) Excitatory amino acids and Alzheimer's disease. Neurobiol Aging 10: 593-602.

Greene JD, Hodges JR, Baddeley AD (1995) Autobiographical memory and executive function in early dementia of Alzheimer type. Neuropsychologia 33: 1647-1670.

Greene LA, Tischler AS (1976) Establishment of a noradrenergic clonal line of rat adrenal pheochromocytoma cells which respond to nerve growth factor. Proc Natl Acad Sci U S A 73: 2424-2428.

Gunawardena S, Her LS, Brusch RG, Laymon RA, Niesman IR, et al. (2003) Disruption of axonal transport by loss of huntingtin or expression of pathogenic polyQ proteins in Drosophila. Neuron 40: 25-40.

Guo Q, Fu W, Sopher BL, Miller MW, Ware CB, et al. (1999) Increased vulnerability of hippocampal neurons to excitotoxic necrosis in presenilin-1 mutant knock-in mice. Nat Med 5: 101-106.

Gusella JF, Wexler NS, Conneally PM, Naylor SL, Anderson MA, et al. (1983) A polymorphic DNA marker genetically linked to Huntington's disease. Nature 306: 234-238.

Gutekunst CA, Li SH, Yi H, Mulroy JS, Kuemmerle S, et al. (1999) Nuclear and neuropil aggregates in Huntington's disease: relationship to neuropathology. J Neurosci 19: 2522-2534.

Haass C, Lemere CA, Capell A, Citron M, Seubert P, et al. (1995) The Swedish mutation causes early-onset Alzheimer's disease by beta-secretase cleavage within the secretory pathway. Nat Med 1: 1291-1296.

Hackam AS, Singaraja R, Wellington CL, Metzler M, McCutcheon K, et al. (1998) The influence of huntingtin protein size on nuclear localization and cellular toxicity. J Cell Biol 141: 1097-1105.

Hall AM, Roberson ED (2012) Mouse models of Alzheimer's disease. Brain Res Bull 88: 3-12.

Halliday GM, McRitchie DA, Macdonald V, Double KL, Trent RJ, et al. (1998) Regional specificity of brain atrophy in Huntington's disease. Exp Neurol 154: 663-672.

Han I, You Y, Kordower JH, Brady ST, Morfini GA (2010) Differential vulnerability of neurons in Huntington's disease: the role of cell type-specific features. J Neurochem 113: 1073-1091.

Hardingham GE, Bading H (2010) Synaptic versus extrasynaptic NMDA receptor signalling: implications for neurodegenerative disorders. Nat Rev Neurosci 11: 682-696.

Hardy J, Cowburn R, Barton A, Reynolds G, Lofdahl E, et al. (1987) Region-specific loss of glutamate innervation in Alzheimer's disease. Neurosci Lett 73: 77-80.

Harper P, Jones L. Huntington’s disease: genetic and molecular studies. In: Bates G, Harper P, Jones L, eds. Huntington’s disease. New York: Oxford University Press, 2002: 113-158.

Hasmann M, Schemainda I (2003) FK866, a highly specific noncompetitive inhibitor of nicotinamide phosphoribosyltransferase, represents a novel mechanism for induction of tumor cell apoptosis. Cancer Res 63: 7436-7442.

HDCRG (1993) A novel gene containing a trinucleotide repeat that is expanded and unstable on Huntington's disease chromosomes. The Huntington's Disease Collaborative Research Group. Cell 72: 971-983.

Herreman A, Hartmann D, Annaert W, Saftig P, Craessaerts K, et al. (1999) Presenilin 2 deficiency causes a mild pulmonary phenotype and no changes in amyloid precursor protein processing but enhances the embryonic lethal phenotype of presenilin 1 deficiency. Proc Natl Acad Sci U S A 96: 11872-11877.

Heston LL (1984) Down's syndrome and Alzheimer's dementia: defining an association. Psychiatr Dev 2: 287-294.

Hickey MA, Kosmalska A, Enayati J, Cohen R, Zeitlin S, et al. (2008) Extensive early motor and non-motor behavioral deficits are followed by striatal neuronal loss in knock-in Huntington's disease mice. Neuroscience 157: 280-295.

Hiruma H, Katakura T, Takahashi S, Ichikawa T, Kawakami T (2003) Glutamate and amyloid beta-protein rapidly inhibit fast axonal transport in cultured rat hippocampal neurons by different mechanisms. J Neurosci 23: 8967-8977.

Ho LW, Brown R, Maxwell M, Wyttenbach A, Rubinsztein DC (2001) Wild type Huntingtin reduces the cellular toxicity of mutant Huntingtin in mammalian cell models of Huntington's disease. J Med Genet 38: 450-452.

Hodges JR, Martinos M, Woollams AM, Patterson K, Adlam AL (2008) Repeat and Point: differentiating semantic dementia from progressive non-fluent aphasia. Cortex 44: 1265-1270.

Hodgson JG, Agopyan N, Gutekunst CA, Leavitt BR, LePiane F, et al. (1999) A YAC mouse model for Huntington's disease with full-length mutant huntingtin, cytoplasmic toxicity, and selective striatal neurodegeneration. Neuron 23: 181-192.

Holcomb L, Gordon MN, McGowan E, Yu X, Benkovic S, et al. (1998) Accelerated Alzheimer-type phenotype in transgenic mice carrying both mutant amyloid precursor protein and presenilin 1 transgenes. Nat Med 4: 97-100.

Hooijmans CR, Van der Zee CE, Dederen PJ, Brouwer KM, Reijmer YD, et al. (2009) DHA and cholesterol containing diets influence Alzheimer-like pathology, cognition and cerebral vasculature in APPswe/PS1dE9 mice. Neurobiol Dis 33: 482-498.

Hsiao K, Chapman P, Nilsen S, Eckman C, Harigaya Y, et al. (1996) Correlative memory deficits, Abeta elevation, and amyloid plaques in transgenic mice. Science 274: 99-102.

Hu M, Schurdak ME, Puttfarcken PS, El Kouhen R, Gopalakrishnan M, et al. (2007) High content screen microscopy analysis of A beta 1-42-induced neurite outgrowth reduction in rat primary cortical neurons: neuroprotective effects of alpha 7 neuronal nicotinic acetylcholine receptor ligands. Brain Res 1151: 227-235.

Hu X, Hicks CW, He W, Wong P, Macklin WB, et al. (2006) Bace1 modulates myelination in the central and peripheral nervous system. Nat Neurosci 9: 1520-1525.

Huse JT, Liu K, Pijak DS, Carlin D, Lee VM, et al. (2002) Beta-secretase processing in the trans-Golgi network preferentially generates truncated amyloid species that accumulate in Alzheimer's disease brain. J Biol Chem 277: 16278-16284.

Imarisio S, Carmichael J, Korolchuk V, Chen CW, Saiki S, et al. (2008) Huntington's disease: from pathology and genetics to potential therapies. Biochem J 412: 191-209.

Irizarry MC, McNamara M, Fedorchak K, Hsiao K, Hyman BT (1997) APPSw transgenic mice develop age-related A beta deposits and neuropil abnormalities, but no neuronal loss in CA1. J Neuropathol Exp Neurol 56: 965-973.

Jackson GR, Salecker I, Dong X, Yao X, Arnheim N, et al. (1998) Polyglutamine-expanded human huntingtin transgenes induce degeneration of Drosophila photoreceptor neurons. Neuron 21: 633-642.

Jankowsky JL, Fadale DJ, Anderson J, Xu GM, Gonzales V, et al. (2004) Mutant presenilins specifically elevate the levels of the 42 residue beta-amyloid peptide in vivo: evidence for augmentation of a 42-specific gamma secretase. Hum Mol Genet 13: 159-170.

Jankowsky JL, Slunt HH, Ratovitski T, Jenkins NA, Copeland NG, et al. (2001) Co-expression of multiple transgenes in mouse CNS: a comparison of strategies. Biomol Eng 17: 157-165.

Jankowsky JL, Younkin LH, Gonzales V, Fadale DJ, Slunt HH, et al. (2007) Rodent A beta modulates the solubility and distribution of amyloid deposits in transgenic mice. J Biol Chem 282: 22707-22720.

Jessen F, Kucharski C, Fries T, Papassotiropoulos A, Hoenig K, et al. (2001) Sensory gating deficit expressed by a disturbed suppression of the P50 event-related potential in patients with Alzheimer's disease. Am J Psychiatry 158: 1319-1321.

Johnson JW, Kotermanski SE (2006) Mechanism of action of memantine. Curr Opin Pharmacol 6: 61-67.

Kalaria RN, Maestre GE, Arizaga R, Friedland RP, Galasko D, et al. (2008) Alzheimer's disease and vascular dementia in developing countries: prevalence, management, and risk factors. Lancet Neurol 7: 812-826.

Kamphuis W, Mamber C, Moeton M, Kooijman L, Sluijs JA, et al. (2012) GFAP isoforms in adult mouse brain with a focus on neurogenic astrocytes and reactive astrogliosis in mouse models of Alzheimer disease. PLoS One 7: e42823.

Kegel KB, Meloni AR, Yi Y, Kim YJ, Doyle E, et al. (2002) Huntingtin is present in the nucleus, interacts with the transcriptional corepressor C-terminal binding protein, and represses transcription. J Biol Chem 277: 7466-7476.

Kipps CM, Knibb JA, Patterson K, Hodges JR (2008) Neuropsychology of frontotemporal dementia. Handb Clin Neurol 88: 527-548.

Kitay BM, McCormack R, Wang Y, Tsoulfas P, Zhai RG (2013) Mislocalization of neuronal mitochondria reveals regulation of Wallerian degeneration and NMNAT/WLD(S)-mediated axon protection independent of axonal mitochondria. Hum Mol Genet 22: 1601-1614.

Klapstein GJ, Fisher RS, Zanjani H, Cepeda C, Jokel ES, et al. (2001) Electrophysiological and morphological changes in striatal spiny neurons in R6/2 Huntington's disease transgenic mice. J Neurophysiol 86: 2667-2677.

Kornhuber J, Bormann J, Retz W, Hubers M, Riederer P (1989) Memantine displaces [3H]MK-801 at therapeutic concentrations in postmortem human frontal cortex. Eur J Pharmacol 166: 589-590.

Kuemmerle S, Gutekunst CA, Klein AM, Li XJ, Li SH, et al. (1999) Huntington aggregates may not predict neuronal death in Huntington's disease. Ann Neurol 46: 842-849.

Lacor PN, Buniel MC, Furlow PW, Clemente AS, Velasco PT, et al. (2007) Abeta oligomer-induced aberrations in synapse composition, shape, and density provide a molecular basis for loss of connectivity in Alzheimer's disease. J Neurosci 27: 796-807.

Laforet GA, Sapp E, Chase K, McIntyre C, Boyce FM, et al. (2001) Changes in cortical and striatal neurons predict behavioral and electrophysiological abnormalities in a transgenic murine model of Huntington's disease. J Neurosci 21: 9112-9123.

Lamb BT, Sisodia SS, Lawler AM, Slunt HH, Kitt CA, et al. (1993) Introduction and expression of the 400 kilobase amyloid precursor protein gene in transgenic mice [corrected]. Nat Genet 5: 22-30.

Lambon Ralph MA, Patterson K (2008) Generalization and differentiation in semantic memory: insights from semantic dementia. Ann N Y Acad Sci 1124: 61-76.

Landwehrmeyer GB, Standaert DG, Testa CM, Penney JB, Jr., Young AB (1995) NMDA receptor subunit mRNA expression by projection neurons and interneurons in rat striatum. J Neurosci 15: 5297-5307.

Lazarov O, Morfini GA, Pigino G, Gadadhar A, Chen X, et al. (2007) Impairments in fast axonal transport and motor neuron deficits in transgenic mice expressing familial Alzheimer's disease-linked mutant presenilin 1. J Neurosci 27: 7011-7020.

Lee MK, Borchelt DR, Kim G, Thinakaran G, Slunt HH, et al. (1997) Hyperaccumulation of FAD-linked presenilin 1 variants in vivo. Nat Med 3: 756-760.

Lee ST, Chu K, Park JE, Kang L, Ko SY, et al. (2006) Memantine reduces striatal cell death with decreasing calpain level in 3-nitropropionic model of Huntington's disease. Brain Res 1118: 199-207.

Lees GJ (1995) Influence of ketamine on the neuronal death caused by NMDA in the rat hippocampus. Neuropharmacology 34: 411-417.

Lerner RP, Trejo Martinez Ldel C, Zhu C, Chesselet MF, Hickey MA (2012) Striatal atrophy and dendritic alterations in a knock-in mouse model of Huntington's disease. Brain Res Bull 87: 571-578.

Letenneur L, Commenges D, Dartigues JF, Barberger-Gateau P (1994) Incidence of dementia and Alzheimer's disease in elderly community residents of south-western France. Int J Epidemiol 23: 1256-1261.

Levine MS, Klapstein GJ, Koppel A, Gruen E, Cepeda C, et al. (1999) Enhanced sensitivity to N-methyl-D-aspartate receptor activation in transgenic and knockin mouse models of Huntington's disease. J Neurosci Res 58: 515-532.

Li H, Li SH, Yu ZX, Shelbourne P, Li XJ (2001) Huntingtin aggregate-associated axonal degeneration is an early pathological event in Huntington's disease mice. J Neurosci 21: 8473-8481.

Li JY, Conforti L (2013) Axonopathy in Huntington's disease. Exp Neurol 246: 62-71.

Li JY, Popovic N, Brundin P (2005) The use of the R6 transgenic mouse models of Huntington's disease in attempts to develop novel therapeutic strategies. NeuroRx 2: 447-464.

Li L, Fan M, Icton CD, Chen N, Leavitt BR, et al. (2003) Role of NR2B-type NMDA receptors in selective neurodegeneration in Huntington disease. Neurobiol Aging 24: 1113-1121.

Li SH, Cheng AL, Li H, Li XJ (1999) Cellular defects and altered gene expression in PC12 cells stably expressing mutant huntingtin. J Neurosci 19: 5159-5172.

Lipton SA (2006) Paradigm shift in neuroprotection by NMDA receptor blockade: memantine and beyond. Nat Rev Drug Discov 5: 160-170.

Lipton SA (2007) Pathologically activated therapeutics for neuroprotection. Nat Rev Neurosci 8: 803-808.

Liu J, Chang L, Roselli F, Almeida OF, Gao X, et al. (2010) Amyloid-beta induces caspase-dependent loss of PSD-95 and synaptophysin through NMDA receptors. J Alzheimers Dis 22: 541-556.

Liu L, Ikonen S, Heikkinen T, Heikkila M, Puolivali J, et al. (2002) Effects of fimbria-fornix lesion and amyloid pathology on spatial learning and memory in transgenic APP+PS1 mice. Behav Brain Res 134: 433-445.

Liu YF (1998) Expression of polyglutamine-expanded Huntingtin activates the SEK1-JNK pathway and induces apoptosis in a hippocampal neuronal cell line. J Biol Chem 273: 28873-28877.

Lucassen EA, Piaggi P, Dsurney J, de Jonge L, Zhao XC, et al. (2014) Sleep extension improves neurocognitive functions in chronically sleep-deprived obese individuals. PLoS One 9: e84832.

Luesse HG, Schiefer J, Spruenken A, Puls C, Block F, et al. (2001) Evaluation of R6/2 HD transgenic mice for therapeutic studies in Huntington's disease: behavioral testing and impact of diabetes mellitus. Behav Brain Res 126: 185-195.

Lunn ER, Perry VH, Brown MC, Rosen H, Gordon S (1989) Absence of Wallerian Degeneration does not Hinder Regeneration in Peripheral Nerve. Eur J Neurosci 1: 27-33.

Luo Y, Bolon B, Kahn S, Bennett BD, Babu-Khan S, et al. (2001) Mice deficient in BACE1, the Alzheimer's beta-secretase, have normal phenotype and abolished beta-amyloid generation. Nat Neurosci 4: 231-232.

Luthi-Carter R, Hanson SA, Strand AD, Bergstrom DA, Chun W, et al. (2002) Dysregulation of gene expression in the R6/2 model of polyglutamine disease: parallel changes in muscle and brain. Hum Mol Genet 11: 1911-1926.

Luthi-Carter R, Strand A, Peters NL, Solano SM, Hollingsworth ZR, et al. (2000) Decreased expression of striatal signaling genes in a mouse model of Huntington's disease. Hum Mol Genet 9: 1259-1271.

Mack TG, Reiner M, Beirowski B, Mi W, Emanuelli M, et al. (2001) Wallerian degeneration of injured axons and synapses is delayed by a Ube4b/Nmnat chimeric gene. Nat Neurosci 4: 1199-1206.

Mahant N, McCusker EA, Byth K, Graham S, Huntington Study G (2003) Huntington's disease: clinical correlates of disability and progression. Neurology 61: 1085-1092.

Maiuri MC, De Stefano D, Farooqi AA (2014) Physiology to the pleiotropic role of RNAs: prospecting novel therapies. Biomed Res Int 2014: 735374.

Mangiarini L, Sathasivam K, Seller M, Cozens B, Harper A, et al. (1996) Exon 1 of the HD gene with an expanded CAG repeat is sufficient to cause a progressive neurological phenotype in transgenic mice. Cell 87: 493-506.

Marangoni M, Adalbert R, Janeckova L, Patrick J, Kohli J, et al. (2014) Age-related axonal swellings precede other neuropathological hallmarks in a knock-in mouse model of Huntington's disease. Neurobiol Aging 35: 2382-2393.

Margolis RL, Ross CA (2003) Diagnosis of Huntington disease. Clin Chem 49: 1726-1732.

Martinez-Coria H, Green KN, Billings LM, Kitazawa M, Albrecht M, et al. (2010) Memantine improves cognition and reduces Alzheimer's-like neuropathology in transgenic mice. Am J Pathol 176: 870-880.

Marutle A, Unger C, Hellstrom-Lindahl E, Wang J, Puolivali J, et al. (2002) Elevated levels of Abeta1-40 and Abeta1-42 do not alter the binding sites of nicotinic receptor subtypes in the brain of APPswe and PS1 double transgenic mice. Neurosci Lett 328: 269-272.

Maurer K, Volk S, Gerbaldo H (1997) Auguste D and Alzheimer's disease. Lancet 349: 1546-1549.

Mayol L, De Stefano D, Campani V, De Falco F, Ferrari E, et al. (2014) Design and characterization of a chitosan physical gel promoting wound healing in mice. J Mater Sci Mater Med 25: 1483-1493.

Mayol L, De Stefano D, De Falco F, Carnuccio R, Maiuri MC, et al. (2014) Effect of hyaluronic acid on the thermogelation and biocompatibility of its blends with methyl cellulose. Carbohydr Polym 112: 480-485.

Mealing GA, Lanthorn TH, Small DL, Murray RJ, Mattes KC, et al. (2001) Structural modifications to an N-methyl-D-aspartate receptor antagonist result in large differences in trapping block. J Pharmacol Exp Ther 297: 906-914.

Melnikova T, Savonenko A, Wang Q, Liang X, Hand T, et al. (2006) Cycloxygenase-2 activity promotes cognitive deficits but not increased amyloid burden in a model of Alzheimer's disease in a sex-dimorphic pattern. Neuroscience 141: 1149-1162.

Menalled L, Zanjani H, MacKenzie L, Koppel A, Carpenter E, et al. (2000) Decrease in striatal enkephalin mRNA in mouse models of Huntington's disease. Exp Neurol 162: 328-342.

Menalled LB (2005) Knock-in mouse models of Huntington's disease. NeuroRx 2: 465-470.

Menalled LB, Chesselet MF (2002) Mouse models of Huntington's disease. Trends Pharmacol Sci 23: 32-39.

Menalled LB, Kudwa AE, Miller S, Fitzpatrick J, Watson-Johnson J, et al. (2012) Comprehensive behavioral and molecular characterization of a new knock-in mouse model of Huntington's disease: zQ175. PLoS One 7: e49838.

Menalled LB, Sison JD, Dragatsis I, Zeitlin S, Chesselet MF (2003) Time course of early motor and neuropathological anomalies in a knock-in mouse model of Huntington's disease with 140 CAG repeats. J Comp Neurol 465: 11-26.

Miguel-Hidalgo JJ, Alvarez XA, Cacabelos R, Quack G (2002) Neuroprotection by memantine against neurodegeneration induced by beta-amyloid(1-40). Brain Res 958: 210-221.

Milde S, Gilley J, Coleman MP (2013) Subcellular localization determines the stability and axon protective capacity of axon survival factor Nmnat2. PLoS Biol 11: e1001539.

Mills PJ, Ancoli-Israel S, von Kanel R, Mausbach BT, Aschbacher K, et al. (2009) Effects of gender and dementia severity on Alzheimer's disease caregivers' sleep and biomarkers of coagulation and inflammation. Brain Behav Immun 23: 605-610.

Milnerwood AJ, Gladding CM, Pouladi MA, Kaufman AM, Hines RM, et al. (2010) Early increase in extrasynaptic NMDA receptor signaling and expression contributes to phenotype onset in Huntington's disease mice. Neuron 65: 178-190.

Minati L, Edginton T, Bruzzone MG, Giaccone G (2009) Current concepts in Alzheimer's disease: a multidisciplinary review. Am J Alzheimers Dis Other Demen 24: 95-121.

Minkeviciene R, Banerjee P, Tanila H (2004) Memantine improves spatial learning in a transgenic mouse model of Alzheimer's disease. J Pharmacol Exp Ther 311: 677-682.

Minkeviciene R, Rheims S, Dobszay MB, Zilberter M, Hartikainen J, et al. (2009) Amyloid beta-induced neuronal hyperexcitability triggers progressive epilepsy. J Neurosci 29: 3453-3462.

Minniti G, Arcella A, Scaringi C, Lanzetta G, Di Stefano D, et al. (2014) Chemoradiation for anaplastic oligodendrogliomas: clinical outcomes and prognostic value of molecular markers. J Neurooncol 116: 275-282.

Minniti G, Scaringi C, Arcella A, Lanzetta G, Di Stefano D, et al. (2014) IDH1 mutation and MGMT methylation status predict survival in patients with anaplastic astrocytoma treated with temozolomide-based chemoradiotherapy. J Neurooncol 118: 377-383.

Mitchell IJ, Cooper AJ, Griffiths MR (1999) The selective vulnerability of striatopallidal neurons. Prog Neurobiol 59: 691-719.

Mohanaruban K, Sastry, B.S.D. & Finucane, P. (1989) Assessment and diagnosis of dementia. Geriatric Medicine: 81-84.

Molnar Z, Soos K, Lengyel I, Penke B, Szegedi V, et al. (2004) Enhancement of NMDA responses by beta-amyloid peptides in the hippocampus in vivo. Neuroreport 15: 1649-1652.

Moran PM, Higgins LS, Cordell B, Moser PC (1995) Age-related learning deficits in transgenic mice expressing the 751-amino acid isoform of human beta-amyloid precursor protein. Proc Natl Acad Sci U S A 92: 5341-5345.

Morfini GA, You YM, Pollema SL, Kaminska A, Liu K, et al. (2009) Pathogenic huntingtin inhibits fast axonal transport by activating JNK3 and phosphorylating kinesin. Nat Neurosci 12: 864-871.

Mott RT, Hulette CM (2005) Neuropathology of Alzheimer's disease. Neuroimaging Clin N Am 15: 755-765, ix.

Mount C, Downton C (2006) Alzheimer disease: progress or profit? Nat Med 12: 780-784.

Moyano-Mendez JR, Fabbrocini G, De Stefano D, Mazzella C, Mayol L, et al. (2014) Enhanced antioxidant effect of trans-resveratrol: potential of binary systems with polyethylene glycol and cyclodextrin. Drug Dev Ind Pharm 40: 1300-1307.

Mullan M, Houlden H, Windelspecht M, Fidani L, Lombardi C, et al. (1992) A locus for familial early-onset Alzheimer's disease on the long arm of chromosome 14, proximal to the alpha 1-antichymotrypsin gene. Nat Genet 2: 340-342.

Muller WE, Mutschler E, Riederer P (1995) Noncompetitive NMDA receptor antagonists with fast open-channel blocking kinetics and strong voltage-dependency as potential therapeutic agents for Alzheimer's dementia. Pharmacopsychiatry 28: 113-124.

Murrell J, Farlow M, Ghetti B, Benson MD (1991) A mutation in the amyloid precursor protein associated with hereditary Alzheimer's disease. Science 254: 97-99.

Myers RH (2004) Huntington's disease genetics. NeuroRx 1: 255-262.

Nathalie P, Jean-Noel O (2008) Processing of amyloid precursor protein and amyloid peptide neurotoxicity. Curr Alzheimer Res 5: 92-99.

Nilsberth C, Westlind-Danielsson A, Eckman CB, Condron MM, Axelman K, et al. (2001) The 'Arctic' APP mutation (E693G) causes Alzheimer's disease by enhanced Abeta protofibril formation. Nat Neurosci 4: 887-893.

Noble W, Olm V, Takata K, Casey E, Mary O, et al. (2003) Cdk5 is a key factor in tau aggregation and tangle formation in vivo. Neuron 38: 555-565.

Nucifora FC, Jr., Ellerby LM, Wellington CL, Wood JD, Herring WJ, et al. (2003) Nuclear localization of a non-caspase truncation product of atrophin-1, with an expanded polyglutamine repeat, increases cellular toxicity. J Biol Chem 278: 13047-13055.

Okamoto S, Pouladi MA, Talantova M, Yao D, Xia P, et al. (2009) Balance between synaptic versus extrasynaptic NMDA receptor activity influences inclusions and neurotoxicity of mutant huntingtin. Nat Med 15: 1407-1413.

Orr AL, Li S, Wang CE, Li H, Wang J, et al. (2008) N-terminal mutant huntingtin associates with mitochondria and impairs mitochondrial trafficking. J Neurosci 28: 2783-2792.

Osterloh JM, Yang J, Rooney TM, Fox AN, Adalbert R, et al. (2012) dSarm/Sarm1 is required for activation of an injury-induced axon death pathway. Science 337: 481-484.

Palmer AM, Gershon S (1990) Is the neuronal basis of Alzheimer's disease cholinergic or glutamatergic? FASEB J 4: 2745-2752.

Parent A, Hazrati LN (1995) Functional anatomy of the basal ganglia. I. The cortico-basal ganglia-thalamo-cortical loop. Brain Res Brain Res Rev 20: 91-127.

Parihar MS, Brewer GJ (2007) Mitoenergetic failure in Alzheimer disease. Am J Physiol Cell Physiol 292: C8-23.

Parsons CG, Danysz W, Quack G (1999) Memantine is a clinically well tolerated N-methyl-D-aspartate (NMDA) receptor antagonist--a review of preclinical data. Neuropharmacology 38: 735-767.

Patterson C, Feightner JW, Garcia A, Hsiung GY, MacKnight C, et al. (2008) Diagnosis and treatment of dementia: 1. Risk assessment and primary prevention of Alzheimer disease. CMAJ 178: 548-556.

Paulsen JS (2011) Cognitive impairment in Huntington disease: diagnosis and treatment. Curr Neurol Neurosci Rep 11: 474-483.

Petersen A, Gabery S (2012) Hypothalamic and Limbic System Changes in Huntington's Disease. J Huntingtons Dis 1: 5-16.

Petrisic MS, Augood SJ, Bicknell RJ (1997) Monoamine transporter gene expression in the central nervous system in diabetes mellitus. J Neurochem 68: 2435-2441.

Pigino G, Morfini G, Pelsman A, Mattson MP, Brady ST, et al. (2003) Alzheimer's presenilin 1 mutations impair kinesin-based axonal transport. J Neurosci 23: 4499-4508.

Pillay NS, Kellaway LA, Kotwal GJ (2008) Early detection of memory deficits and memory improvement with vaccinia virus complement control protein in an Alzheimer's disease model. Behav Brain Res 192: 173-177.

Plaza JA, De Stefano D, Suster S, Prieto VG, Kacerovska D, et al. (2014) Intradermal spitz nevi: a rare subtype of spitz nevi analyzed in a clinicopathologic study of 74 cases. Am J Dermatopathol 36: 283-294; quiz 295-287.

Politis M, Pavese N, Tai YF, Tabrizi SJ, Barker RA, et al. (2008) Hypothalamic involvement in Huntington's disease: an in vivo PET study. Brain 131: 2860-2869.

Porrero C, Rubio-Garrido P, Avendano C, Clasca F (2010) Mapping of fluorescent protein-expressing neurons and axon pathways in adult and developing Thy1-eYFP-H transgenic mice. Brain Res 1345: 59-72.

Quon D, Wang Y, Catalano R, Scardina JM, Murakami K, et al. (1991) Formation of beta-amyloid protein deposits in brains of transgenic mice. Nature 352: 239-241.

Raina P, Santaguida P, Ismaila A, Patterson C, Cowan D, et al. (2008) Effectiveness of cholinesterase inhibitors and memantine for treating dementia: evidence review for a clinical practice guideline. Ann Intern Med 148: 379-397.

Ramaswamy S, McBride JL, Kordower JH (2007) Animal models of Huntington's disease. ILAR J 48: 356-373.

Ranen NG, Stine OC, Abbott MH, Sherr M, Codori AM, et al. (1995) Anticipation and instability of IT-15 (CAG)n repeats in parent-offspring pairs with Huntington disease. Am J Hum Genet 57: 593-602.

Ranju V, Sathiya S, Kalaivani P, Priya RJ, Saravana Babu C (2015) Memantine exerts functional recovery by improving BDNF and GDNF expression in 3-nitropropionic acid intoxicated mice. Neurosci Lett 586: 1-7.

Rapoport M, Dawson HN, Binder LI, Vitek MP, Ferreira A (2002) Tau is essential to beta -amyloid-induced neurotoxicity. Proc Natl Acad Sci U S A 99: 6364-6369.

Raymoned LA. Excitotoxicity in Huntington disease. Clin Neurosci Res 3(3): 121-128, 2003.

Reading SA, Yassa MA, Bakker A, Dziorny AC, Gourley LM, et al. (2005) Regional white matter change in pre-symptomatic Huntington's disease: a diffusion tensor imaging study. Psychiatry Res 140: 55-62.

Reddy PH, Williams M, Charles V, Garrett L, Pike-Buchanan L, et al. (1998) Behavioural abnormalities and selective neuronal loss in HD transgenic mice expressing mutated full-length HD cDNA. Nat Genet 20: 198-202.

Reiner A, Albin RL, Anderson KD, D'Amato CJ, Penney JB, et al. (1988) Differential loss of striatal projection neurons in Huntington disease. Proc Natl Acad Sci U S A 85: 5733-5737.

Reisberg B. An overview of current concepts of Alzheimer's disease, senile dementia, and age-associated cognitive decline. In: Reisberg B eds. Alzheimer's disease, the standard reference. New York: The Free Press, 1983.

Reiserer RS, Harrison FE, Syverud DC, McDonald MP (2007) Impaired spatial learning in the APPSwe + PSEN1DeltaE9 bigenic mouse model of Alzheimer's disease. Genes Brain Behav 6: 54-65.

Rigamonti D, Bauer JH, De-Fraja C, Conti L, Sipione S, et al. (2000) Wild-type huntingtin protects from apoptosis upstream of caspase-3. J Neurosci 20: 3705-3713.

Rigamonti D, Sipione S, Goffredo D, Zuccato C, Fossale E, et al. (2001) Huntingtin's neuroprotective activity occurs via inhibition of procaspase-9 processing. J Biol Chem 276: 14545-14548.

Rigby M, Le Bourdelles B, Heavens RP, Kelly S, Smith D, et al. (1996) The messenger RNAs for the N-methyl-D-aspartate receptor subunits show region-specific expression of different subunit composition in the human brain. Neuroscience 73: 429-447.

Roberds SL, Anderson J, Basi G, Bienkowski MJ, Branstetter DG, et al. (2001) BACE knockout mice are healthy despite lacking the primary beta-secretase activity in brain: implications for Alzheimer's disease therapeutics. Hum Mol Genet 10: 1317-1324.

Rogawski MA, Wenk GL (2003) The neuropharmacological basis for the use of memantine in the treatment of Alzheimer's disease. CNS Drug Rev 9: 275-308.

Roos RA (2010) Huntington's disease: a clinical review. Orphanet J Rare Dis 5: 40.

Rosales-Corral S, Acuna-Castroviejo D, Tan DX, Lopez-Armas G, Cruz-Ramos J, et al. (2012) Accumulation of exogenous amyloid-beta peptide in hippocampal mitochondria causes their dysfunction: a protective role for melatonin. Oxid Med Cell Longev 2012: 843649.

Rosas HD, Salat DH, Lee SY, Zaleta AK, Pappu V, et al. (2008) Cerebral cortex and the clinical expression of Huntington's disease: complexity and heterogeneity. Brain 131: 1057-1068.

Roselli F, Tirard M, Lu J, Hutzler P, Lamberti P, et al. (2005) Soluble beta-amyloid1-40 induces NMDA-dependent degradation of postsynaptic density-95 at glutamatergic synapses. J Neurosci 25: 11061-11070.

Rui Y, Tiwari P, Xie Z, Zheng JQ (2006) Acute impairment of mitochondrial trafficking by beta-amyloid peptides in hippocampal neurons. J Neurosci 26: 10480-10487.

Salehi A, Delcroix JD, Belichenko PV, Zhan K, Wu C, et al. (2006) Increased App expression in a mouse model of Down's syndrome disrupts NGF transport and causes cholinergic neuron degeneration. Neuron 51: 29-42.

Saraceno C, Musardo S, Marcello E, Pelucchi S, Luca MD (2013) Modeling Alzheimer's disease: from past to future. Front Pharmacol 4: 77.

Sasaki Y, Araki T, Milbrandt J (2006) Stimulation of nicotinamide adenine dinucleotide biosynthetic pathways delays axonal degeneration after axotomy. J Neurosci 26: 8484-8491.

Sasaki Y, Vohra BP, Baloh RH, Milbrandt J (2009) Transgenic mice expressing the Nmnat1 protein manifest robust delay in axonal degeneration in vivo. J Neurosci 29: 6526-6534.

Sasaki YF, Rothe T, Premkumar LS, Das S, Cui J, et al. (2002) Characterization and comparison of the NR3A subunit of the NMDA receptor in recombinant systems and primary cortical neurons. J Neurophysiol 87: 2052-2063.

Saudou F, Finkbeiner S, Devys D, Greenberg ME (1998) Huntingtin acts in the nucleus to induce apoptosis but death does not correlate with the formation of intranuclear inclusions. Cell 95: 55-66.

Saura CA, Choi SY, Beglopoulos V, Malkani S, Zhang D, et al. (2004) Loss of presenilin function causes impairments of memory and synaptic plasticity followed by age-dependent neurodegeneration. Neuron 42: 23-36.

Savonenko A, Xu GM, Melnikova T, Morton JL, Gonzales V, et al. (2005) Episodic-like memory deficits in the APPswe/PS1dE9 mouse model of Alzheimer's disease: relationships to beta-amyloid deposition and neurotransmitter abnormalities. Neurobiol Dis 18: 602-617.

Schneck MK, Reisberg B, Ferris SH (1982) An overview of current concepts of Alzheimer's disease. Am J Psychiatry 139: 165-173.

Schwarcz R, Whetsell WO, Jr., Mangano RM (1983) Quinolinic acid: an endogenous metabolite that produces axon-sparing lesions in rat brain. Science 219: 316-318.

Selkoe DJ (1989) Biochemistry of altered brain proteins in Alzheimer's disease. Annu Rev Neurosci 12: 463-490.

Selkoe DJ (2002) Alzheimer's disease is a synaptic failure. Science 298: 789-791.

Semaka A, Collins JA, Hayden MR (2010) Unstable familial transmissions of Huntington disease alleles with 27-35 CAG repeats (intermediate alleles). Am J Med Genet B Neuropsychiatr Genet 153B: 314-320.

Shelbourne PF, Killeen N, Hevner RF, Johnston HM, Tecott L, et al. (1999) A Huntington's disease CAG expansion at the murine Hdh locus is unstable and associated with behavioural abnormalities in mice. Hum Mol Genet 8: 763-774.

Shen J, Kelleher RJ, 3rd (2007) The presenilin hypothesis of Alzheimer's disease: evidence for a loss-of-function pathogenic mechanism. Proc Natl Acad Sci U S A 104: 403-409.

Singh NK, Dsouza RN, Grasselli M, Fernandez-Lahore M (2014) High capacity cryogel-type adsorbents for protein purification. J Chromatogr A 1355: 143-148.

Sipione S, Rigamonti D, Valenza M, Zuccato C, Conti L, et al. (2002) Early transcriptional profiles in huntingtin-inducible striatal cells by microarray analyses. Hum Mol Genet 11: 1953-1965.

Slow EJ, van Raamsdonk J, Rogers D, Coleman SH, Graham RK, et al. (2003) Selective striatal neuronal loss in a YAC128 mouse model of Huntington disease. Hum Mol Genet 12: 1555-1567.

Smith KD, Kallhoff V, Zheng H, Pautler RG (2007) In vivo axonal transport rates decrease in a mouse model of Alzheimer's disease. Neuroimage 35: 1401-1408.

Snowden JS, Craufurd D, Griffiths HL, Neary D (1998) Awareness of involuntary movements in Huntington disease. Arch Neurol 55: 801-805.

Snowden JS, Craufurd D, Thompson J, Neary D (2002) Psychomotor, executive, and memory function in preclinical Huntington's disease. J Clin Exp Neuropsychol 24: 133-145.

Song C, Zhang Y, Parsons CG, Liu YF (2003) Expression of polyglutamine-expanded huntingtin induces tyrosine phosphorylation of N-methyl-D-aspartate receptors. J Biol Chem 278: 33364-33369.

Song MS, Rauw G, Baker GB, Kar S (2008) Memantine protects rat cortical cultured neurons against beta-amyloid-induced toxicity by attenuating tau phosphorylation. Eur J Neurosci 28: 1989-2002.

Sorrentino G, Bonavita V (2007) Neurodegeneration and Alzheimer's disease: the lesson from tauopathies. Neurol Sci 28: 63-71.

Squitieri F, Gellera C, Cannella M, Mariotti C, Cislaghi G, et al. (2003) Homozygosity for CAG mutation in Huntington disease is associated with a more severe clinical course. Brain 126: 946-955.

St George-Hyslop PH, Petit A (2005) Molecular biology and genetics of Alzheimer's disease. C R Biol 328: 119-130.

Starling AJ, Andre VM, Cepeda C, de Lima M, Chandler SH, et al. (2005) Alterations in N-methyl-D-aspartate receptor sensitivity and magnesium blockade occur early in development in the R6/2 mouse model of Huntington's disease. J Neurosci Res 82: 377-386.

Stefano DD, Villella VR, Esposito S, Tosco A, Sepe A, et al. (2014) Restoration of CFTR function in patients with cystic fibrosis carrying the F508del-CFTR mutation. Autophagy.

Steffan JS, Kazantsev A, Spasic-Boskovic O, Greenwald M, Zhu YZ, et al. (2000) The Huntington's disease protein interacts with p53 and CREB-binding protein and represses transcription. Proc Natl Acad Sci U S A 97: 6763-6768.

Stokin GB, Lillo C, Falzone TL, Brusch RG, Rockenstein E, et al. (2005) Axonopathy and transport deficits early in the pathogenesis of Alzheimer's disease. Science 307: 1282-1288.

Sun Y, Savanenin A, Reddy PH, Liu YF (2001) Polyglutamine-expanded huntingtin promotes sensitization of N-methyl-D-aspartate receptors via post-synaptic density 95. J Biol Chem 276: 24713-24718.

Suzuki N, Cheung TT, Cai XD, Odaka A, Otvos L, Jr., et al. (1994) An increased percentage of long amyloid beta protein secreted by familial amyloid beta protein precursor (beta APP717) mutants. Science 264: 1336-1340.

Swerdlow NR, Paulsen J, Braff DL, Butters N, Geyer MA, et al. (1995) Impaired prepulse inhibition of acoustic and tactile startle response in patients with Huntington's disease. J Neurol Neurosurg Psychiatry 58: 192-200.

Szegedi V, Juhasz G, Budai D, Penke B (2005) Divergent effects of Abeta1-42 on ionotropic glutamate receptor-mediated responses in CA1 neurons in vivo. Brain Res 1062: 120-126.

Tagliavini F, Giaccone G, Frangione B, Bugiani O (1988) Preamyloid deposits in the cerebral cortex of patients with Alzheimer's disease and nondemented individuals. Neurosci Lett 93: 191-196.

Takeuchi H, Mizuno T, Zhang G, Wang J, Kawanokuchi J, et al. (2005) Neuritic beading induced by activated microglia is an early feature of neuronal dysfunction toward neuronal death by inhibition of mitochondrial respiration and axonal transport. J Biol Chem 280: 10444-10454.

Thinakaran G, Parent AT (2004) Identification of the role of presenilins beyond Alzheimer's disease. Pharmacol Res 50: 411-418.

Thompson SB. Dementia: A guide for health care professionals. Aldershot: Arena, 1997.

Tremblay R, Chakravarthy B, Hewitt K, Tauskela J, Morley P, et al. (2000) Transient NMDA receptor inactivation provides long-term protection to cultured cortical neurons from a variety of death signals. J Neurosci 20: 7183-7192.

Van Gool F, Galli M, Rongvaux A, Andris F, Leo O (2009) [A new inflammatory pathway linked to NAD]. Med Sci (Paris) 25: 551-553.

Velier J, Kim M, Schwarz C, Kim TW, Sapp E, et al. (1998) Wild-type and mutant huntingtins function in vesicle trafficking in the secretory and endocytic pathways. Exp Neurol 152: 34-40.

Vessie PR. On the transmission of Huntington's chorea for 300 years: the Bures family group. J Nerv Ment Dis 76: 553-573, 1932.

von Kanel R, Mausbach BT, Patterson TL, Dimsdale JE, Aschbacher K, et al. (2008) Increased Framingham Coronary Heart Disease Risk Score in dementia caregivers relative to non-caregiving controls. Gerontology 54: 131-137.

Walker FO (2007) Huntington's disease. Lancet 369: 218-228.

Wang H, He J, Zhang R, Zhu S, Wang J, et al. (2012) Sensorimotor gating and memory deficits in an APP/PS1 double transgenic mouse model of Alzheimer's disease. Behav Brain Res 233: 237-243.

Wang J, Tanila H, Puolivali J, Kadish I, van Groen T (2003) Gender differences in the amount and deposition of amyloidbeta in APPswe and PS1 double transgenic mice. Neurobiol Dis 14: 318-327.

Wang J, Tanila H, Puolivali J, Kadish I, van Groen T (2003) Gender differences in the amount and deposition of amyloidbeta in APPswe and PS1 double transgenic mice. Neurobiol Dis 14: 318-327.

Wang J, Zhai Q, Chen Y, Lin E, Gu W, et al. (2005) A local mechanism mediates NAD-dependent protection of axon degeneration. J Cell Biol 170: 349-355.

Warby SC, Visscher H, Collins JA, Doty CN, Carter C, et al. (2011) HTT haplotypes contribute to differences in Huntington disease prevalence between Europe and East Asia. Eur J Hum Genet 19: 561-566.

Weaver KE, Richards TL, Liang O, Laurino MY, Samii A, et al. (2009) Longitudinal diffusion tensor imaging in Huntington's Disease. Exp Neurol 216: 525-529.

Wenk GL (2006) Neuropathologic changes in Alzheimer's disease: potential targets for treatment. J Clin Psychiatry 67 Suppl 3: 3-7; quiz 23.

Wenk GL, Olton DS (1989) Cognitive enhancers: potential strategies and experimental results. Prog Neuropsychopharmacol Biol Psychiatry 13 Suppl: S117-139.

Wenk GL, Olton DS. Basal forebrain cholinergic neurons and Alzheimer's disease. In: Coyle J, eds. Experimental models of dementing disorders: A synaptic neurochemical prospective. New York: Alan R Liss Inc., 1987: 81-101.

Wenk GL, Parsons CG, Danysz W (2006) Potential role of N-methyl-D-aspartate receptors as executors of neurodegeneration resulting from diverse insults: focus on memantine. Behav Pharmacol 17: 411-424.

Wexler NS, Lorimer J, Porter J, Gomez F, Moskowitz C, et al. (2004) Venezuelan kindreds reveal that genetic and environmental factors modulate Huntington's disease age of onset. Proc Natl Acad Sci U S A 101: 3498-3503.

Wheeler VC, White JK, Gutekunst CA, Vrbanac V, Weaver M, et al. (2000) Long glutamine tracts cause nuclear localization of a novel form of huntingtin in medium spiny striatal neurons in HdhQ92 and HdhQ111 knock-in mice. Hum Mol Genet 9: 503-513.

Wheelock VL, Tempkin T, Marder K, Nance M, Myers RH, et al. (2003) Predictors of nursing home placement in Huntington disease. Neurology 60: 998-1001.

Willem M, Garratt AN, Novak B, Citron M, Kaufmann S, et al. (2006) Control of peripheral nerve myelination by the beta-secretase BACE1. Science 314: 664-666.

Witt A, Macdonald N, Kirkpatrick P (2004) Memantine hydrochloride. Nat Rev Drug Discov 3: 109-110.

Woollams AM, Cooper-Pye E, Hodges JR, Patterson K (2008) Anomia: a doubly typical signature of semantic dementia. Neuropsychologia 46: 2503-2514.

Wyttenbach A, Carmichael J, Swartz J, Furlong RA, Narain Y, et al. (2000) Effects of heat shock, heat shock protein 40 (HDJ-2), and proteasome inhibition on protein

aggregation in cellular models of Huntington's disease. Proc Natl Acad Sci U S A 97: 2898-2903.

Yamaguchi F, Richards SJ, Beyreuther K, Salbaum M, Carlson GA, et al. (1991) Transgenic mice for the amyloid precursor protein 695 isoform have impaired spatial memory. Neuroreport 2: 781-784.

Yamamoto A, Lucas JJ, Hen R (2000) Reversal of neuropathology and motor dysfunction in a conditional model of Huntington's disease. Cell 101: 57-66.

Young AB, Shoulson I, Penney JB, Starosta-Rubinstein S, Gomez F, et al. (1986) Huntington's disease in Venezuela: neurologic features and functional decline. Neurology 36: 244-249.

Zala D, Colin E, Rangone H, Liot G, Humbert S, et al. (2008) Phosphorylation of mutant huntingtin at S421 restores anterograde and retrograde transport in neurons. Hum Mol Genet 17: 3837-3846.

Zala D, Hinckelmann MV, Yu H, Lyra da Cunha MM, Liot G, et al. (2013) Vesicular glycolysis provides on-board energy for fast axonal transport. Cell 152: 479-491.

Zeitlin S, Liu JP, Chapman DL, Papaioannou VE, Efstratiadis A (1995) Increased apoptosis and early embryonic lethality in mice nullizygous for the Huntington's disease gene homologue. Nat Genet 11: 155-163.

Zeron MM, Chen N, Moshaver A, Lee AT, Wellington CL, et al. (2001) Mutant huntingtin enhances excitotoxic cell death. Mol Cell Neurosci 17: 41-53.

Zhang B, Higuchi M, Yoshiyama Y, Ishihara T, Forman MS, et al. (2004) Retarded axonal transport of R406W mutant tau in transgenic mice with a neurodegenerative tauopathy. J Neurosci 24: 4657-4667.

Zhang S, Boyd J, Delaney K, Murphy TH (2005) Rapid reversible changes in dendritic spine structure in vivo gated by the degree of ischemia. J Neurosci 25: 5333-5338.

Zuccato C, Cattaneo E (2007) Role of brain-derived neurotrophic factor in Huntington's disease. Prog Neurobiol 81: 294-330.

Zuccato C, Cattaneo E (2009) Brain-derived neurotrophic factor in neurodegenerative diseases. Nat Rev Neurol 5: 311-322.

Zuccato C, Ciammola A, Rigamonti D, Leavitt BR, Goffredo D, et al. (2001) Loss of huntingtin-mediated BDNF gene transcription in Huntington's disease. Science 293: 493-498.

Zuccato C, Marullo M, Conforti P, MacDonald ME, Tartari M, et al. (2008) Systematic assessment of BDNF and its receptor levels in human cortices affected by Huntington's disease. Brain Pathol 18: 225-238.

Zuccato C, Valenza M, Cattaneo E (2010) Molecular mechanisms and potential therapeutical targets in Huntington's disease. Physiol Rev 90: 905-981.